

Electronic Thesis and Dissertation Repository

2-23-2017 12:00 AM

Postnatal β 1 Integrin Deficiency in Pancreatic Beta-Cells Impairs Function and Survival

Jason E. Peart, *The University of Western Ontario*

Supervisor: Rennian Wang, *The University of Western Ontario*

A thesis submitted in partial fulfillment of the requirements for the Master of Science degree in Pathology

© Jason E. Peart 2017

Follow this and additional works at: <https://ir.lib.uwo.ca/etd>



Part of the [Endocrine System Diseases Commons](#)

Recommended Citation

Peart, Jason E., "Postnatal β 1 Integrin Deficiency in Pancreatic Beta-Cells Impairs Function and Survival" (2017). *Electronic Thesis and Dissertation Repository*. 4437.
<https://ir.lib.uwo.ca/etd/4437>

This Dissertation/Thesis is brought to you for free and open access by Scholarship@Western. It has been accepted for inclusion in Electronic Thesis and Dissertation Repository by an authorized administrator of Scholarship@Western. For more information, please contact wlsadmin@uwo.ca.

Abstract

Integrin $\beta 1$ is essential for pancreatic beta-cell development and maintenance throughout life in rodents and human fetal islets. However, the effects of a postnatal *$\beta 1$ integrin knockout* ($\beta 1$ KO) specific to pancreatic beta-cells of mice is undetermined. We generated mice with CreERT recombinase specific to the *mouse insulin promoter* (MIP), allowing us to induce a $\beta 1$ KO upon injection of tamoxifen (MIP $\beta 1$ KO model).

At 3-4 weeks of age tamoxifen was injected and mice were sacrificed at 8 (male) and 16 weeks (female) post-tamoxifen. MIP $\beta 1$ KO mice had impaired glucose tolerance, reduced beta-cell mass and islet density. The impairment in glucose tolerance remained in aged mice. Male MIP $\beta 1$ KO mice also had impaired insulin expression and secretion, along with reduced Pdx-1, p-FAK, p-ERK, and p-Akt protein levels. Insulin exocytosis proteins were also reduced in male MIP $\beta 1$ KO mice. These findings demonstrate a significant role for $\beta 1$ integrin in the survival and function of adult murine beta-cells.

Keywords

$\beta 1$ integrin, mouse insulin promoter (MIP), Diabetes mellitus, tamoxifen-inducible, glucose tolerance test, beta-cell mass, FAK signalling

Co-Authorship Statement

The methodology described in Chapter 2 was conducted by Jason Peart in Dr. Rennian Wang's laboratory. The following contributions were made by other members within the lab.

Jinming Li provided technical assistance with genotyping, immunofluorescence staining, and conducting western blots. Jinming Li conducted all qRT-PCR experiments presented in this dissertation. Hojun Lee aided in morphometric analyses of 16 week post-tamoxifen pancreata in Figure 3.10. Dr. Matthew Riopel conducted western blot experiments that were included in Figures 3.11B and 3.13A-D. Dr. Zhi-Chao Feng conducted western blot experiments that were used in Figures 3.13A-C and 3.13E, and contributed to the GSIS data in Figure 3.5A. All studies were designed by Dr. Rennian Wang, who generated the MIP β 1KO mice, provided insight into interpreting findings, and helped revise the final manuscript.

Acknowledgments

I would like to thank my supervisor Dr. Rennian Wang for allowing me to pursue a masters degree within her lab. Diabetes has impacted my family in so many ways, myself included, and Dr. Wang gave me the chance to contribute in a meaningful way to something I am so passionate about. In addition, Dr. Wang was always pushing for me to be more self-sufficient, a skill that essential to so many aspects of daily life, yet she was always there if I needed guidance and motivation and for that I am thankful. As a lab technician Jinming Li has provided his expertise in experimental methods countless times throughout my thesis, without him, I would not have been able to fulfill my project in its entirety. I would also like to thank all Wang Lab members for their encouraging words, assistance when needed, and their comments and feedback.

Thank you Dr. Zia Khan and Dr. Andrew Leask for being members on my committee and for providing insightful feedback regarding my project.

To my mother, Marianne, thank you for all your love and support through the years.

Lastly, thank you to the Children's Health Research Institute and the Pathology Department at Western University for their financial support.

Table of Contents

Abstract.....	i
Co-Authorship Statement.....	ii
Acknowledgments.....	iii
Table of Contents.....	iv
List of Tables.....	vii
List of Figures.....	viii
List of Appendices.....	x
List of Abbreviations.....	xi
Chapter 1 - Introduction.....	1
1.1 Significance of the study.....	1
1.2 The pancreas and its development.....	1
1.3 Beta-cells and Insulin Secretion.....	3
1.4 Diabetes mellitus.....	7
1.5 Integrin receptors and the ECM.....	8
1.6 $\beta 1$ integrin and islet development.....	11
1.7 $\beta 1$ integrin in islet survival and function.....	11
1.8 Signalling pathways involving $\beta 1$ integrin in islet survival and function.....	14
1.9 Rationale and objectives of the present study.....	18
Chapter 2 – Materials and Methods.....	19
2.1 Generation of the beta-cell $\beta 1$ integrin knockout mouse model.....	19
2.2 Mouse genotyping.....	21
2.3 Tamoxifen preparation and administration.....	23
2.4 Glucose metabolism studies.....	23
2.5 Islet isolation.....	24

2.6 Ex vivo GSIS	24
2.7 Insulin ELISA	24
2.8 Tissue processing and immunohistological analyses	25
2.9 RNA extraction	30
2.10 qRT-PCR quantification	30
2.11 Reverse transcription and cDNA synthesis.....	34
2.12 Protein extraction and western blot analyses	34
2.13 Statistical analyses	35
Chapter 3 - Results	36
3.1 Characterization of $\beta 1$ integrin expression in beta-cells of MIP β 1KO mice.....	36
3.2 MIP β 1KO mice display impaired glucose tolerance	41
3.3 Deficient glucose-stimulated insulin secretion in male but not female MIP β 1KO mice.....	46
3.4 Reduction of insulin secretory molecules in MIP β 1KO mice	49
3.5 Reduced beta-cell mass in MIP β 1KO mice	56
3.6 Reduction of Pdx-1 mRNA and protein levels in male MIP β 1KO mice.....	64
3.7 $\beta 1$ integrin deficiency in beta-cells does not affect islet vasculature.....	69
3.8 Reduction of phosphorylated-FAK, ERK1/2, and Akt protein levels with altered cell proliferation pathways in male MIP β 1KO mice	72
3.9 Expression of other integrin subunits in male MIP β 1KO mice	75
3.10 Glucose intolerance was maintained in aged MIP β 1KO mice	80
Chapter 4 - Discussion	83
4.1 Knockdown of $\beta 1$ integrin in MIP β 1KO mice	83
4.2 Do MIP β 1KO mice have impaired glucose tolerance and insulin secretion?.....	84
4.3 Are insulin secretory molecules altered in MIP β 1KO mice?	85
4.4 Is $\beta 1$ integrin required for proper islet morphology?.....	86
4.5 Vasculature in the islets of MIP β 1KO mice	88

4.6 Signalling in MIP β 1KO mice	88
4.7 Aged MIP β 1KO mice and a lack of functional compensation by other integrins .	89
4.8 Limitations of the study	90
4.9 Conclusions and future directions	92
Chapter 5 - References	95
Appendices.....	111
Curriculum Vitae	116

List of Tables

Table 2.1 Primary antibodies used for immunostaining and Western Blots.....	28
Table 2.2 Sequences of primers used in qRT-PCR.....	31

List of Figures

Figure 1.1 SNARE mediated insulin exocytosis in beta-cells	6
Figure 1.2 The association of α and β integrins and their ligands	10
Figure 1.3 β 1 integrin signalling pathway	17
Figure 2.1 Breeding schematic for generation of MIP β 1KO mice.....	20
Figure 2.2 Representative PCR images for mouse genotyping	22
Figure 2.3. The derivative melting curves of qRT-PCR products.....	33
Figure 3.1 Confirmation of β 1 integrin knockdown in 8 weeks post-tamoxifen male MIP β 1KO mice.....	38
Figure 3.2 Confirmation of β 1 integrin knockdown in 16 weeks post-tamoxifen female MIP β 1KO mice.....	40
Figure 3.3 Metabolic analyses of 8 weeks post-tamoxifen male MIP β 1KO mice	43
Figure 3.4 Metabolic analyses of 16 weeks post-tamoxifen female MIP β 1KO mice	45
Figure 3.5 In vivo and ex vivo GSIS analyses.....	48
Figure 3.6 qRT-PCR analyses of insulin exocytosis machinery mRNA in 8 weeks post- tamoxifen male MIP β 1KO mice.....	51
Figure 3.7 Immunofluorescence staining for insulin exocytosis proteins in 8 weeks post- tamoxifen male MIP β 1KO mice.....	53
Figure 3.8 qRT-PCR analysis for insulin exocytosis proteins in 16 weeks post-tamoxifen female MIP β 1KO mice	55
Figure 3.9 Morphometric analyses of 8 weeks post-tamoxifen male MIP β 1KO mice	59

Figure 3.10 E-cadherin and Glut2 co-localization in 8 week post-tamoxifen male MIP β 1KO mice.....	61
Figure 3.11 Morphometric analyses of 16 weeks post-tamoxifen female MIP β 1KO mice ...	63
Figure 3.12 Examination of Pdx-1 expression in 8 weeks post-tamoxifen male MIP β 1KO mice.....	66
Figure 3.13 Transcription factor expression in 8 week post-tamoxifen male MIP β 1KO mice	68
Figure 3.14 Measurement of islet vascularization in MIP β 1KO mice	71
Figure 3.15 Cell signalling, proliferation, and apoptosis in 8 weeks post-tamoxifen male MIP β 1KO mice.....	74
Figure 3.16 qRT-PCR analyses for integrin alpha subunits in 8 weeks post-tamoxifen male MIP β 1KO mice.....	77
Figure 3.17 Immunofluorescence staining for integrin alpha subunits in 8 weeks post-tamoxifen male MIP β 1KO mice.....	79
Figure 3.18 Metabolic analyses of aged MIP β 1KO mice.....	82
Figure 4.1 Impact of the MIP β 1KO model in male mice	94

List of Appendices

Appendix A: Animal use protocol.....	112
Appendix B: Classification II laboratory approval form.....	113
Appendix C: Biosafety approval form	115

List of Abbreviations

Akt	v-akt murine thymoma viral oncogene
AUC	Area under the curve
β 1KO	Collagen type I α 2 driven β 1 integrin knockout mice
BP	Base pair
Bcl2	B-cell lymphoma 2
BSA	Bovine serum albumin
BW	Body weight
Col1a2	Collagen type I α 2 chain
CreERT	Tamoxifen inducible Cre recombinase
CDK5	Cyclin-dependent kinase 5
DAPI	4'-6-Diamidino-2-phenylindole
DM	Diabetes mellitus
EDTA	Ethylenediaminetetraacetic acid
ECM	Extracellular matrix
ELISA	Enzyme-linked immunosorbent assay
ERK	Extracellular signal-related kinase
FAK	Focal adhesion kinase
FERM	Band 4.1, ezrin, radixin and moesin homology domain
g	Units of times gravity
Gcg	Glucagon
Glut-2	Glucose transporter 2
Grb2	Growth factor receptor-bound protein 2
GSIS	Glucose-stimulated insulin secretion
HEPES	4-(2-hydroxyethyl)-1-piperazineethanesulfonic acid

Hes1	hairy and enhancer of split-1
Ins	Insulin
INS-1	Rat insulinoma-1 cell line
I.P.	Intraperitoneal
IPGTT	Intraperitoneal glucose tolerance test
IPITT	Intraperitoneal insulin tolerance test
IR	Insulin receptor
Itg	Integrin
ISL-1	Islet-1
KO	Knockout
MAPK	Mitogen-activated protein kinase
MafA	v-maf avian musculoaponeurotic fibrosarcoma homolog A
MIP	Mouse insulin promoter
MIP β 1KO	Mouse insulin promoter-driven β 1 integrin knockout mice
mSOS1	Son of sevenless homolog 1
Munc18-1	Mammalian homologue of unc-18
Ngn3	Neurogenin3
Nkx2.2	NK2 homeobox 2
Nkx6.1	NK6 homeobox 1
p	Phosphorylated
p110	phosphatidylinositol-4,5-bisphosphate 3-kinase, catalytic subunit alpha
p35	NCK5a neuronal Cdk5 activator
P70s6k	Ribosomal protein S6 kinase beta-1
Pax4	Paired box 4
PaSC	Pancreatic stellate cell
PBS	Phosphate buffered saline

PCR	Polymerase chain reaction
Pdx-1	Pancreatic duodenal homeobox-1
PECAM	Platelet endothelial cell adhesion molecule
PFA	Paraformaldehyde
PI3K	Phosphoinositide 3-kinase
Ptf1a	Pancreas specific transcription factor 1a
qRT-PCR	Quantitative real-time reverse transcriptase PCR
RGD	Arg-Gly-Asp (Arginine-Glycine-Aspartic acid)
RIP β 1KO	Rat insulin promoter-driven β 1 integrin knockout mice
RIPFAKKO	Rat insulin promoter-driven FAK knockout mice
RPM	Revolutions per minute
S473	Serine residue 473
SEM	Standard error of the mean
SH2	Src homology 2 domain
SH3	Src homology 3 domain
SNAP-25	Synaptosome associated protein-25
Stx1a	Syntaxin1a
Stx3	Syntaxin3
TBST	Tris-buffered saline with Tween 20
VAMP-2	Vesicle associated membrane protein-2
Y118	Tyrosine residue 118
Y397	Tyrosine residue 397

Chapter 1 - Introduction

1.1 Significance of the study

The most promising avenue for the treatment of diabetes is transplantation of pancreatic islets, yet an inadequate donor supply and short-term survival of transplanted islets are limiting factors. Finding optimal conditions for isolation of islets, transplantation, and generation of functional beta-like cells from stem cells is of critical importance to circumvent these issues. The loss of $\beta 1$ integrin, a protein critical in cell-extracellular matrix (ECM) interactions, has not been studied in beta-cells of adult mice. Further understanding of the relationship of the ECM and postnatal beta-cells in their native environment will help us understand the ideal way to handle beta-cells in therapeutic conditions.

1.2 The pancreas and its development

The pancreas is a glandular organ that can be divided into two morphologically distinct regions: the exocrine and endocrine pancreas. The exocrine tissue comprises 97% of the pancreas and consists of the acinar cells which secrete a variety of digestive enzymes (proteases, lipases, and amylase) and the ductal system, responsible for transporting enzyme secretions into the duodenum. The remaining 3% of the pancreas are the highly vascularized pancreatic islets of Langerhans which were first discovered by Paul Langerhans in 1869 during his PhD studies (Langerhans, 1869). Islets are dense clusters of 5 different hormone secreting cell types (alpha-cells, beta-cells, delta-cells, gamma-cells, and epsilon-cells), that secrete the hormones glucagon, insulin, somatostatin, pancreatic polypeptide, and ghrelin respectively. Islet architecture varies between frequently studied mammalian species, with different cellular compositions in porcine, canine, murine, and human islets (Kim et al. 2009, Wang et al. 1999). Murine islets consist of a beta-cell rich core that comprises ~87% of the islet, surrounded by an outer layer of alpha-cells (7% of the islet), with the remaining cell types making up the remaining 6% (Rothers & Harlan 2004). However, human islets contain a higher percentage of alpha-cells (36%), with beta-cells accounting for 54% of the islet (Rothers

& Harlan 2004). Regulation of glucose metabolism is a highly intricate process carried out through the release of glucagon and insulin. In response to hypoglycemia (low blood glucose), glucagon is released from alpha-cells and stimulates glucose production from the liver through conversion of glycogen into glucose. Alternatively, insulin is secreted by beta-cells after a meal or in hyperglycemic conditions (high blood glucose), which binds to the insulin receptor found on peripheral cells such as those in the liver, muscle, and adipose, which uptake and store excess glucose.

The pancreas is derived from an outgrowth of endodermal epithelium in the foregut that expresses Sry-related HMG box 17 protein (Sox17) (Tateishi et al. 2008). The primary transition of pancreatic development begins on mouse embryonic (e) day 8.5, where the outgrowth begins to divide into two buds known as the dorsal and ventral buds that express key transcription factors pancreatic duodenal homeobox 1 (Pdx-1) and pancreatic transcription factor 1a (Ptf1a) (Offield et al. 1996, Kagawauchi et al. 2002, Krapp et al. 1996, Hald et al. 2008, Meulen & Huisin, 2015). The pancreatic buds fuse at the beginning of the secondary transition of pancreatic development (e12.5-e18.5) and form one cohesive organ with a definitive tip region (cells destined for an exocrine cell fate expressing Ptf1a) and interior trunk region (cells destined to become either endocrine or ductal cells expressing NK6 homeobox 1 (Nkx6.1)) that is dependent on high levels of Notch activity (Afelik & Jensen 2012, Afelik et al. 2012). Most tip cells have fully differentiated into acinar cells by e15.5 (Pan et al. 2013). Within the trunk, high levels of Notch activity result in activation of hairy and enhancer of split-1 (Hes1), an inhibitor of Neurogenin 3 (Ngn3). However, lowered levels of Notch leads to a loss of Hes1 with continued activation of Sox9, an activator of Ngn3, and these cells migrate away from the ducts to commit to an endocrine cell fate (Shih et al. 2012). Endocrine cells further differentiate into the five aforementioned cell types, and it is the expression of Pdx-1, Nkx6.1 and paired box 4 (Pax4) that lead to a beta-cell fate (Collombat et al. 2003, Gannon et al. 2008, Henseleit et al. 2005, Holland et al. 2002, Shih et al. 2013, Sosa-Pineda et al. 1997). Endocrine cells begin to cluster into islet-like structures around e16 (Shih et al. 2013, Habener et al. 2005). The tertiary period of pancreatic development (e19.5 – post natal day (p) 21), is a period of remodelling where beta-cell neogenesis, proliferation and apoptosis occurs, leading to the final pancreatic structure observed in

adults (Kaung 1994, Scaglia et al. 1997). By postnatal day 21, the islets are fully mature and beta-cells are capable of maintaining normoglycemia through secretion of insulin into the plasma in response to increased blood glucose levels.

1.3 Beta-cells and Insulin Secretion

Glucose-stimulated insulin secretion is a tightly regulated process beginning with up-take of glucose by pancreatic beta-cells via the glucose transporter type 2 (Glut2) protein in rodents. Intracellular glucose leads to increased production of ATP, and an increase in the ATP/ADP ratio leading to closing of voltage-gated potassium channels, initiating depolarization of the cell (Ashcroft et al. 1984). This causes an influx of Ca^{2+} into the cell via L-type Ca^{2+} channels (Hoenig & Sharp 1986, Straub & Sharp 2002, Wollheim & Sharp 1981) and results in docking of insulin containing granules to the plasma membrane with the aid of soluble N-ethylmaleimide-sensitive attachment protein receptors (SNAREs), tethering proteins such as Rab (Ungar & Hughson 2003), and microtubule remodelling (Kalwat & Thurmond 2013). Insulin exocytosis is a biphasic phenomenon. The first phase of insulin release begins approximately 1-2 minutes after glucose is ingested. Insulin release plateaus 3-4 minutes after glucose ingestion and declines rapidly until 8 minutes afterwards as part of the K_{ATP} -dependent (triggering) pathway (Straub & Sharp 2002). This initial phase releases insulin from an immediately available pool of insulin granules (known as the readily releasable pool), which are pre-docked insulin granules on the cell membrane (Straub & Sharp 2002, Wang & Thurmond 2009). The second phase of insulin release begins after the first, with an increasing release of insulin into the plasma that peaks at 25-30 minutes post glucose intake and this is referred to as the K_{ATP} -independent (augmenting) pathway (Straub & Sharp 2002). During the second phase of insulin release, insulin exocytosis occurs from a pool of insulin granules known as the storage granule pool and the release of these granules can be influenced by acetylcholine and glucagon like peptide-1 (GLP-1), which lead to increased levels of diacylglycerol (DAG) and cyclic adenosine monophosphate (cyclic AMP) respectively (Straub & Sharp 2002, Wang & Thurmond 2009). Once in circulation, insulin interacts with the insulin receptor found on multiple peripheral cell types (such as liver, fat, muscle and beta-cells) and leads to the phosphorylation of insulin

receptor substrates (IRS). Phosphorylated IRS subsequently interacts with signalling pathways (e.g. phosphoinositide 3-kinase (PI3K)/v-akt murine thymoma viral oncogene (Akt) and mitogen activated protein kinase (MAPK)/ extracellular signal-related kinase (ERK)) that control cell metabolism, differentiation, and proliferation (Giancotti & Guo 2004). Within the beta-cell, the binding of insulin to the insulin receptor plays a positive autocrine role that regulates subsequent insulin secretion (Leibiger et al. 2001). When insulin binds to insulin receptor type A expressed on the beta-cell surface, PI3K class Ia and ribosomal protein S6 kinase beta-1 (p70s6k) are upregulated leading to enhanced insulin gene transcription (Leibiger et al. 2001). The implications of insulin and its downstream signalling are vast and vary between cell types, and the topic is beyond the scope of this thesis, however, the way by which insulin exocytosis takes place is worthy of examination.

Exocytosis is mediated by SNARE proteins, which work in a coordinated fashion. In general, a SNARE protein consists of a conserved 60-70 amino acid heptad repeat (the SNARE motif) with a transmembrane domain in the C-terminus and independently folded domains at the N-terminus (Weimbs et al. 1997, Jahn & Scheller 2006). SNAREs can be loosely defined as either target-SNAREs (t-SNAREs) which reside on the plasma membrane, or vesicle-SNAREs (v-SNAREs) which are present on vesicles (Jahn & Scheller 2006). The formation of SNARE complexes varies between organism and tissue types (Kasai et al. 2012). Studies of insulin exocytosis in beta-cells of rats and the rat cell lines HIT-T15, β TC6-F7, and RIN1056A, have shown that protein components of t-SNAREs syntaxins (1-4) and synaptosome associated protein 25 (SNAP-25), and that of v-SNAREs vesicle associated membrane protein-2 (VAMP-2) and synaptotagmin III are expressed (Wheeler et al. 1996). Among the syntaxin family of proteins, syntaxin1A and syntaxin3 have been shown to be key mediators of insulin exocytosis. A Cre-mediated beta-cell specific knockout of syntaxin1A in mice lead to impaired first and second phase insulin secretion (Liang et al. 2017). Syntaxin3 siRNA in INS-1 cells and isolated mouse islets (3-6 months old) lead to a reduction in new comer insulin granules, whereas overexpression of syntaxin3 enhanced both phases of insulin exocytosis (Zhu et al. 2013).

A general schematic illustrating the function of SNAREs is presented (**Figure 1.1**) t-SNAREs and v-SNAREs form a four-helix structure at the site of exocytosis and is dissociated by *N*-ethylmaleimide-sensitive factor (NSF) after exocytosis is complete (Jahn & Scheller 2006). The formation of this four-helix structure is due to the contribution of helices by individual proteins in the complex: SNAP-25 contributes two helices, while syntaxin1A and VAMP2 each contribute one helix, allowing for membrane fusion and exocytosis (Fasshauer 2002).

Beyond the core components mentioned above, there are a multitude of other factors that are responsible for the regulation of exocytosis, two of which are Mammalian unc18 (Munc18) and synaptotagmin III. Munc18 has three known isoforms, Munc18a, Munc18b, and Munc18c (Tellam et al. 1995). Munc18a shares exact homology with Munc18, whereas Munc18b has 61% homology, and Munc18c has 51% (Tellam et al. 1995). Studies have shown that Munc18a and Munc18b have highest affinity towards syntaxins 1-3, whereas Munc18c affinity for binding is preferential to syntaxin 4 (Oh & Thurmond 2009). Studies have best characterized the relationship between Munc18 and syntaxin1A, demonstrating that Munc18 regulates Syntaxin1A by maintaining it in a closed conformation, preventing formation of the SNARE complex by inhibiting interactions with VAMP2 and that these interactions are highly dependent on a 1:1 syntaxin:Munc18 molar ratio, and this seems to hold true for all Munc18 and syntaxin proteins (Reviewed in Thurmond 2013). Since insulin exocytosis is Ca^{2+} mediated, it is intuitive to think that part of the SNARE complex would sense calcium, and synaptotagmin III plays this role (Brown et al. 2000, Wheeler et al. 1996). Synaptotagmin III is found within secretory vesicles along with insulin, and its cytoplasmic Ca^{2+} sensing region leads to a conformational change upon influx of Ca^{2+} into the cell, allowing its interaction with syntaxin and SNAP25 on the plasma membrane (Brown et al. 2000). Impairment of insulin secretion and/or the signalling pathways at one or multiple areas leads to the development of diabetes mellitus (DM). There are several forms of DM with different treatment options available depending on the pathology of the disease.

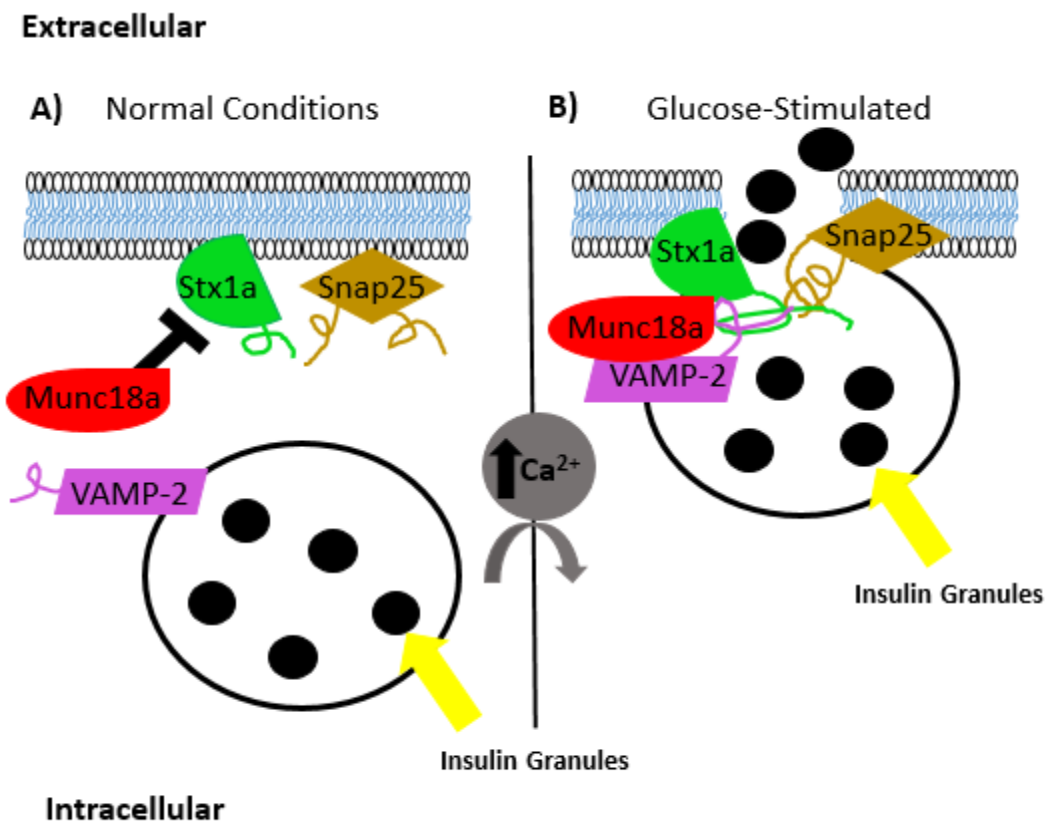


Figure 1.1 SNARE mediated insulin exocytosis in beta-cells

A) In normal conditions the helices contributed by syntaxin1A (Stx1A), SNAP25, and VAMP-2 remain apart and Munc18a maintains Stx1A in a closed conformation. **B)** Influx of calcium (Ca²⁺) into the cell results in the open conformation of Stx1A through release of inhibition by Munc18, which now aids in stabilizing the SNARE complex at the plasma membrane. At this time, the helices from Stx1A, SNAP25, and VAMP-2 come together and result in fusion of the vesicle with the plasma membrane and subsequent insulin exocytosis.

1.4 Diabetes mellitus

DM is diagnosed as one of two types based on the pathology of the disease. Type 1 diabetes (T1D) is the result of autoimmune destruction of the pancreatic beta-cells, leading to insufficient insulin production. In T1D, individuals develop severe hyperglycemia unless exogenous insulin is administered. In contrast, the development of type 2 diabetes (T2D) is multi-factorial, ranging from inefficient beta-cell mass to reduced sensitivity to insulin in peripheral tissues. T2D also results in hyperglycemia, but less severe cases can be treated with modifications in diet and increased physical activity. Medications often come in one of two forms: those that aid in maintaining sufficient beta-cell function, such as glucagon-like peptide 1 (GLP1) agonists or DPP4 inhibitors (Lamber et al. 2003, Versophl et al. 2009), or medications like metformin that target peripheral tissues to increase glucose uptake (e.g. muscle (Bailey & Puaah 1986, Rosetti et al. 1990, Galsuka et al. 1994) and fat (Cigolini et al. 1984)) or decrease glucose production (e.g. liver) (Bailey & Wollen 1988, Bailey 1992, Bailey 1993). A promising avenue for the treatment for T1D is the restoration of functioning beta-cells in diabetic patients using islet transplantations. The Edmonton protocol, established during the 1990s and still in effect today, involves isolating islets from human cadaveric donors and transplanting them in the hepatic portal vein of transplant recipients (Shapiro et al. 2000). However, islet transplantation currently has many shortcomings that limit the long-term production of endogenous insulin. Transplant recipients must balance taking immunosuppressant drugs to prevent rejection while avoiding beta-cell toxicity (Zeng et al. 1993). In addition, cells are often damaged during the isolation process leading to impaired integrin and ECM interactions, induced cell death and reduced cell function, and a shortage of donor tissue, leading to inadequate beta-cell mass over time (Shapiro et al. 2000, Ryan et al. 2005). To circumvent these issues, designing optimal culture conditions for maintaining islet architecture and transplant environments for donor tissue and/or beta-like cells derived from stem cells is essential. One way to do this is to study how the integrin family of receptors, essential in cellular adhesion, interacts with the surrounding extracellular matrix (ECM) to maintain islet integrity, beta-cell function and survival.

1.5 Integrin receptors and the ECM

Integrins are heterodimeric proteins consisting of α and β subunits (18 α and 8 β subunits in mammals) that combine to form 24 different combinations (Takada et al. 2007, Barczyk et al. 2010). The ligands for integrins are proteins that comprise the extracellular matrix (ECM). The ECM consists of negatively charged glycosaminoglycans that form a porous, yet hydrated, gel-like substance in which a variety of proteins such as collagens, fibronectin, laminins, and vitronectin reside. These proteins provide stability and support for cells, while at the same time having profound influence on cell differentiation, function, proliferation, and survival (Aszódi et al. 2006, Streuli 1999, Rosso et al. 2004, Kleinmen et al. 2003). The ability of the ECM to influence the fate of cells is ultimately dependent on a variety of adhesion molecules that act to govern interactions with the environment around them. Cell adhesion molecules can be broadly defined into one of four categories: Immunoglobulin superfamily cell adhesion molecules (IGSF CAMs), integrins, cadherins, and selectins. Although there is a multitude of resources providing in-depth information on the different types of cell adhesion molecules, integrin-ECM interactions are the focus of this thesis.

Integrins can be divided into four general classes based on the extracellular ligands they bind to as dictated by the α -subunit that governs ligand binding specificity (**Figure 1.2**): arginine-glycine-aspartic acid (RGD) receptors (e.g., fibronectin and vitronectin), GFOGER receptors (collagens), leukocyte-specific receptors, and laminin receptors combinations (Takada et al. 2007, Barczyk et al. 2010). Integrins exist in an inactive conformation with low affinity for binding to their ligands (Springer & Dustin 2012). Inside-out signalling is a process by which integrins become activated into a high affinity ligand binding state, and talin binding to the cytoplasmic tail of the β -integrin subunit has been implicated as the key protein required for the conformational change (reviewed in Wang 2012). The binding of talin makes a direct connection between an integrin, the ECM, and the actin cytoskeleton. The kindlin family of focal adhesion proteins has been shown to activate integrins, with loss of integrin activation seen in kindlin inhibition studies (Kloeker et al. 2004, Harburger & Calderwood 2009). After the initial binding of talin and kindlins, the now activated integrin will bind to extracellular ligands leading to

outside-in signalling and resulting in further scaffolding of signalling proteins within the cell into groupings known as focal adhesions. Focal adhesions, mediated by focal adhesion kinase (FAK), can lead to a variety of downstream signalling processes involving the activation of RhoGTPases, serine/threonine kinases, and tyrosine kinases such as ERK1/2 as well as Akt (Danen & Sonneberg 2003). The multitude of proteins that coalesce together during outside-in signalling is vast and reviewed in Harburger & Calderwood (2009), but a more detailed description of $\beta 1$ integrin-FAK related signalling is discussed in **section 1.8**.

$\beta 1$ integrin is the most abundant β -integrin subunit and is expressed ubiquitously. $\beta 1$ integrin associates with 12 different α subunits ($\alpha 1$ - $\alpha 11$ and αv) (Barczyk et al. 2010). Signalling through $\beta 1$ integrin is dependent on the cytoplasmic domain, in which a NPxY motif is present and leads to inside-out activation of $\beta 1$ (Cordes et al. 2006) and outside-in activation of FAK (Wennerberg et al. 2000). $\beta 1$ integrin through its affinity with 12 different α subunits, binds to all major categories of ECM proteins and is involved in actin remodelling, cell polarity, movement, and induction and maintenance of cellular differentiation and function (Brakebusch & Fassler, 2005); including cartilage and bone formation (Aszódi et al. 2006), skeletal muscle development (Burkin et al. 2001, Schwander et al. 2003), epidermis formation (Brakebusch et al. 2000), development of the cerebral cortex (Belvindrah et al. 2007), and angiogenesis (Mettouchi & Meneguzzi 2006). Researchers have begun to uncover the role of $\beta 1$ integrin in the pancreas, specifically with regard to islet development, function and survival, but substantial work remains to be done.

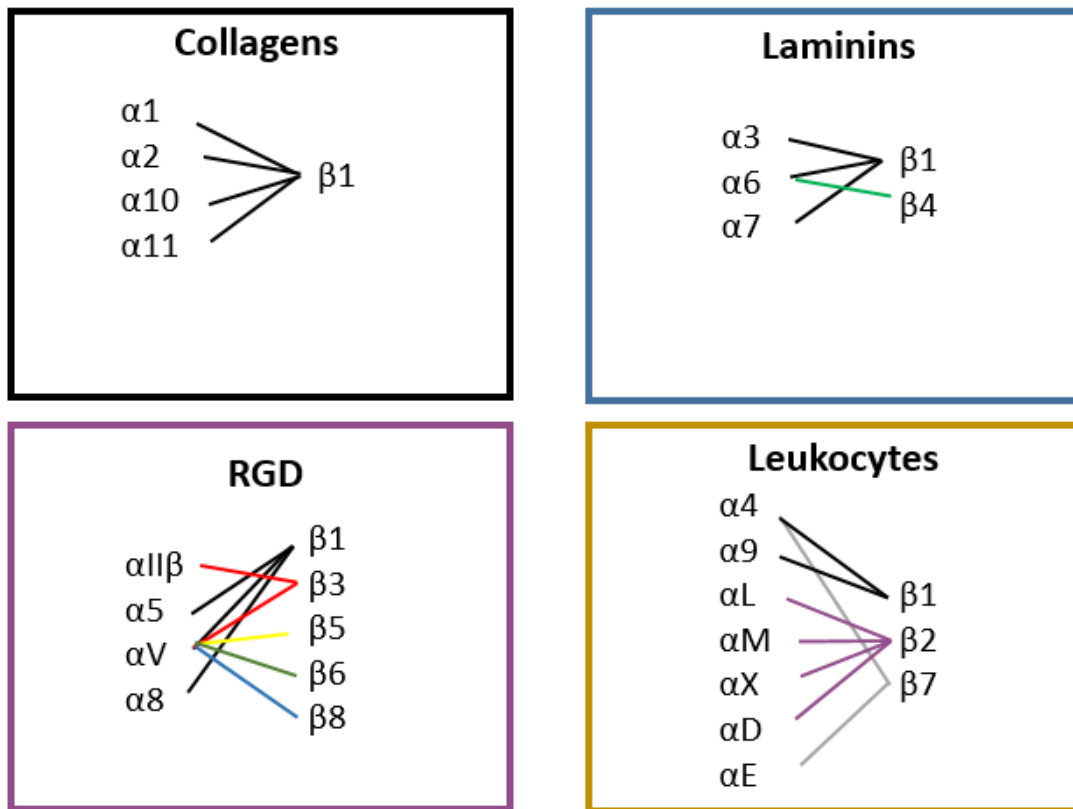


Figure 1.2 The association of α and β integrins and their ligands

The formation of potential $\alpha\beta$ integrin heterodimers is highlighted along with their preferred ligands. As indicated, $\beta 1$ integrin associates with 12 different α integrins allowing it to bind to all four major types of extracellular ligands (collagens, laminins, RGD motif containing proteins such as fibronectin, and leukocytes).

1.6 β 1 integrin and islet development

Development of islets depend on the interactions between cells and the surrounding ECM. During rat pancreatic development, the alpha subunits that commonly associate with β 1 integrin: α 3, α 5, and α 6, all have higher mRNA levels at e18 and p28 compared to day of birth (p0) where there is a marked decrease (Yashpal et al. 2005). β 1 integrin along with α 3 and α 6 protein also significantly increase over the period from p0 to p28 implicating its important role during the maturation and proliferative phase of rat pancreas development (Yashpal et al. 2005). Human fetal islets demonstrate a similar trend, with an increase in α 3 β 1 and α 6 β 1 observed by 16-20 weeks of development (Wang et al. 2005). Previous studies demonstrated that human fetal pancreatic cells migrate and interact with collagen IV matrix protein exclusively through interactions with α 1 β 1 integrin (Kaido et al. 2004a). Similarly, α v β 1 in 19-21 week old human fetal islets has been shown to be essential for spreading and migration on vitronectin, an ECM component expressed by epithelial cells and insulin-expressing cells emerging from the ductal epithelium (Cirulli et al. 2000, Kaido et al. 2004b). In studies examining developing human and rat islets, a significant reduction of islet cell adhesion to the ECM was observed when cells were treated with a functional blocking β 1 integrin antibody (Yashpal et al. 2005, Wang et al. 2005). Recently, Diaferia and colleagues (2013) generated a beta-cell specific β 1 integrin knockout model using Cre recombinase downstream of the rat insulin-1 promoter (RIP β 1KO mice). This model, in which β 1 integrin was knocked out from conception, resulted in a significant reduction in beta-cell mass (18% of that seen in controls) (Diaferia et al. 2013). These results show that the interaction between beta-cells and the ECM surrounding them, as mediated by β 1 integrin, is essential for proper beta-cell proliferation during development and into adulthood.

1.7 β 1 integrin in islet survival and function

A lot of work has been done to elucidate the role of β 1 integrin in islet cell survival and function. Early studies examining isolated canine islets found that they underwent apoptosis due to destruction of the perinsular-basement membrane, but had improved survival when cultured in the presence of collagen I and fibronectin, which are two ECM

ligands of $\beta 1$ integrin (Wang & Rosenberg, 1999). Most work regarding $\beta 1$ in pancreatic islets has been conducted *in vitro*. One of the first studies found that $\alpha 3\beta 1$ represents nearly half of the $\beta 1$ integrins on primary and transformed (RIN-2A line) rat islet cells, and when this interaction is blocked, the islets have reduced attachment and spreading on bovine corneal ECM or ECM produced by A-431 cells (Kantengwa et al. 1997). Similarly, Parnaud (2006) found that blocking the interaction between $\beta 1$ integrin and laminin-5, led to reduced insulin secretion and beta-cell spreading, whereas culturing rat islets on an 804G matrix that is rich in laminin-5 enhanced insulin secretion. Furthermore, the 804G matrix protects beta-cells from apoptosis via activation of the FAK/MAPK/ERK1/2 pathway (Hammer et al. 2004). Although the primary ligand of $\alpha 3\beta 1$ is laminin, it has been shown that it can bind to a series of other matrix proteins including collagen, fibronectin, and laminin, and this is typically found in situations where another primary integrin is absent (Kantengwa et al. 1997). Studies using the insulinoma-1 cell line (INS-1), a beta-cell cancer line that secretes insulin in response to glucose within physiological ranges (Asfari et al. 1992), observed that $\beta 1$ integrin associates with $\alpha 1$ - $\alpha 6$ and αV in these cells, and $\alpha 3\beta 1$ was the most highly expressed (Krishnamurthy et al. 2008). INS-1 cells also showed beneficial effects when cultured on collagen I and IV, whereby increased levels of spreading, survival, proliferation, and FAK activation are observed, and these beneficial effects are negated when $\alpha 3\beta 1$ is blocked (Krishnamurthy et al. 2008). Studies using human fetal islets have found similar results, where interfering with $\beta 1$ integrin either through blockade or siRNA leads to reduced *Insulin* gene expression, increased apoptosis, reduced ECM adhesion, and reduced p-FAK and p-ERK1/2 levels (Wang et al. 2005, Kaido et al. 2004b, Saleem et al. 2009). Examination of rat and human fetal islets also showed that either transfections with siRNA against $\beta 1$ or utilization of a $\beta 1$ immunoneutralizing antibody leads to an increase in apoptosis and a reduction in *Pdx-1* and *Insulin* mRNA (Wang et al. 2005, Yashpal et al. 2005). Important to note is that *Pdx-1* is not only responsible for proper development of the pancreas, it also plays a key role in insulin gene expression in mature beta-cells (Fujimoto and Polonsky, 2009). All of these *in vitro* studies highlight a role for $\beta 1$ integrin in maintaining islet function and survival, however the *in vivo* role of $\beta 1$ integrin has only recently begun to be elucidated.

In more recent years with the advancement of *in vivo* gene knockdown techniques, mouse models have been generated to study the relationship between integrins, the ECM and beta-cells. One study analyzed the role of $\beta 1$ integrin by conditionally removing it in collagen Ia2-producing cells of adult mice using a CreERT-loxP system ($\beta 1$ KO mice) (Riopel et al. 2011). This knockout impacted beta-cells, but also affected a variety of other cell types; this includes pancreatic stellate cells (PaSC), which are fibroblast-like cells that are a major contributor of ECM proteins in the pancreas (Apte et al. 2012). In this model the pancreas became very dissociated, with some islets having no contact with exocrine cells, presumably due to the reduction in collagen fibers and connective tissue that was observed. In addition, $\beta 1$ KO mice developed glucose intolerance while still responding normally to exogenous insulin, indicating that hyperglycemia in mice was due to beta-cell defects (Riopel et al. 2011). The $\beta 1$ KO mice had reduced beta-cell mass due to a decrease in proliferation and an increase in apoptosis, a decrease in islet insulin content and reduced Pdx-1 protein levels. A decrease in FAK/ERK1/2 were also seen in $\beta 1$ KO mice, which corroborates previous *in vitro* studies that imply that $\beta 1$ regulates survival and function of islets through this pathway (Hammer et al. 2004, Krishnamurthy et al. 2008, Saleem 2009). Since the ablation of $\beta 1$ integrin was not specific to beta-cells, it is unclear whether the loss of $\beta 1$ integrin played a direct or indirect role in islet cell function and survival.

As previously mentioned, the RIP $\beta 1$ KO model has been generated for use as a beta-cell specific $\beta 1$ knockout mouse model (Diaferia et al. 2013). However, the knockout is present in beta-cells as soon as the *Insulin* gene is transcribed at the beginning of embryonic development. Despite the significantly reduced beta-cell mass in adult RIP $\beta 1$ KO mice (~18% of that seen in wild-type), islet architecture was unchanged and insulin content was significantly increased in the remaining beta-cell population (Diaferia et al. 2013). These islets lacking $\beta 1$ integrin also secreted significantly more insulin in response to glucose during an IPGTT and resulted in maintenance of normoglycemia. One possible explanation proposed is that $\beta 3$ and $\beta 5$ integrins have crosstalk capabilities that can compensate for $\beta 1$ integrin when it is blocked or genetically ablated (Diaferia et al. 2013). The ability for these integrin subunits to compensate, and the fact that the knockout was induced at conception, leaves ample time during development for this

compensatory response. Although other integrins may have been able to maintain the functional role of beta-cells, this study shows that $\beta 1$ is a key regulator of cellular proliferation in beta-cells. Positive regulators of cell-cycle arrest were up-regulated in RIP $\beta 1$ KO mice, such as *cyclin dependent kinase 1A*, *cyclin dependent kinase 5 regulatory subunit associated protein 1*, and ERK-dependent tumour suppressors (e.g., *deleted in malignant brain tumors 1*). Paralleling these findings was a reduction in cyclin D1, a protein required for progression through the G1 phase of the cell cycle that has been established to be essential in postnatal beta-cell growth (Kushner et al. 2005). The formation of focal-adhesions is the way by which integrins regulate outside-in signalling, and the RIP $\beta 1$ KO model showed a significant decrease in p-ERK1/2 and p-Akt within these islets. The mechanism by which these proteins regulate beta-cells and the specific proteins involved are discussed now.

1.8 Signalling pathways involving $\beta 1$ integrin in islet survival and function

When integrins are activated they interact with the band 4.1, ezrin, radixin and moesin homology (FERM) domain on FAK (Lim et al. 2008), which leads to autophosphorylation of tyrosine residue 397 either through direct interaction with integrins or through the phosphorylation of FAK tyrosine residues 576 and 577 by proto-oncogene tyrosine kinase Src (Schaller 2001). Src can be activated by a variety of tyrosine phosphatases (Brakebusch & Fassler, 2003) and it interacts with the focal adhesion complex through its SH2 domain which binds to FAK autophosphorylation domains, or through its SH3 domain which interacts with paxillin (Clark & Brugge, 1995). The binding of Src leads to recruitment of SH2-SH3 adaptor proteins through further modifications of FAK (Clark & Brugge, 1995), one of which being the phosphorylation of FAK at tyrosine 925 (p-FAK^{Y925}), leading to the subsequent binding of growth factor receptor-bound protein 2 (Grb2) and the Ras guanine nucleotide exchange factor mSOS1 (son of sevenless homolog 1) (Giancotti & Ruoslahti, 1999). This leads to downstream phosphorylation of kinases Ras and rapidly accelerated fibrosarcoma (Raf), which causes activation of the MAPK/ERK1/2 pathway. ERK1/2 can regulate cell proliferation and survival in a variety of ways once activated. ERK1/2 has

been shown to induce NCK5a neuronal CDK5 activator (p35) expression, a known activator of cyclin-dependent kinase 5 (CDK5) (Harada et al. 2001). Together, CDK5 and ERK1/2 can promote cell cycle progression and prevent apoptosis through phosphorylating the anti-apoptotic protein b-cell lymphoma 2 (Bcl2) on residues threonine 56, 74 or serine 84 which promotes the release of apoptotic proteins from the mitochondria (Wang et al. 2006, Stupack & Cheresch, 2002). Additionally, ERK1/2 can prevent caspase-mediated apoptosis by inhibiting caspase 9 activity (Allan et al. 2003). One group of researchers generated a *rat insulin 1* promoter-driven FAK knockout (RIPFAKKO) and found that when beta-cell FAK is diminished, CDK5, ERK1/2 and Bcl2 activity are significantly reduced along with decreased beta-cell mass (Cai et al. 2012). This finding brings together the multitude of studies that have previously shown links between reduced beta-cell survival and decreased FAK/ERK1/2 pathway signalling due to an impairment of normal β 1 function or levels (Hammer et al. 2004, Krishnamurthy et al. 2008, Saleem 2009, Riopel et al. 2011, Diaferia et al. 2013).

As mentioned before, the activation of Src by FAK can lead to the recruitment of SH2-SH3 adaptor proteins, one of which is the p85 subunit of PI3K, which allows for the catalytic activity of phosphatidylinositol-4,5-bisphosphate 3-kinase, catalytic subunit alpha (p110) (Xia et al. 2004). Downstream of PI3K/p110 activation, Akt becomes phosphorylated at serine 473 (p-Akt^{S473}) (McLean et al. 2005, Xia et al. 2004). The activation of Akt^{S473} has been shown to prevent apoptosis in a variety of different manners, like that of ERK1/2 through the regulation of capase-9 and BAD which directly interacts with Bcl2, preventing its anti-apoptotic properties (Song et al. 2005). In addition, reduced p-Akt^{S473} signaling was found in RIP β 1KO mice, which suggests a role in the reduction in beta-cell mass and increased cell death (Cai et al. 2012). The RIPFAKKO model also showed a significant reduction in p-Akt^{S473} which could be playing a similar role in this model regarding cell survival (Cai et al. 2012).

The role of FAK mediated signalling has also been shown to play a role in glucose stimulated insulin secretion through cytoskeletal remodelling (Kalwat & Thurmond 2013, Ronadas et al. 2011, Rondas et al. 2012, Cai et al. 2012). Once activated by FAK phosphorylation, paxillin directly interacts with the cytoskeleton through interactions

with vinculin and actopaxin, and these interactions are partly responsible for actin remodeling through depolymerization (reviewed in Turner 2000). A recent study used MIN6B1 cells (Rondas et al. 2012) to knock down β 1 integrin or FAK and found that glucose-induced disruption of F-actin, which is required for proper granule movement to the plasma membrane, was hindered. Additionally, phosphorylated paxillin at tyrosine 118 (p-paxillin^{Y118}), along with p- ERK1/2 were decreased during glucose stimulation along with the glucose-induced activation of the Akt/AS160 signalling pathway (Rondas et al. 2012). Using rat beta-cells or isolated islets (Rondas et al. 2011) and hindering FAK or paxillin function, similar results were noted along with a reduction in SNARE proteins such as SNAP25 and syntaxin 1. Using the RIPFAKKO mouse model, a reduction in FAK also lead to reduced p-paxillin^{Y118} and colocalization of it with SNAP25 and syntaxin 1 on the plasma membrane was reduced (Cai et al. 2012). These findings highlight the essential role of FAK mediated signalling not only in beta-cell survival but also in mediating insulin exocytosis through cytoskeletal remodeling (**Figure 1.3**)

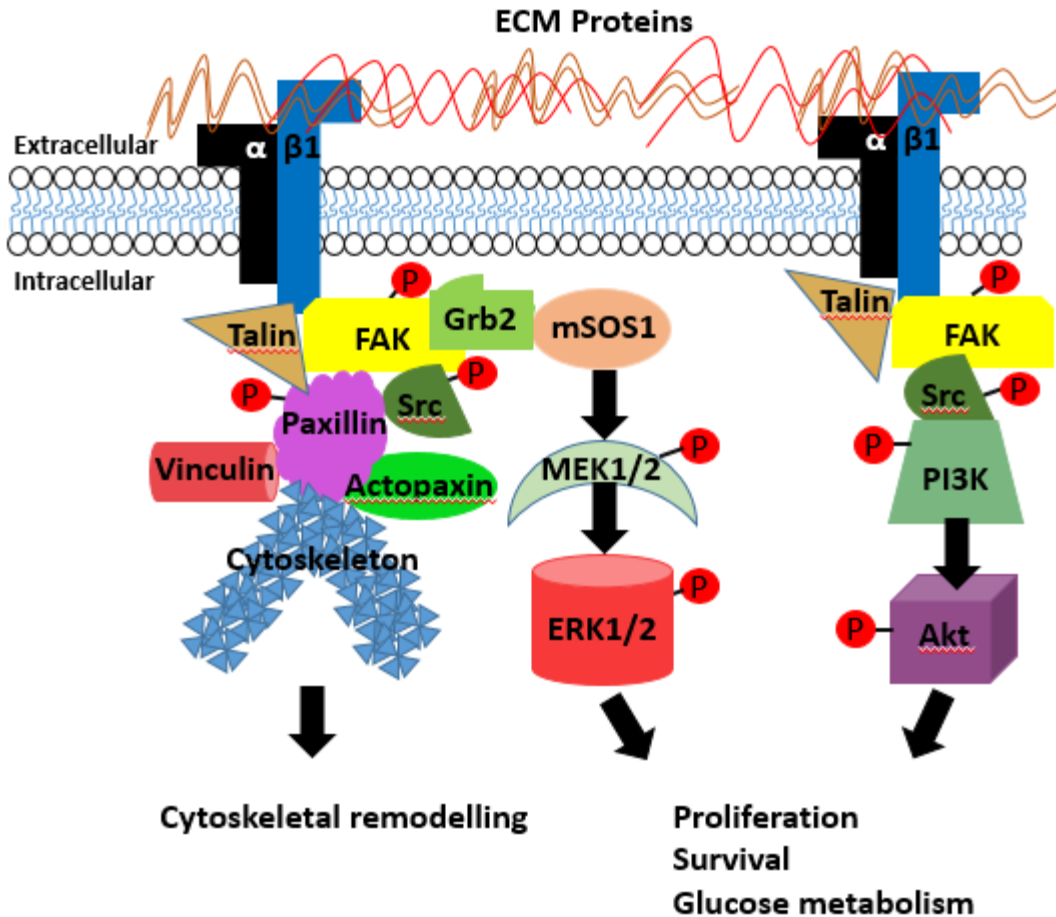


Figure 1.3 $\beta 1$ integrin signalling pathway

Outside-in signalling as mediated by $\beta 1$ integrin is due to the formation of focal adhesion complexes. When focal adhesion kinase (FAK) becomes phosphorylated it leads to the activation of downstream signalling molecules through a kinase cascade resulting in regulation of cell proliferation, survival, differentiation and glucose metabolism. Additionally, the focal adhesion complex is responsible for cytoskeletal remodelling essential for insulin exocytosis.

1.9 Rationale and objectives of the present study

The rationale of this project is to elucidate the role of $\beta 1$ integrin in beta-cells of adult mice without the confounding variables of development (Diaferia et al. 2013) or non-beta cell specificity (Riopel et al. 2011) seen in previous mouse models. A new inducible $\beta 1$ KO model where CreERT is downstream of the *mouse insulin-1 promoter* (MIP) was generated (MIP $\beta 1$ KO) to remove these variables and determine the precise role of $\beta 1$ integrin in beta-cells of adult mice.

Objective

To utilize the MIP $\beta 1$ KO mouse model to elucidate the role of $\beta 1$ integrin specifically in the beta-cells of adult mice.

Hypothesis

Beta-cell specific $\beta 1$ integrin knockout in adult mice will lead to glucose intolerance, impaired beta-cell function, and survival.

Specific Questions

1. Do adult MIP $\beta 1$ KO mice display impaired glucose tolerance and insulin secretion?
2. Are insulin secretory molecules altered in MIP $\beta 1$ KO mice?
3. Does a beta-cell specific knockout of $\beta 1$ integrin in adult mice lead to reduced beta-cell mass and increased beta-cell death?
4. Are there alterations in transcription factor expression in MIP $\beta 1$ KO mice?
5. Does a beta-cell specific knockout of $\beta 1$ integrin in adult mice affect islet vascularization?
6. Are associated intracellular signaling pathways affected in MIP $\beta 1$ KO islets?
7. Does α integrin expression change in MIP $\beta 1$ KO mice?
8. Do aged MIP $\beta 1$ KO mice recover from the initial knockout of $\beta 1$ integrin?

Chapter 2 – Materials and Methods

2.1 Generation of the beta-cell $\beta 1$ integrin knockout mouse model

The *mouse insulin 1 promoter*-driven Cre recombinase mouse line (*MIP-CreER*) was a gift from Dr. Louis Philipson's laboratory (University of Chicago, Chicago, IL, USA) (Tamarina et al. 2014). To verify the specificity of the *CreER* transgene, *MIP-CreER* mice were crossed with *B6;129S6-Gt(ROSA)26Sor^{tm9(CAG-tdTomato)Hze/J}* mice (Jackson Laboratory, Stock # 007905). Cre expression in the *MIP-CreER* mice excised the *LoxP-stop-LoxP* signal 5' to the *tdTomato* gene and activated expression of the red fluorescence reporter protein exclusively in beta-cells of isolated islets (Trinder et al. 2016). To generate the beta-cell specific $\beta 1$ integrin knockout (MIP $\beta 1$ KO) mouse line, C57Bl/6 mice with a *LoxP* floxed $\beta 1$ integrin gene (*B6;129-Itgb1^{tm1Efu/J}*), obtained from Jackson Laboratory (Stock #004605) were crossed with *MIP-CreER* mice within our vivarium (Victoria Research Laboratories, Victoria Hospital, London, ON, CA), producing *MIP-CreER^{+/-}; $\beta 1$ itg^{fl/+}* mice. The *MIP-CreER^{+/-}; $\beta 1$ itg^{fl/+}* mice were subsequently mated to generate the tamoxifen inducible $\beta 1$ integrin knockout experimental mouse model **MIP $\beta 1$ KO** (*MIP-CreER⁺; $\beta 1$ itg^{fl/f}*) and **control** mice (*MIP-CreER⁻; $\beta 1$ itg^{fl/fl}* and *MIP-CreER⁺; $\beta 1$ itg^{+/+}*) (**Figure 2. 1**). All protocols were approved by the Animal Use Subcommittee at the University of Western Ontario in accordance with the guidelines of the Canadian Council of Animal Care (**Appendix A**).

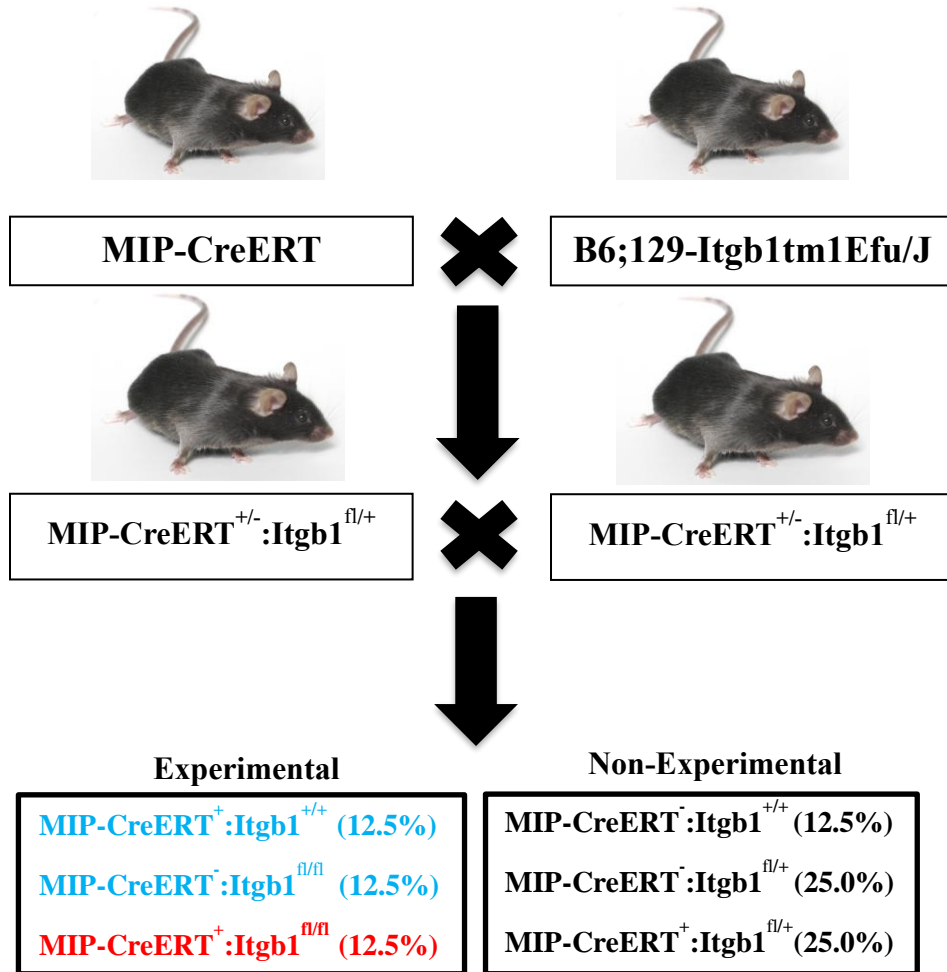


Figure 2.1 Breeding schematic for generation of MIPβ1KO mice

Heterozygote mice obtained from the initial crossing of *MIP-CreERT* mice with *B6;129-Itgb1tm1Efu/J* mice lead to six different potential phenotypic combinations. The experimental mice that were used were the control mice (MIP-CreERT⁺;Itgb1^{+/+} and MIP-CreERT⁻;Itgb1^{fl/fl}, blue) and MIPβ1KO mice (MIP-CreERT⁺;Itgb1^{fl/fl}, red). Percentages of the likelihood of any given genotype are listed.

2.2 Mouse genotyping

For genotyping, approximately 1-3mm of tail from each mouse was collected at weaning, then dissolved and heated in 50 μ L base solution (25 mM NaOH; 0.2 mM EDTA) at 95°C for 30 minutes, and allowed to cool to room temperature for 1 hour. Subsequently, 50 μ L of Tris-HCl (pH 5.5) was then added to neutralize each sample and were centrifuged at 15000 x g for 1 minute. Polymerase chain reactions (PCR) were used to confirm the genotype using the following primers: *MIP* (5'-CCT GGC GAT CCC TGA ACA TGT CCT-3') and *CreERT* (5'-TGG ACT ATA AAG CTG GTG GGC AT-3'), whereas β *litg*^{fl/fl} was detected using *oIMR1906* (5'-CGG CTC AAA GCA GAG TGT CAG TC-3') and *oIMR1907* (5'-CCA CAA CTT TCC CAG TTA GCT CTC-3'). A 2% agarose gel with ethidium bromide was used to verify the PCR amplicons. The gels were run at 80 V for 90 minutes and imaged using the Gene Genius Bio Imaging System (SynGene, Frederick, MD, USA) along with GeneSnap 7.12 software (SynGene). *MIPCreERT*⁺ mice were identified by the corresponding *MIPCreERT* DNA fragment at 268 base pairs (BP) (**Figure 2.2A**), while β *litg*^{+/+} and β *litg*^{fl/fl} mice produced a single DNA fragment size of either 160bp or 280bp, respectively (**Figure 2.2B**).

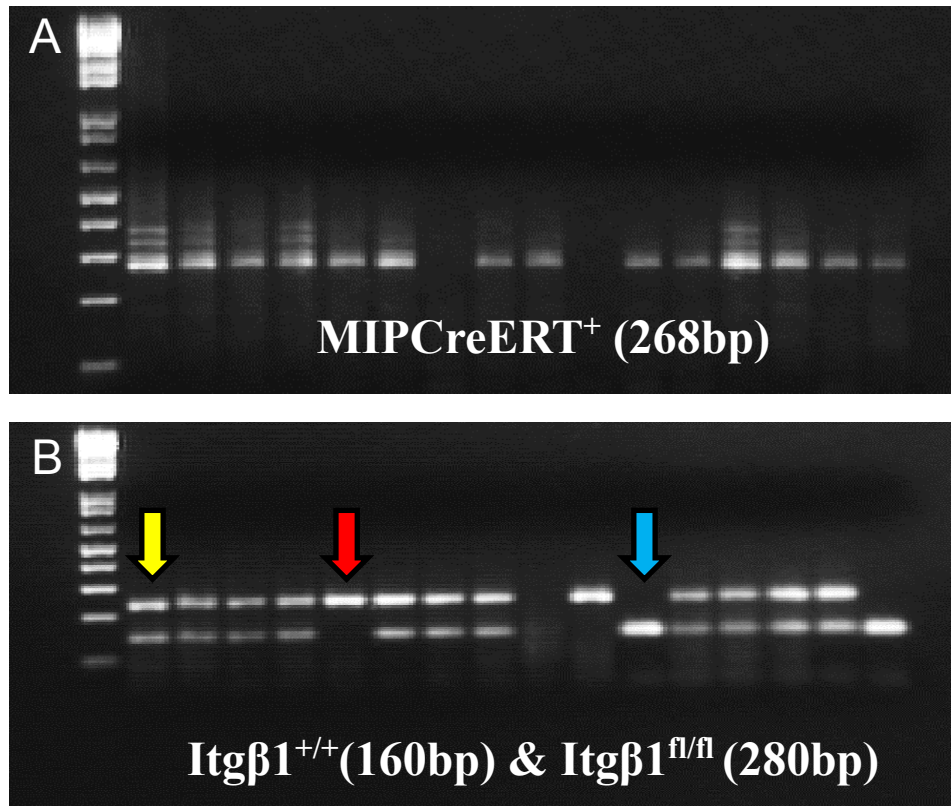


Figure 2.2 Representative PCR images for mouse genotyping

A) MIPCreERT⁺ positive mice are indicated by one distinct band located at 268bp. **B)** Itgβ1 mice are either heterozygous for the wildtype and mutant alleles and display two bands at 160bp and 280bp (Itgβ1^{+/fl}, yellow arrow), homozygous for the wildtype alleles at 160bp (Itgβ1^{+/+}, blue arrow) or homozygous for the mutant alleles at 280bp (Itgβ1^{fl/fl}, red arrow).

2.3 Tamoxifen preparation and administration

Tamoxifen (Sigma-Aldrich, St. Louis, MO, USA) was dissolved in 100% ethanol to a final concentration of 300 mg/mL. The sample was heated at 60°C and vortexed until the tamoxifen was completely dissolved. For injections, the ethanol-suspended tamoxifen was diluted in corn oil (Sigma-Aldrich, St. Louis, MO, USA) to a final concentration of 30 mg/mL. Mice were injected intraperitoneally (I.P.) at 3-4 weeks of age for three consecutive days at a dosage of 4 mg per 20 g of body weight (BW).

2.4 Glucose metabolism studies

An intraperitoneal glucose tolerance test (IPGTT) was conducted at 4, 8, 16 (females only), or 25-35 weeks post-tamoxifen injection in MIP β 1KO and control mice to measure the response of mice to high glucose levels. For the IPGTT, glucose (D-(+)-glucose; dextrose; Sigma-Aldrich, St. Louis, MO, USA) was administered intraperitoneally at a dose of 2 mg/g of BW after a 16 hour overnight fast, and blood glucose levels were measured at 0, 15, 30, 60, 90, and 120 minutes post injection (as reported in Riopel et al. 2011). Area under the curve (AUC) was used to quantify glucose responsiveness using units of ([mmol/L x minute]) (Allison et al. 1995, Krishnamurthy et al. 2007).

Glucose-stimulated insulin secretion (GSIS) was performed at 8 weeks (males) or 16 weeks (females) post-tamoxifen, following an overnight fast of 16 hours. Plasma blood samples via tail vein were collected at 0 minutes before an IP glucose injection (2 mg/g BW), and at 5 and 35 minutes after glucose loading (Riopel et al. 2011). The blood samples were centrifuged for 20 minutes at 15871 x g at 4°C and plasma was stored at -20°C.

An intraperitoneal insulin tolerance test (IPITT) was conducted at 8 weeks (male) and 16 weeks (female) in MIP β 1KO and control mice to insulin sensitivity. Following a 4 hour fast (starting at 9AM), 1 U/kg BW of human insulin (Humalin, Eli Lilly, Toronto, Ontario, Canada) was administered via IP injection, and blood glucose levels were measured at 0, 15, 30, 60, 90, and 120 minutes post injection (Riopel et al. 2011). Data

was expressed as the percent change from basal blood glucose levels and AUC was used for quantification [(mmol/L x minute)] (Allison et al. 1995, Krisnamurthy et al. 2007, Feng et al. 2013).

2.5 Islet isolation

Islets from both MIP β 1KO and control mice at 8 weeks and 16-week post-tamoxifen injection were isolated using the following methodology: the common bile duct was sutured closed via surgical string in close proximity to the duodenum and 3 mL of collagenase V (1 mg/mL, Sigma-Aldrich, St. Louis, MO, USA) was injected via bile duct to perfuse the pancreas. The pancreas was then dissociated in a 15 mL falcon tube with 3 mL dissociation buffer (Hank's balanced salt solution with HEPES) and incubated in a 37°C hot water bath for 30 minutes. Islet purification was performed using a Ficoll gradient as previously described (Wang et al. 2004), and processed for RNA or protein extraction as well as for *ex vivo* GSIS.

2.6 *Ex vivo* GSIS

For *ex vivo* GSIS, duplicate samples with 10 islets per experimental group were hand-picked and incubated in RPMI 1640 (11% glucose) overnight for recovery culture. The overnight culture media was collected for basal insulin secretion levels. Islets were washed in glucose-free media and incubated in the following manner: a low glucose media (2.2 mM) for 1 hour, then in a high glucose solution (22 mM) for 1 hour, and a final 1 hour incubation in an additional low glucose media (2.2 mM) (Feng et al. 2012). The media from each incubation stage was collected and stored at -20°C, and islets were washed and stored in PBS at -20°C. Insulin secretion and content were measured using the Mouse Ultrasensitive Insulin Enzyme Linked Immunosorbent Assay (ELISA) kit (ALPCO, Salem, NH, USA).

2.7 Insulin ELISA

Islet insulin secretion and content was measured using a mouse ultrasensitive insulin ELISA kit (ALPCO, Salem, NH, USA) with a sensitivity of 0.15 ng/mL, according to the manufacturer's instructions. Insulin release was expressed as ng/mL. A static glucose

stimulation index in isolated islets was calculated by dividing the insulin output from the high glucose (22 mM) incubation by the insulin output during the low glucose (2.2 mM) incubation.

2.8 Tissue processing and immunohistological analyses

Mice were sacrificed at 8 weeks (male) or 16 weeks (female) post-tamoxifen, or at 25-35 weeks post-tamoxifen for aged cohorts, and their pancreata were fixed in 4% paraformaldehyde overnight at 4°C (Fisher Scientific Company, Ottawa, ON, Canada). Tissue was washed in phosphate buffered saline (PBS) and subjected to a series of dehydration steps (70%-100% ethanol), toluene, and paraffin wax (Fisher Scientific Company, Ottawa, ON, Canada) using the Shandon Citadel™ Tissue Processor 1000 (Thermo Electron Corporation, Waltham, MA, USA). Embedded tissue was cut into 3 µm thick sections using the Leica RM2245 microtome (Leica Biosystems, Concord, ON, Canada) and placed on a heat plate at 37°C overnight.

For immunofluorescence staining, slides were deparaffinized and rehydrated starting with three separate xylene washes and a series of ethanol (100% to 70%) solutions, and finally washed in PBS. To recover epitopes masked during paraformaldehyde fixation, slides were placed in a sodium citrate antigen retrieval solution (pH 6.0) (Bouwens et al. 1997) and heated in a microwave for 20 minutes. A 10% normal goat serum solution (Invitrogen, Frederick, MD, USA) was applied for 30 minutes at room temperature to prevent non-specific antibody binding. Primary antibodies were applied using the manufacturers' recommended dilutions listed in **Table 2.1**, and incubated overnight at 4°C. Secondary antibodies were used at a 1:50 dilution as follows: fluorescein isothiocyanate (FITC anti-mouse, anti-rat, or anti-rabbit) or TexRed (anti-mouse, anti-rat, or anti-rabbit) (Jackson ImmunoResearch, West Grove, PA, USA). Nuclei were stained with DAPI (4',6-diamidino-2-phenylindole) (Sigma-Aldrich, St. Louis, MO, USA) at a dilution of 1:1000 (coverslips were subsequently secured and the slides were stored at -20°C away from light exposure. Images were obtained using the Leica DMIRE2 fluorescence microscope (Improvision, Lexington, MA, USA) and quantified using Image-Pro software (MediaCybernetics, Rockville, MD, USA).

Immunohistochemical staining was conducted for detection of the transcription factor MafA. The rehydration and blocking steps were the same as previously mentioned. For secondary antibody application, streptavidin-biotin horseradish peroxidase complex and aminoethyl carbazole substrate kit was used (Invitrogen, Frederick, MD, USA) after incubation with the primary antibody. The slides were counter-stained using Hematoxylin (Thermo Scientific, Burlington, ON, Canada). Images were obtained with the Leica upright light microscope (Improvision, Lexington, MA, USA) and quantified using Image-Pro software (MediaCybernetics Rockville, MD, USA).

An islet was defined as any cluster of 3 or more insulin⁺ cells with at least one non-beta cell. Islet density (islet number per mm²) was obtained by measuring all islets on the pancreatic sections and dividing that number by the total pancreas area. Islet size was calculated by measuring all islets' area (μm²) per tissue section and then sorted into subgroups based on size, with data being expressed as a percentage of total islet number. Alpha and beta-cell mass was determined by manually tracing the glucagon⁺ or insulin⁺ area and pancreatic section area, and the data was calculated as follows: alpha-cell mass (mg) = (glucagon⁺ area x pancreas mass)/pancreas area; beta-cell mass (mg) = (insulin⁺ area x pancreas mass)/pancreas area, as previously described (Wang et al. 1994).

Quantification of beta-cell nuclear proteins was conducted using double immunofluorescence staining for Ki67, Pdx-1, Nkx6.1, Nkx2.2 or Isl-1 with insulin. A total of 10 random islets were selected per sample and analyzed using Image-Pro software (MediaCybernetics). Insulin⁺ cells that co-stained with a nuclear transcription factor (TF) were quantified and expressed as a percentage of double positive labelling cells divided by the total number of insulin⁺ cells.

Platelet endothelial cell adhesion molecule (PECAM) was used as a co-stain with insulin to identify vasculature in islets. For analyses, 10 random islets were selected and their capillaries and total islet size was manually traced. Islet capillary area was measured by taking the combined area of all capillaries within an islet and dividing it by the total islet area, and was expressed as a percentage. The average islet capillary diameter was measured

as the total diameter of all islet capillaries divided by the total number of capillaries and expressed as a mean (μm^2) (Feng et al. 2015).

Table 2.1 Primary antibodies used for immunostaining and Western Blots

Primary Antibodies		Dilution	Company
Anti-Akt	Rabbit polyclonal	1:3000*	Cell Signaling (Temecula, CA, USA)
Anti-Cyclin D1	Mouse monoclonal	1:2000*	Cell Signaling (Temecula, CA, USA)
Anti-E-Cadherin	Rabbit polyclonal	1:200	Cell Signaling (Temecula, CA, USA)
Anti-ERK	Rabbit polyclonal	1:3000*	Cell Signaling (Temecula, CA, USA)
Anti-FAK	Rabbit polyclonal	1:1000*	Cell Signaling (Temecula, CA, USA)
Anti-Glucagon	Rabbit polyclonal	1:800	Sigma-Aldrich (St Louis, MO, USA)
Anti-Glut2	Rabbit polyclonal	1:200	Abcam (Cambridge, MA, USA)
Anti-Insulin	Mouse monoclonal	1:800	Sigma-Aldrich (St Louis, MO, USA)
Anti-Insulin	Rabbit polyclonal	1:50	Santa Cruz (Santa Cruz, CA, USA)
Anti-Integrin α 3	Rabbit polyclonal	1:50	Chemicon (Temecula, CA, USA)
Anti-Integrin α 5	Rabbit polyclonal	1:50	Chemicon (Temecula, CA, USA)
Anti-Integrin α 6	Rabbit polyclonal	1:50	Santa Cruz (Santa Cruz, CA, USA)
Anti-Integrin α V	Rabbit polyclonal	1:100	Abcam (Cambridge, MA, USA)
Anti-Integrin β 1	Rabbit polyclonal	1:500*	Abcam (Cambridge, MA, USA)
Anti-Integrin β 1	Rat monoclonal	1:100	Milipore (Etobicoke, ON, CA)
Anti-Islet1	Mouse monoclonal	1:100	DSHB (Iowa City, IA, USA)
Anti-Ki67	Rabbit polyclonal	1:100	Abcam (Cambridge, MA, USA)
Anti-MafA	Rabbit polyclonal	1:100	Bethyl Laboratory (Montgomery, TX, USA)
Anti-Munc18-1	Rabbit polyclonal	1:100	Abcam (Cambridge, MA, USA)

Anti-Nkx2.2	Mouse monoclonal	1:100	DSHB (Iowa City, IA, USA)
Anti-Nkx6.1	Mouse monoclonal	1:100	DSHB (Iowa City, IA, USA)
Anti-PARP	Rabbit polyclonal	1:1000*	Cell Signaling (Temecula, CA, USA)
Anti-Pdx-1	Rabbit polyclonal	1:800 1:2000*	Dr. Wright (University of Vanderbilt, Nashville, TN, USA)
Anti-PECAM	Rabbit polyclonal	1:200	Santa Cruz (Santa Cruz, CA, USA)
Anti-phospho-Akt (Ser473)	Mouse monoclonal	1:2000*	Cell Signaling (Temecula, CA, USA)
Anti-phospho- Cleaved PARP	Rabbit polyclonal	1:1000*	Abcam (Cambridge, MA, USA)
Anti-phospho-ERK (Thr202/Tyr204)	Rabbit polyclonal	1:3000*	Cell Signaling (Temecula, CA, USA)
Anti-phospho-FAK (Tyr397)	Rabbit polyclonal	1:2000*	Cell Signaling (Temecula, CA, USA)
Anti-SNAP25	Mouse monoclonal	1:50	Santa Cruz (Santa Cruz, CA, USA)
Anti-Syntaxin 1A	Mouse monoclonal	1:50	Santa Cruz (Santa Cruz, CA, USA)
Anti-VAMP2	Rabbit polyclonal	1:200	Abcam (Cambridge, MA, USA)
Anti- β -actin	Mouse monoclonal	1:5000*	Sigma-Aldrich (St Louis, MO, USA)

* Indicates dilution factor used when conducting a western blot. DSHB stands for Developmental Studies Hybridoma Bank at the University of Iowa.

2.9 RNA extraction

RNA was extracted from isolated mouse islets via the RNAqueous-4 PCR Kit as per the manufacturer's instructions (Ambion, Austin, TX, USA). Cell lysate was then vortexed intermittently and washed with 64% ethanol (Life Technologies, Carlsbad, CA, USA). A collection filter was used to isolate RNA (Life Technologies, Carlsbad, CA, USA), and heated elution solution (Life Technologies, Carlsbad, CA, USA) was applied to collect the RNA from the filter. DNA contamination was eliminated by DNase treatment (Life Technology, Carlsbad, CA, USA). The concentration of RNA was measured using a Multiskan Spectrometer (Thermo Scientific, Burlington, ON, Canada), and only samples with a concentration greater than 0.1 $\mu\text{g}/\mu\text{L}$ were used. RNA quality was confirmed by observation of a 28S and 18S band when run on a 1% agaroses ethidium bromide infused gel.

2.10 qRT-PCR quantification

Quantitative real-time reverse transcriptase PCR (qRT-PCR) was conducted with 0.1 μg of cDNA using the iQ SYBR Green Supermix kit (Bio-Rad Laboratories, Mississauga, ON, Canada), along with 0.5 μL forward and reverse primers (**Table 2.2**). To verify primer specific amplification, the reactions were performed by omitting reverse transcriptase (RT-), cDNA, or DNA polymerase and no reaction bands were observed. Reactions were run using the Bio-Rad CFX Connect™ real-time PCR detection system (Bio-Rad Laboratories, Mississauga, ON, Canada) and analyzed using CFX Manager software (Bio-Rad Laboratories). Relative mRNA levels were calculated using the $2^{-\Delta\Delta\text{CT}}$ method, where ΔCT is the difference between the threshold cycle of a given cDNA transcript and the internal standard gene 18S rRNA subunit cDNA (Schmittgen et al. 2008). The derivative melting curves were analyzed to assess amplification specificity of the target gene sequence (**Figure. 2.3**).

Table 2.2 Sequences of primers used in qRT-PCR

Primer	Accession Definition	Sequence 5'-3' (Sense/Antisense)	Fragment Size (bp)	Annealing Temp (°C)
Glucagon	NM_008100.4	GAT CAT TCC CAG CTT CCC AG CGG TTC CTC TTG GTG TTC AT	163	56.5
Ins1&2	NM_008386.3 NM_008387.4	GGC TTC TTC TAC ACA CCC A CAG TAG TTC TCC AGC TGG TA	182	53.9
Itga3 (α 3)	NM_013565.2	GCC ATC CGC CCT GCT ACT GT AGT ACG GGC TGC AAG TTG TCC	219	60.9
Itga5 (α 5)	NM_010577.3	GGC ACC CAA GGC TAA CAC TA CGA ACT GTT GCT CCG AAC CA	204	57.7
Itga6 (α 6)	NM_008397.3	TGG CTT CCT CGT TTG GCT ATG GAA TCG GCT TCA CAT TAC TC	168	54.2
ItgaV (α V)	NM_008402.2	ACC TGG ACG TCG AAA GTC CC CCG GCG GCT GGA TGA GCA TT	194	59.4
Itgb1 (β 1)	NM_010578.2	GGC AAC AAT GAA GCT ATC GTG TTC GGA TTG ACC ACA GTT GTC	257	55.1
Pdx1	NM_008814.3	CCA CCC CAG TTT ACA AGC TCG GTA GGC AGT ACG GGT CCT CT	324	57.5
Snap25	NM_011428.3	GGC TTC ATC CGC AGG GTA AC CTG GCG ATT CTG GGT GTC AAT	138	58.9

Syntaxin1A	NM_016801.3	AAG GAC AGC GAT GAC GAC GAC TTC GGC AAT CTT GTC AAT AA	114	55.5
Syntaxin3	NM_001025307.1	GTC GGC ACA AGG ACA TCG TA TGT TCT CAA TGC GGT CAA TCA	117	56.5
Vamp2	NM_009497.3	GAG CGG GAC CAG AAG TTG TC TCC ACC AGT ATT TGC GCT TG	109	57.8
18S	NR_003278.3	GTA ACC CGT TGA ACC CCA TTC CCA TCC AAT CGG TAG TAG CG	151	55.6

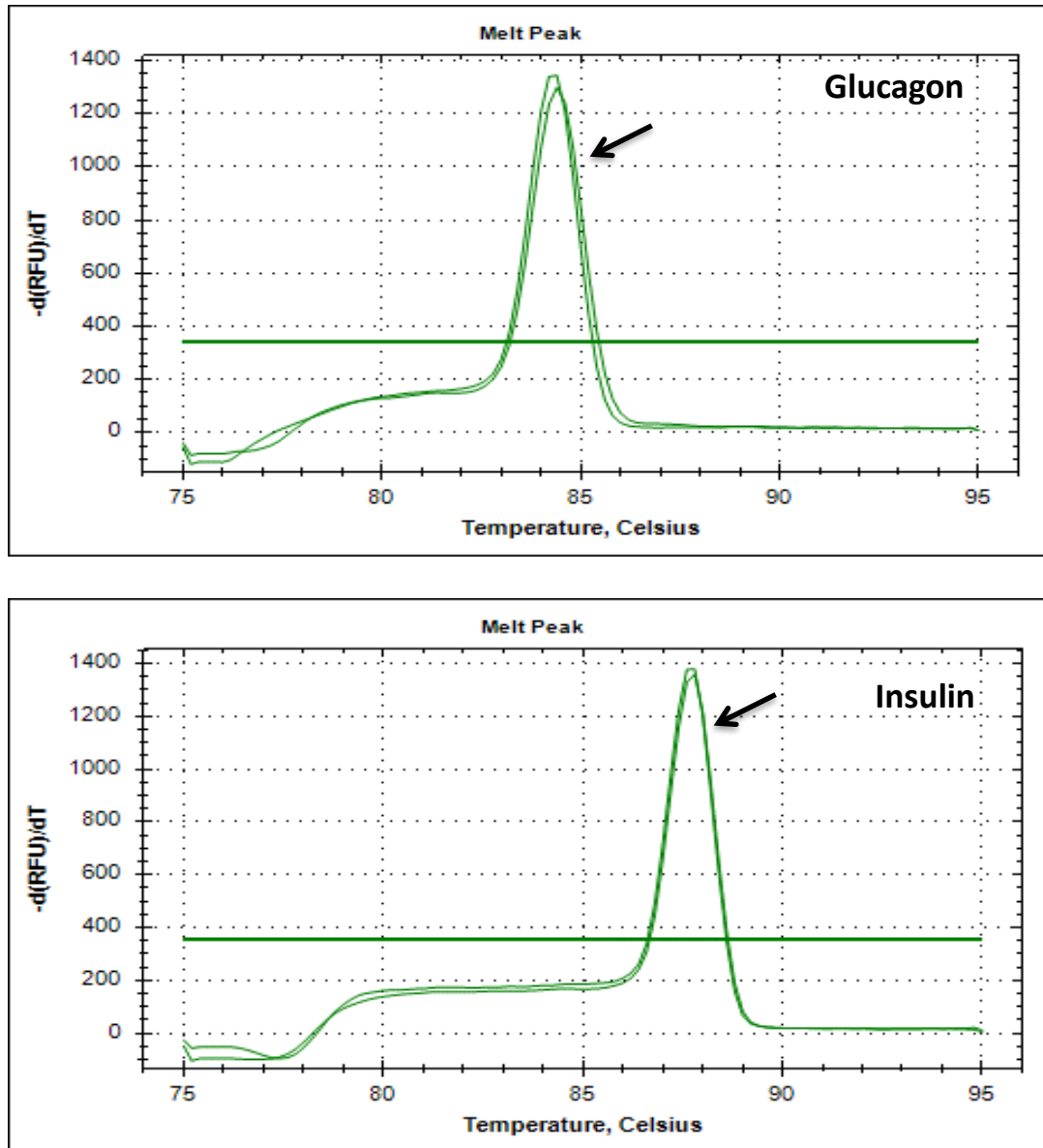


Figure 2.3. The derivative melting curves of qRT-PCR products.

The derivative melting curves (arrows) of glucagon and insulin show that qRT-PCR assays have amplified specific target sequences.

2.11 Reverse transcription and cDNA synthesis

Oligo-(dT) (500 µg/ml), DEPC, and random hexamers (3000 ng/mL) were added to the RNA and heated for 5 minutes at 60°C and then cooled down to 4°C for 5 minutes using the GeneAmp PCR System 2400 (Applied Biosystems INC., Foster City, CA, USA). Afterwards, 4 µL of 5x buffer, 2 µL of DTT, 2 µL of 10 mM dNTPs and 0.5 µL of RNAsin was mixed together and added to the RNA sample. The GeneAmp PCR System (Applied Biosystems) was used to heat samples in the following order: 42°C for 90 minutes, 94°C for 5 minutes, and 4°C for 60 minutes. SuperScript® II Reverse Transcriptase (200 units) (Invitrogen) was added with the samples at 42°C and a final concentration of 6 µg/ 8 µL was obtained by dilution with sterile H₂O and stored at -20°C. Samples omitting SuperScript® II Reverse Transcriptase were used as negative controls.

2.12 Protein extraction and western blot analyses

Isolated islets were lysed in Nonident-P40 lysis buffer (Nonident-P40, phenylmethylsulfonyl fluoride, sodium orthovanadate) (Sigma-Aldrich, St. Louis, MO, USA) and a cOmplete™ protease-inhibitor cocktail tablet (Roche Applied Science, Quebec City, QC, Canada) using a sonicator, and then placed on ice for 30 minutes afterwards and spun down at 15871 x g for 20 minutes at 4°C before storage at -80°C (Rioped et al. 2011). A Bradford protein assay was conducted using the Bio-Rad dye reagent (Bio-Rad Laboratories, Mississauga, ON, Canada). Bovine serum albumin (BSA) standard concentrations at 0, 0.05, 0.1, 0.2, 0.3, 0.4, and 0.5 mg/mL were used for the standard curve. 10 µL of each standard and 1 µL of sample (added to 9 µL of sterile H₂O) was pipetted onto a micro titer plate in duplicate. Once the dye was added to the samples, they were placed on a shaker for 20 minutes at room temperature. A Multiskan Spectrum spectrophotometer (Thermo Scientific, Burlington, ON, Canada) was used to read the optical density values at 595 nm.

Protein was loaded at a concentration ranging from 15-20 µg into either a 7.5%, 10%, or 12.5% sodium dodecyl sulphate-polyacrylamide (SDS-PAGE) resolving gel.

Electrophoresis was conducted at a rate of 40 V as it ran through the 4% stacking gel, and 80 V for the remaining duration required to run to the bottom of the resolving gel. Nitrocellulose membranes (Bio-Rad Laboratories, Mississauga, ON, Canada) were used for protein transfer. The transfer was conducted at 250 mA for 150 minutes in an ice encased chamber containing transfer buffer (195 mM glycine, 25 mM Tris, and methanol at a volume of 20%). Membranes were treated with Ponceau S for approximately 1 minute, whereas gels were treated with Coomassie Blue for 30 minutes at room temperature to subjectively assess overall protein transfer. Membranes were then washed in Tris-buffered saline containing 0.1% Tween-20 (Zymed Laboratories, San Fran, CA, USA) to remove the Ponceau S. Blocking buffer was applied to the membranes for 30 minutes at room temperature (5% non-fat dairy milk, containing 2.5 mL 1x TBST and 50 μ L NP-40 (Zymed Laboratories)). Primary antibodies (**Table 2.1**) were applied for 2 hours at room temperature, or overnight at 4°C, and the membranes were washed 3 times for 10 minutes in 1x TBST wash buffer prior to incubation with secondary antibodies. Anti-rabbit or anti-mouse horseradish peroxidase-conjugated secondary antibodies were applied for 1 hour at room temperature (Cell Signaling Temecula, CA, USA). Proteins were detected using ECL™-Plus Western Blot detecting reagents (Perkin-Elmer, Wellesley, MA, USA) and imaged using the Versadoc Imaging System (Bio-Rad Laboratories). Image Lab (Bio-Rad Laboratories) was used to quantify the bands using densitometry and data were normalized to appropriate loading controls (e.g., β -Actin).

2.13 Statistical analyses

Data are expressed as means \pm SEM. Statistical significance was determined using an unpaired student's *t*-test (GraphPad software; La Jolla, CA, USA). Differences were considered statistically significant when $p < 0.05$.

Chapter 3 - Results

3.1 Characterization of $\beta 1$ integrin expression in beta-cells of MIP $\beta 1$ KO mice

To confirm and quantify the knockdown of $\beta 1$ integrin in MIP $\beta 1$ KO mice, both mRNA and protein from isolated islets were analyzed. qRT-PCR analysis showed a significant reduction of $\beta 1$ integrin mRNA ($p < 0.01$ vs. control, **Figure 3.1A**) and protein level ($p < 0.01$, **Figure 3.1B**) of approximately 60% in the male MIP $\beta 1$ KO islets compared to controls at 8 weeks post-tamoxifen. Immunofluorescence staining was used to qualitatively examine $\beta 1$ integrin knockdown and showed a reduction of $\beta 1$ integrin in the islets of MIP $\beta 1$ KO mice compared to control mice (**Figure 3.1C**). However, the reduction of *$\beta 1$ integrin* mRNA in isolated female MIP $\beta 1$ KO islets at 16 weeks post-tamoxifen showed no statistical significance due to high variability among the samples (**Figure 3.2A**). Both western blot and immunofluorescence staining showed slightly reduced levels of $\beta 1$ integrin protein in the islets of female MIP $\beta 1$ KO mice compared to controls (**Figure 3.2B,C**).

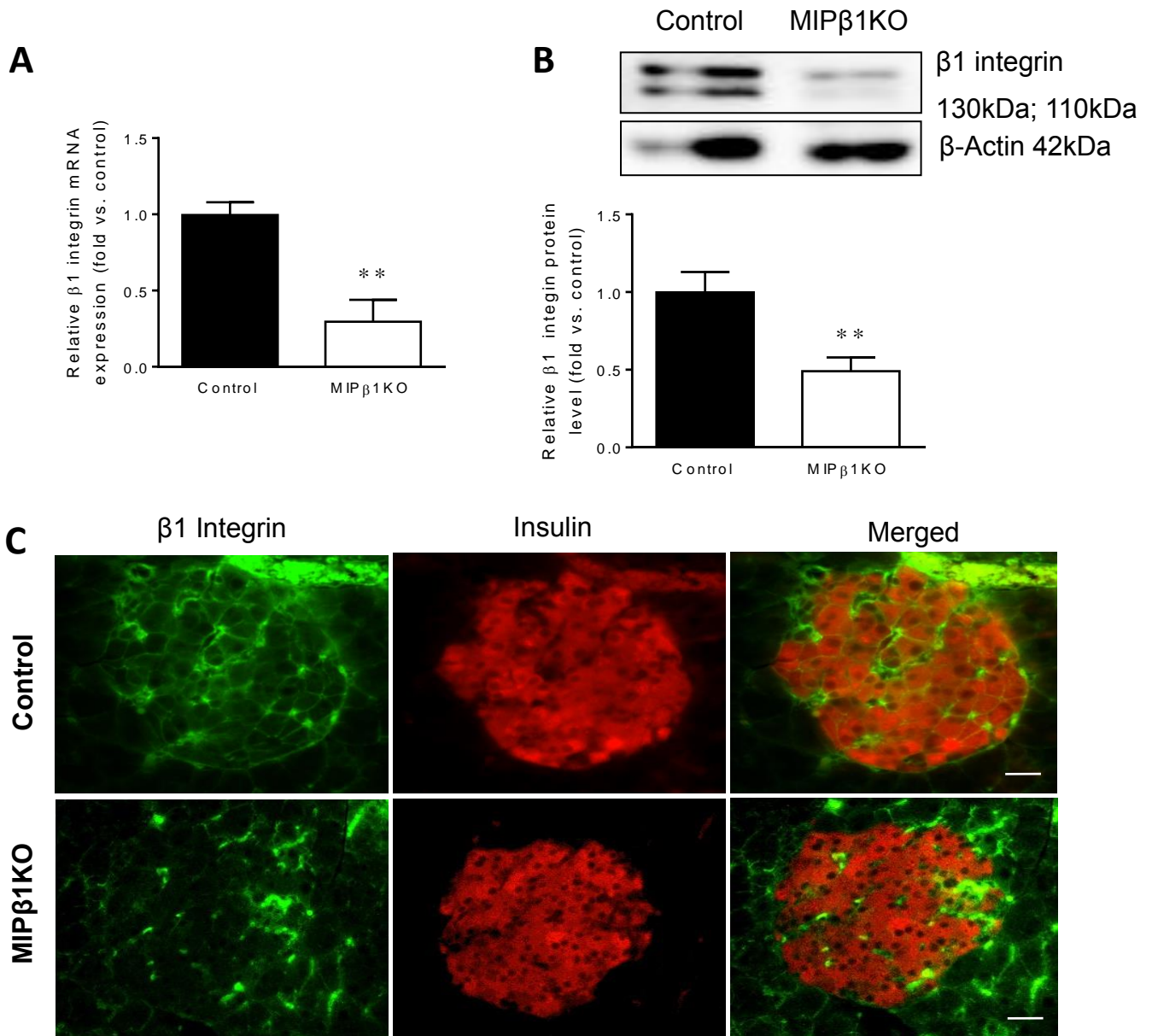


Figure 3.1 Confirmation of $\beta 1$ integrin knockdown in 8 weeks post-tamoxifen male MIP $\beta 1$ KO mice

A) qRT-PCR for *$\beta 1$ integrin* mRNA and **B)** western blot analysis for $\beta 1$ integrin protein in control and MIP $\beta 1$ KO islets, with a representative blot shown. **C)** Representative double immunofluorescence staining for $\beta 1$ integrin (green) and insulin (red) in the islets of control and MIP $\beta 1$ KO mice. Scale bar: 25 μm . Black bars: control, white bars: MIP $\beta 1$ KO group. Data are expressed as mean \pm SEM ($n = 3-5/\text{group}$) $^{***}p < 0.01$ vs. control group.

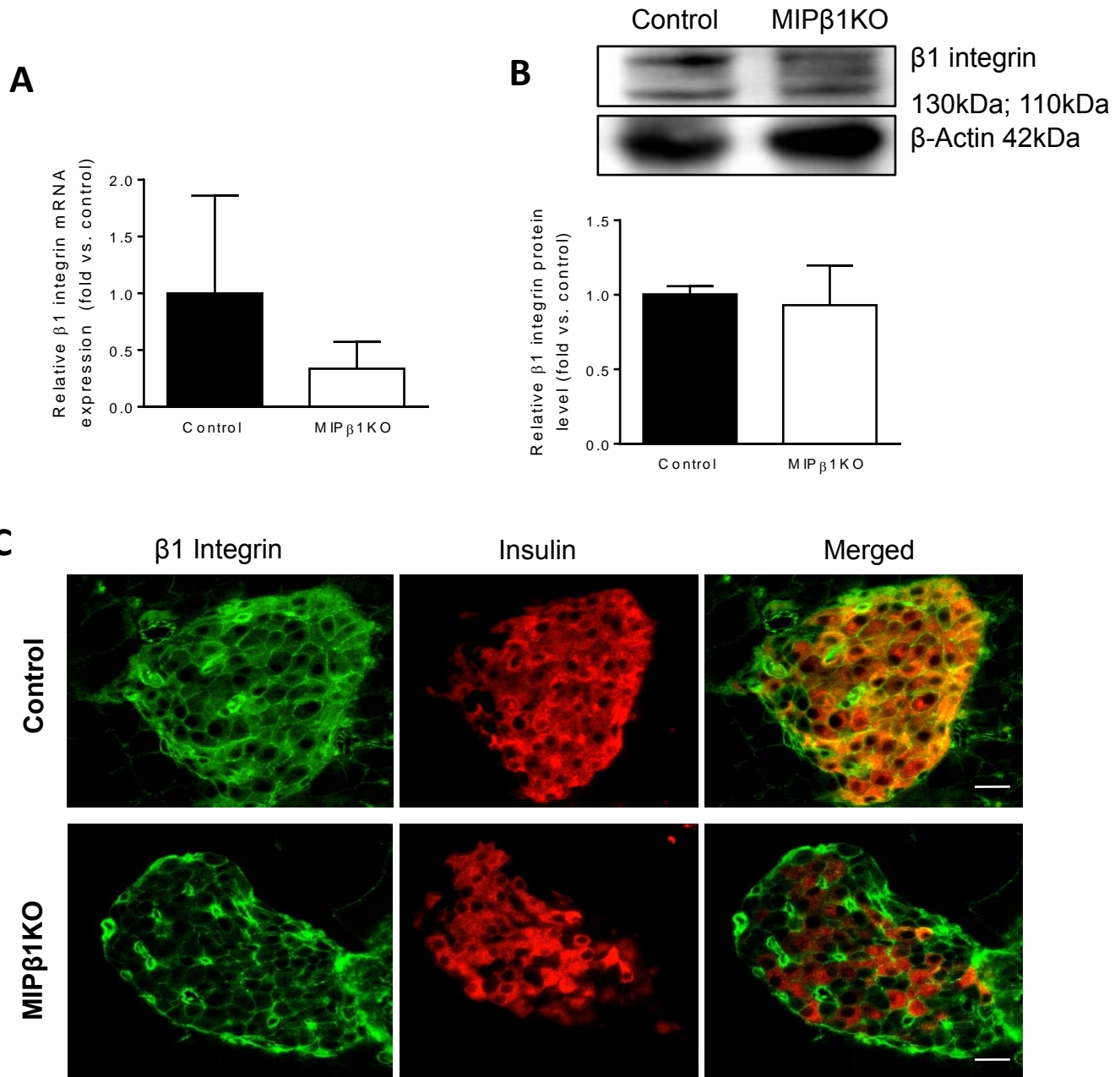


Figure 3.2 Confirmation of $\beta 1$ integrin knockdown in 16 weeks post-tamoxifen female MIP $\beta 1$ KO mice

A) qRT-PCR for $\beta 1$ integrin mRNA and **B)** western blot analysis for $\beta 1$ integrin protein in control and MIP $\beta 1$ KO islets, with a representative blot shown. **C)** Representative double immunofluorescence staining for $\beta 1$ integrin (green) and insulin (red) in the islets of control and MIP $\beta 1$ KO mice. Scale bar: 25 μ m. Black bars: control, white bars: MIP $\beta 1$ KO group. Data are expressed as mean \pm SEM ($n = 3/group$).

3.2 MIP β 1KO mice display impaired glucose tolerance

Fasting blood glucose levels were taken along with body weight measurements to assess phenotypic abnormalities. Male MIP β 1KO mice at 8 weeks post-tamoxifen showed no change in fasting blood glucose and BW compared to control mice (**Figure 3.3A,B**). However, fasting blood glucose level in female MIP β 1KO mice at 16 weeks post-tamoxifen were significantly elevated ($p < 0.05$, **Figure 3.4A**) with no change in BW (**Figure 3.4B**). IPGTT and IPITT tests were performed to assess glucose metabolism. Male MIP β 1KO mice subjected to an IPGTT showed statistically significant elevations in blood glucose at 15, 30, and 90 minutes post glucose injection which corresponded with an significant increase in the overall AUC ($p < 0.05$, **Figure 3.3C**). Impaired glucose tolerance was also observed in female MIP β 1KO mice at 16 weeks post-tamoxifen with a significant elevation of blood glucose at 30 minutes, and a significant increase in the overall AUC ($p < 0.05$, **Figure 3.4C**). To examine if peripheral insulin sensitivity was altered in MIP β 1KO mice, an IPITT was conducted and both MIP β 1KO mice and control mice responded in a similar fashion at all time points with unchanged AUC in all testing groups (**Figure 3.3D and Figure 3.4D**).

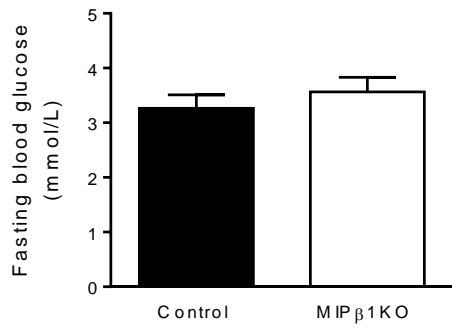
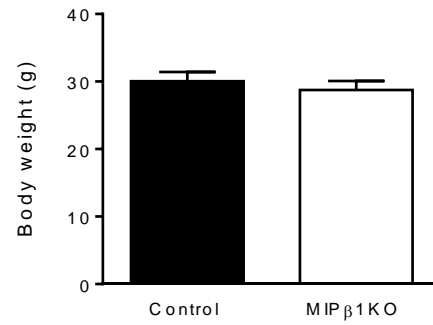
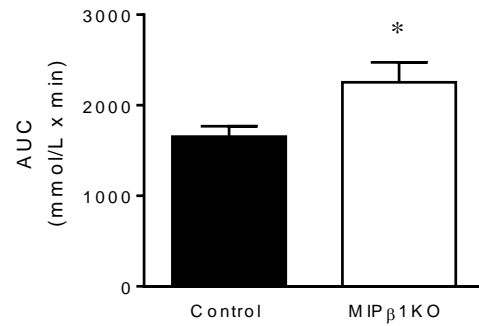
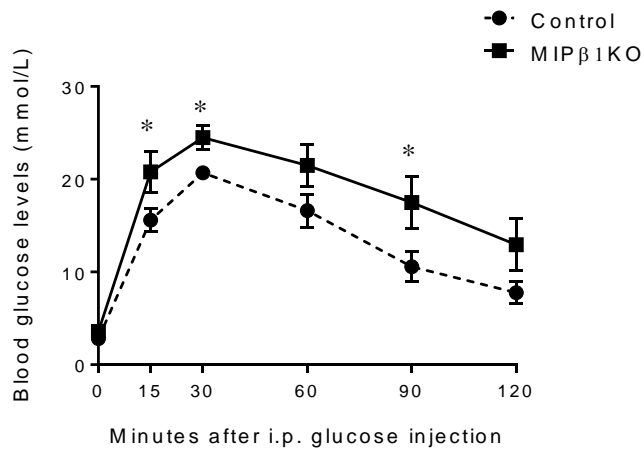
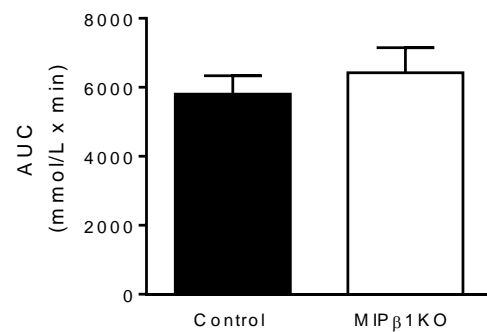
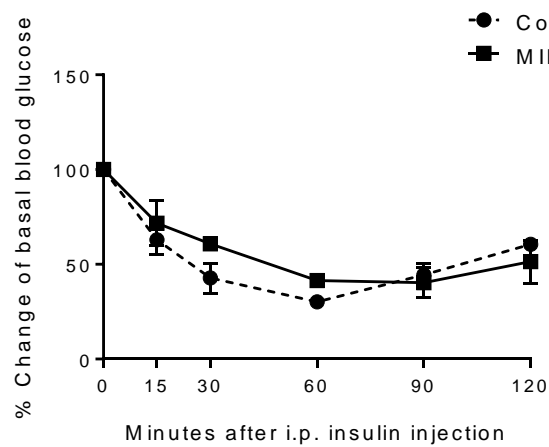
A**B****C****D**

Figure 3.3 Metabolic analyses of 8 weeks post-tamoxifen male MIP β 1KO mice

A) Fasting blood glucose (16 hours) and **B)** body weight of male control and MIP β 1KO mice. **C)** IPGTT and **D)** IPITT analyses and their corresponding AUC data for control and MIP β 1KO mice. Black bars: control, white bars: MIP β 1KO group. Data are expressed as mean \pm SEM ($n = 3-8/group$). $*p < 0.05$ vs. control group.

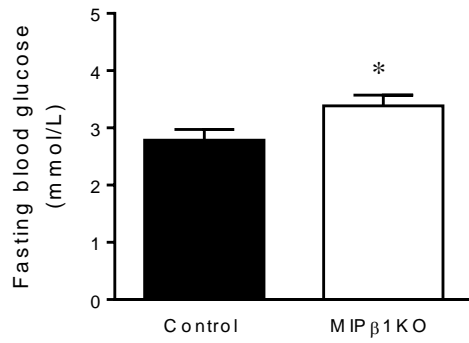
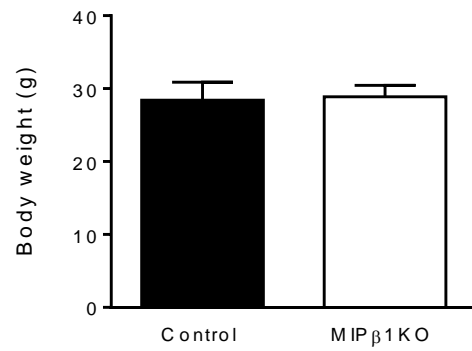
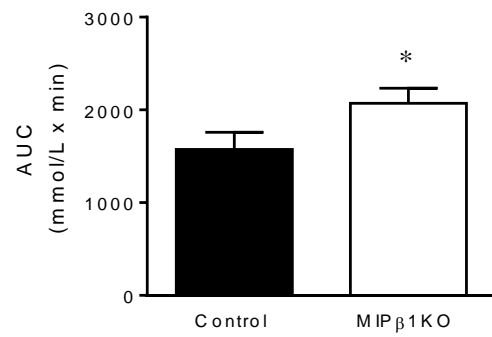
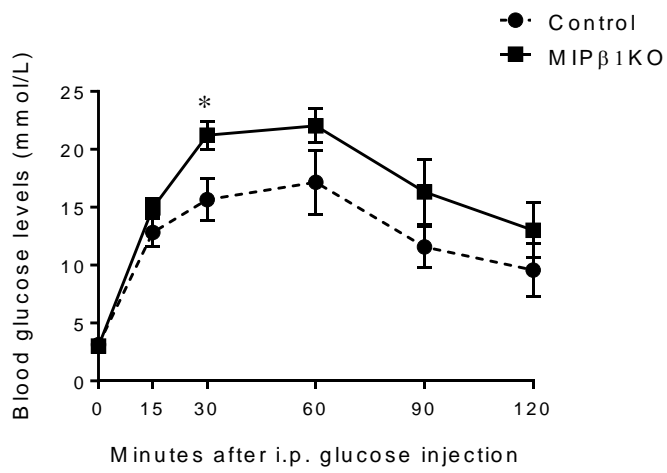
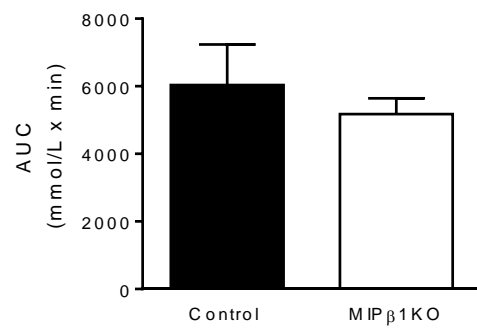
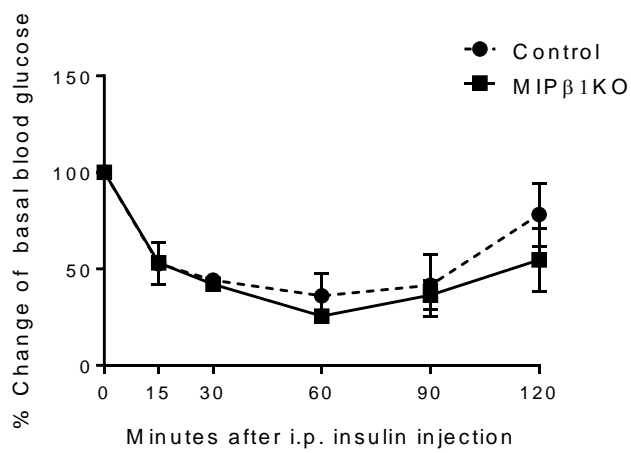
A**B****C****D**

Figure 3.4 Metabolic analyses of 16 weeks post-tamoxifen female MIP β 1KO mice

A) Fasting blood glucose (16 hours) and **B)** body weight of female control and MIP β 1KO mice. **C)** IPGTT and **D)** IPITT analyses and their AUC for control and MIP β 1KO mice. Black bars: control, white bars: MIP β 1KO group. Data are expressed as mean \pm SEM ($n = 3-8/group$). * $p < 0.05$ vs. control group.

3.3 Deficient glucose-stimulated insulin secretion in male but not female MIP β 1KO mice

Because the MIP β 1KO mice showed impairment in glucose tolerance, glucose-stimulated insulin secretion (GSIS) was measured both *in vivo* and *ex vivo* to determine beta-cell functional responsiveness. An *in vivo* GSIS test was performed in male MIP β 1KO mice at 8 weeks post-tamoxifen and showed significantly lower levels of plasma insulin at 5 and 35 minutes post glucose injection, along with significantly elevated blood glucose at 35 minutes when compared to littermate controls ($p < 0.05$, **Figure 3.5A**). To directly assess beta-cell function, isolated islets from male MIP β 1KO and control mice were incubated overnight and basal insulin levels were measured using an insulin ELISA. Basal insulin secretion in male MIP β 1KO islets was significantly lower with ~50% the amount of insulin compared to control islets ($p < 0.001$, **Figure 3.5C**). When male MIP β 1KO islets were subjected to an *ex vivo* GSIS test, a significant reduction of insulin secretion in response to glucose challenge was observed compared to control islets ($p < 0.05$, **Figure 3.5E**). The impairment in proper blood glucose management during fasting and under high glucose loading conditions in female MIP β 1KO mice at 16 weeks post-tamoxifen led to the subsequent analyses of insulin release *in vivo* and *ex vivo* using isolated islets. Female MIP β 1KO mice subjected to a GSIS test had similar levels of plasma insulin as controls (**Figure 3.5B**). Isolated islets of female MIP β 1KO also had no change in basal insulin secretion (**Figure 3.5D**), and no significant reduction during the *ex vivo* GSIS test was observed (**Figure 3.5F**).

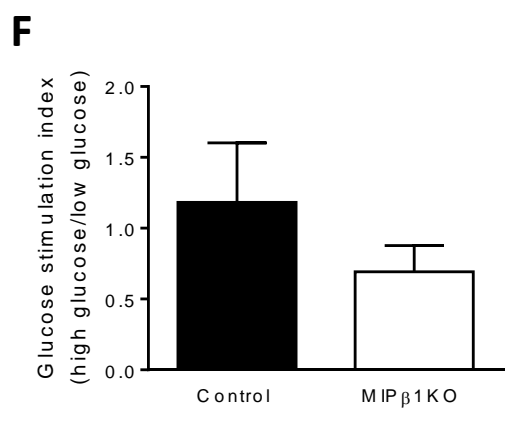
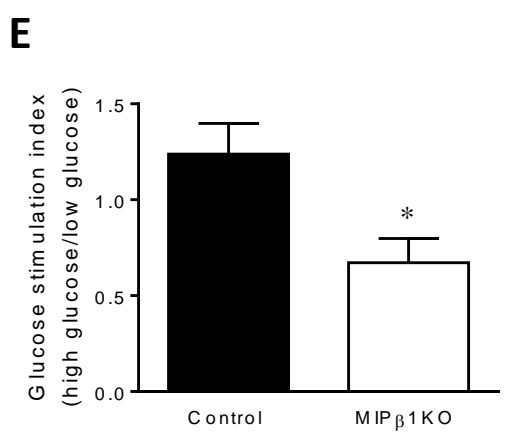
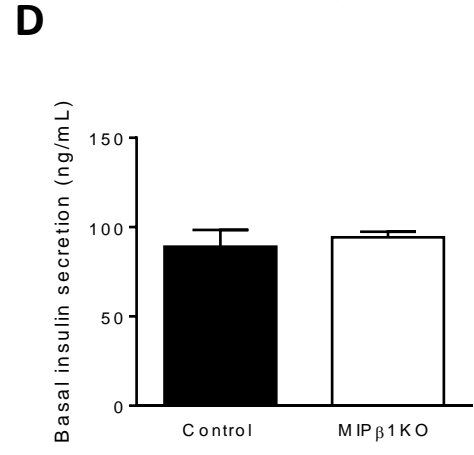
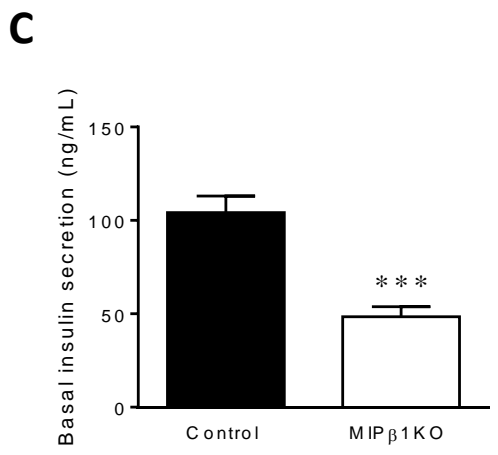
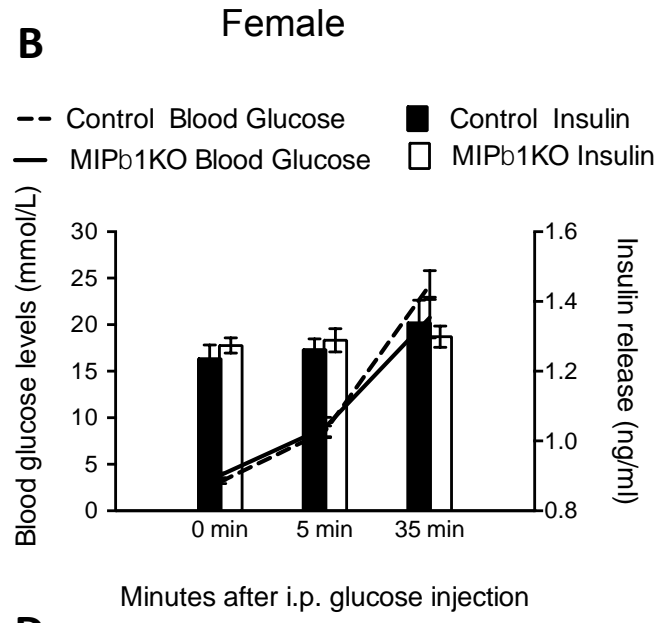
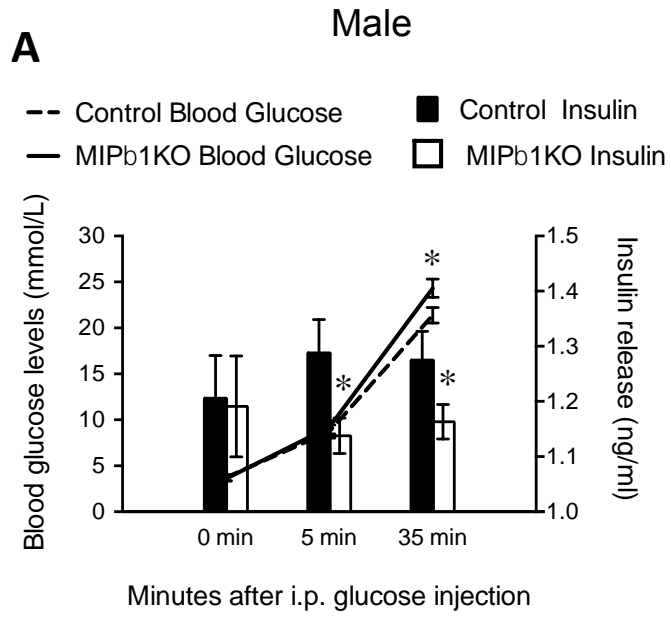


Figure 3.5 *In vivo* and *ex vivo* GSIS analyses

In vivo GSIS assay showing blood glucose and plasma insulin levels after 16-hour fast in **A)** male and **B)** female control and MIP β 1KO mice. Basal insulin secretion from isolated islet of **C)** male and **D)** female control and MIP β 1KO mice. *Ex vivo* insulin secretion in response to high glucose conditions in isolated islet of **E)** male and **F)** female control and MIP β 1KO mice. Black bars: control, white bars: MIP β 1KO group. Data are expressed as mean \pm SEM ($n = 4-7/group$). * $p < 0.05$; *** $p < 0.001$ vs. control group.

3.4 Reduction of insulin secretory molecules in MIP β 1KO mice

An investigation into the molecules involved in exocytosis of insulin granules was conducted. A significant reduction in the mRNA of *Snap25* ($p < 0.05$, **Figure 3.6A**) and *Vamp2* ($p < 0.01$, **Figure 3.6B**) was observed in male MIP β 1KO islets at 8 weeks post-tamoxifen compared to controls. Immunofluorescence staining showed a clear reduction in SNAP25 and VAMP2 in beta-cells in alignment with the reduction in mRNA in male MIP β 1KO mice (**Figure 3.7A,B**). Both *Syntaxin 1A* (*Stx1a*) and *Syntaxin 3* (*Stx3*) mRNA in male MIP β 1KO islets was unchanged compared to control mice (**Figure 3.6C,D**). Immunofluorescence staining for Munc18 showed a reduction in the beta-cells of male MIP β 1KO mice (**Figure 3.7C**). Female MIP β 1KO mice at 16 weeks post-tamoxifen showed a similar trend with reductions of *Snap25*, *Vamp2*, *Syntaxin1A* and *Syntaxin3* mRNA, but it was not statistically different compared to controls (**Figure 3.8A-D**).

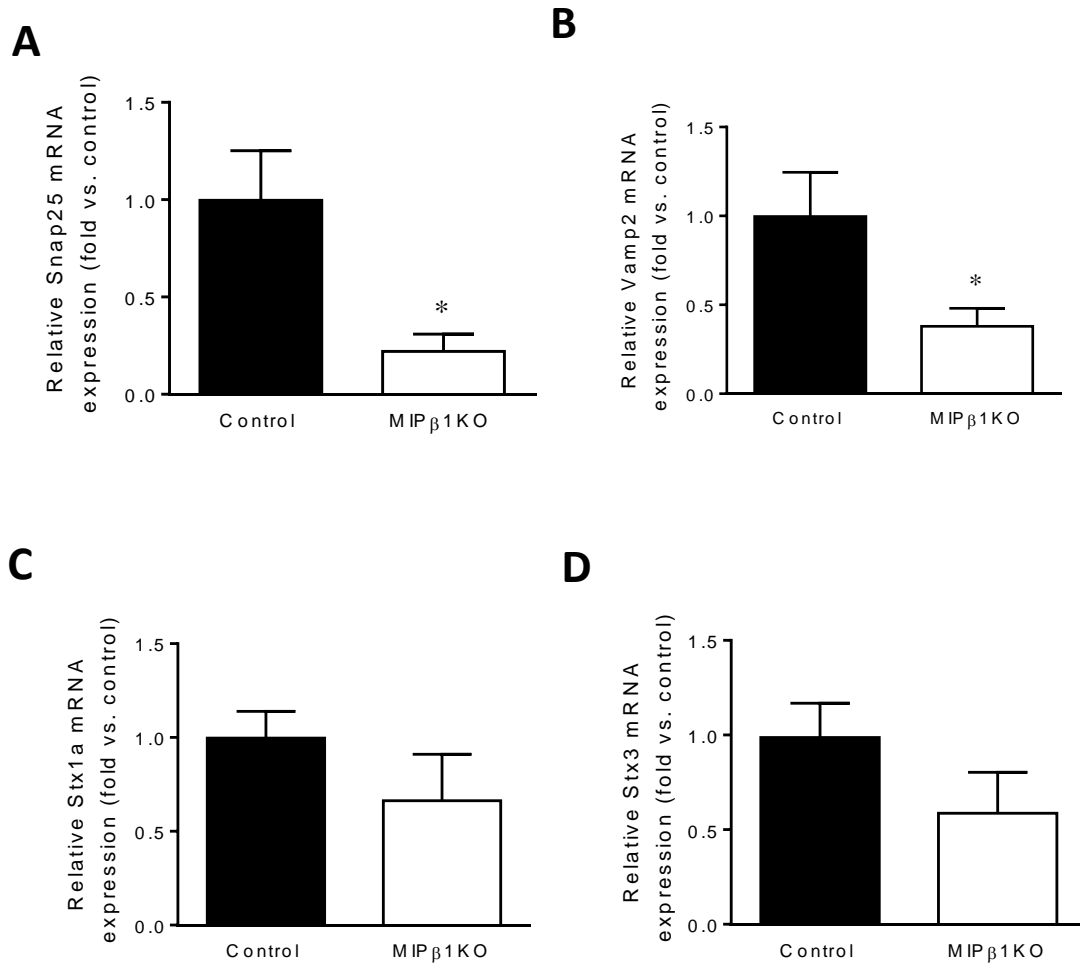


Figure 3.6 qRT-PCR analyses of insulin exocytosis machinery mRNA in 8 weeks post-tamoxifen male MIP β 1KO mice

Relative gene expression of control and male MIP β 1KO mice for **A)** *Snap25*, **B)** *Vamp2*, **C)** *Syntaxin1A (Stx1a)*, and **D)** *Syntaxin3 (Stx3)*. Black bars: control, white bars: MIP β 1KO group. Data are expressed as mean \pm SEM ($n = 3-4/group$). * $p < 0.05$ vs. control.

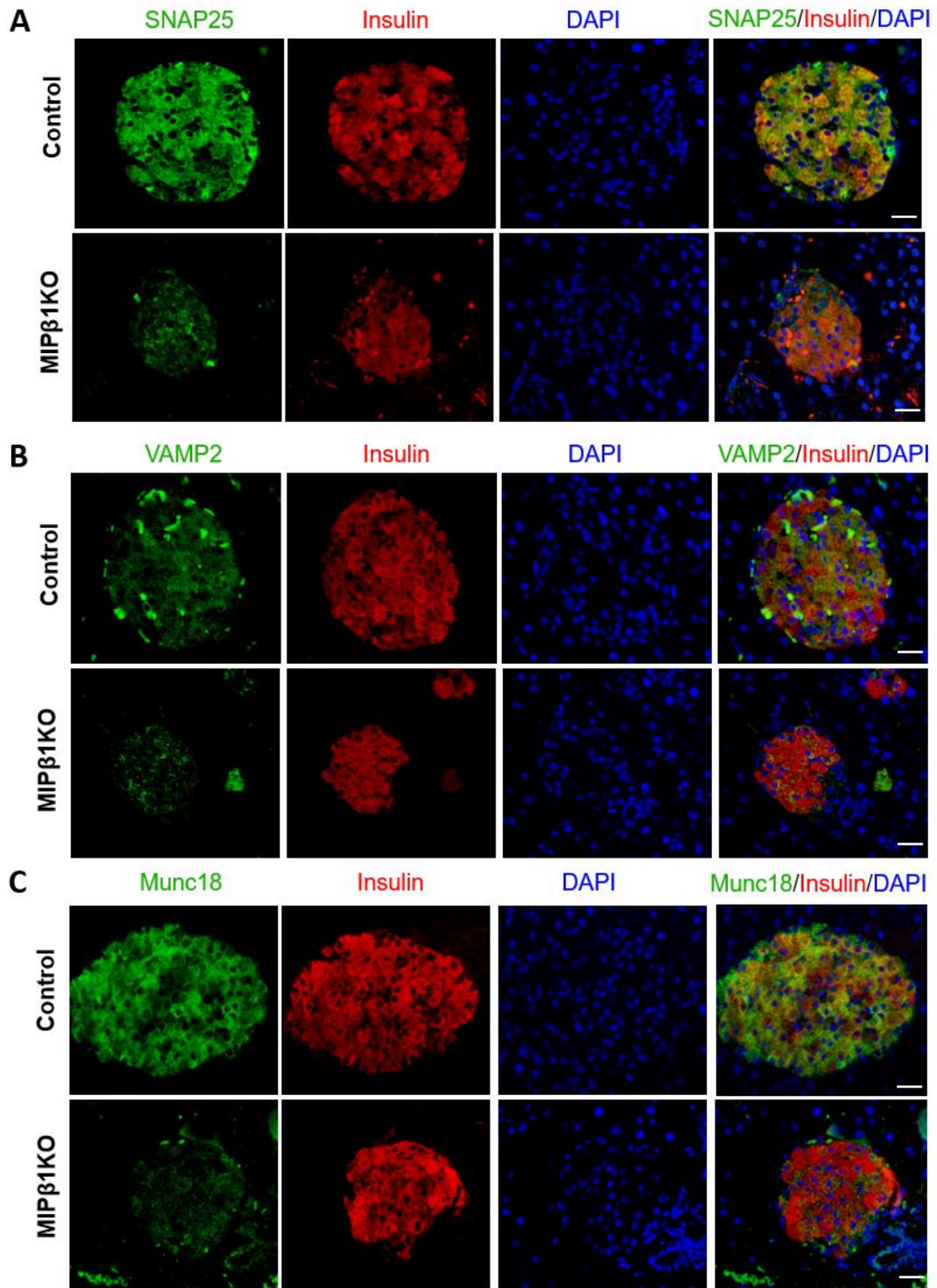


Figure 3.7 Immunofluorescence staining for insulin exocytosis proteins in 8 weeks post-tamoxifen male MIP β 1KO mice

Representative immunofluorescence staining images with separated fluorescent channels for **A)** Snap25, **B)** Vamp2, and **C)** Munc18 (green), with insulin (red) in control and MIP β 1KO mice. Nuclei were stained with DAPI (blue) ($n=3/group$). Scale bar: 25 μ m.

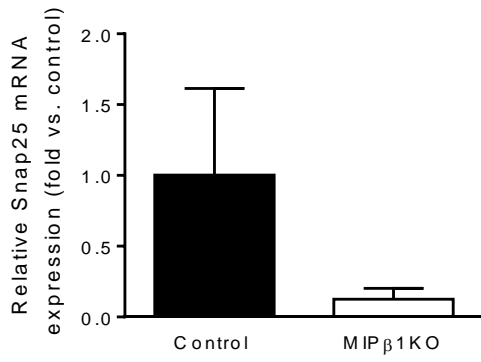
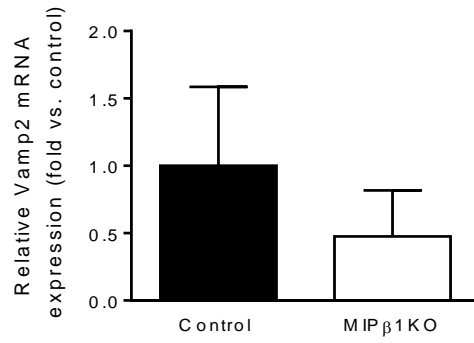
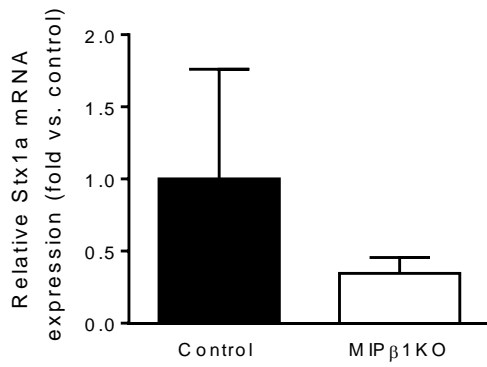
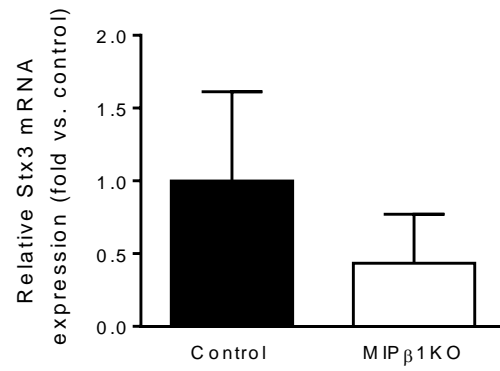
A**B****C****D**

Figure 3.8 qRT-PCR analysis for insulin exocytosis proteins in 16 weeks post-tamoxifen female MIP β 1KO mice

Relative mRNA expression of control and female MIP β 1KO mice for **A)** *Snap25*, **B)** *Vamp2*, **C)** *Syntaxin1A (Stx1a)*, and **D)** *Syntaxin3 (Stx3)*. Black bars: control, white bars: MIP β 1KO group. Data are expressed as mean \pm SEM ($n = 3/group$).

3.5 Reduced beta-cell mass in MIP β 1KO mice

Morphological studies of male MIP β 1KO (8 weeks post-tamoxifen) and control pancreata showed that the overall architecture of the pancreas was unaltered and islets remained intact in tight clusters (**Figure 3.9A**). Morphometric analyses of islet density (islets per mm²) showed a significant reduction in male MIP β 1KO mice compared to the controls ($p < 0.05$, **Figure 3.9B**). When islets were grouped based on their size, it was found that there were significantly more small islets (501-2500 μm^2), and less of the large islets (2501-10000 μm^2) in the male MIP β 1KO pancreas ($p < 0.05$, **Figure 3.9C**). The decrease in size seen in large islets was clearly related to a significant decrease (~60%) in beta-cell mass in male MIP β 1KO mice ($p < 0.05$, **Figure 3.9D**), yet there was no accompanied reduction in alpha-cell mass (**Figure 3.9E**). Because a reduction in beta-cell mass was seen, *insulin* (*Ins*) mRNA was examined using isolated islets from male MIP β 1KO mice and was found to be significantly decreased compared to control islets ($p < 0.05$, **Figure 3.9F**). There was no change in the expression of *glucagon* (*Gcg*) mRNA in male MIP β 1KO mice (**Figure 3.9G**). Immunofluorescence staining was also used to examine E-cadherin (**Figure 3.10A**) and Glut2 (**Figure 3.10B**), proteins known to be important in maintaining beta-cell function and glucose-sensing, and no change was detected in male MIP β 1KO mice.

Morphological examination of female MIP β 1KO mice 16 weeks post-tamoxifen and control pancreata showed relatively smaller islets (**Figure 3.11A**); however, quantitative assessment of islet number per mm² of pancreas was not significantly altered in female MIP β 1KO mice (**Figure 3.11B**). When examining female MIP β 1KO islet size, there was a significant increase in very small islets ($< 500 \mu\text{m}^2$), but larger islets did not display any clear reduction ($p < 0.05$, **Figure 3.11C**). Although islet density and size was not significantly impacted, there was a significant reduction in beta-cell mass (~50%), implying that there is either a reduction in beta-cell proliferation or increase in apoptosis in female MIP β 1KO mice compared to controls ($p < 0.01$, **Figure 3.11D**). Unlike that seen in male MIP β 1KO, female MIP β 1KO showed a significant reduction in alpha-cell mass ($p < 0.05$, **Figure 3.11E**). Both *Ins* and *Gcg* mRNA levels were reduced in isolated

islets of female MIP β 1KO and control mice, but significance was not reached due to high variability among the samples (**Figure 3.11F,G**).

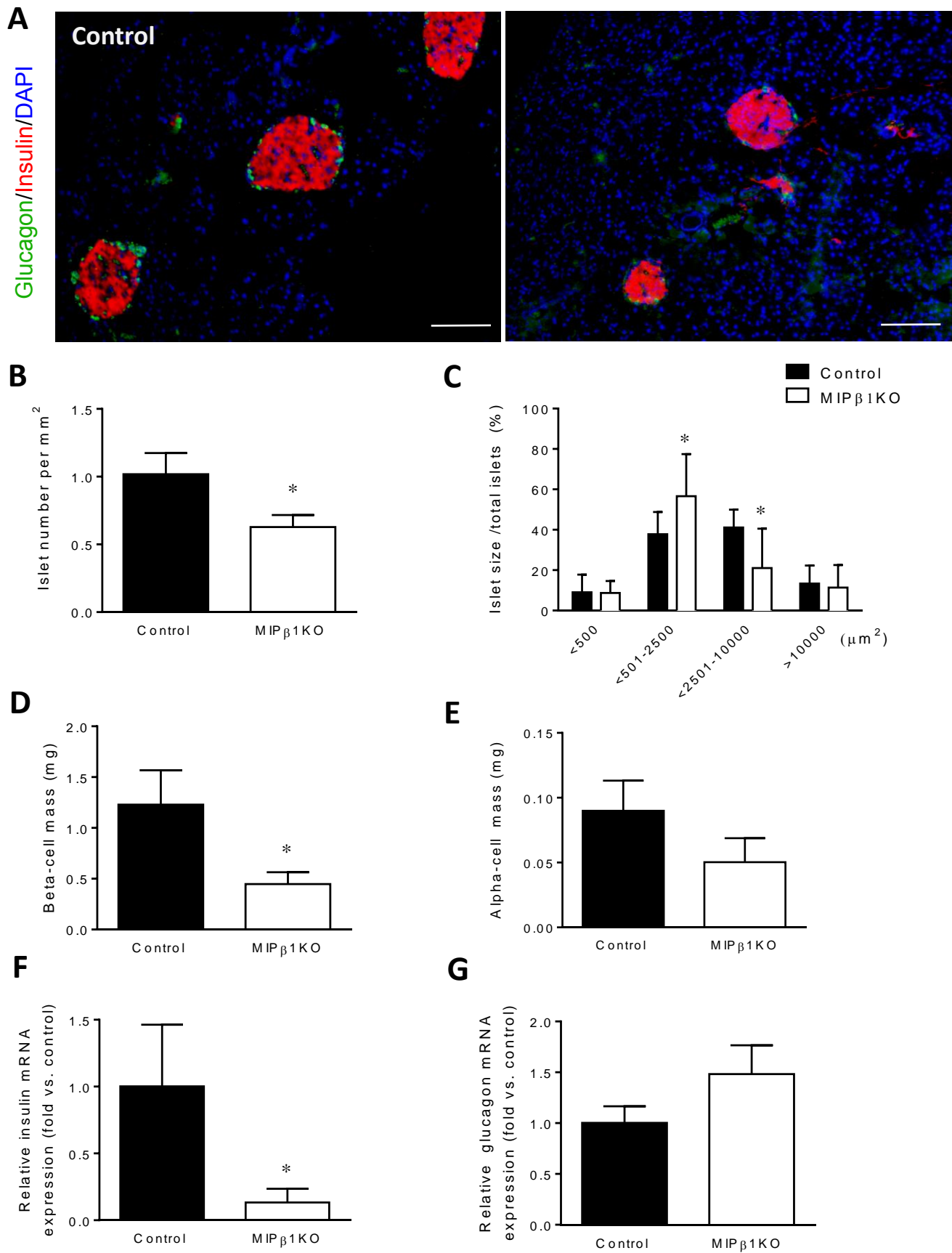


Figure 3.9 Morphometric analyses of 8 weeks post-tamoxifen male MIP β 1KO mice

A) Representative immunofluorescence images showing insulin⁺ staining (red) and DAPI (blue) in control (left) and MIP β 1KO (right) mice. Scale bar: 200 μ m. **B)** Islet number, **C)** islet size, **D)** beta-cell mass and **E)** alpha-cell mass of control and MIP β 1KO mice ($n = 5-6/group$). qRT-PCR analysis for **F)** *Insulin* and **H)** *Glucagon* mRNA of control and MIP β 1KO mice ($n = 3-4/group$). Black bars: control, white bars: MIP β 1KO group. Data are expressed as mean \pm SEM. * $p < 0.05$ vs. control group.

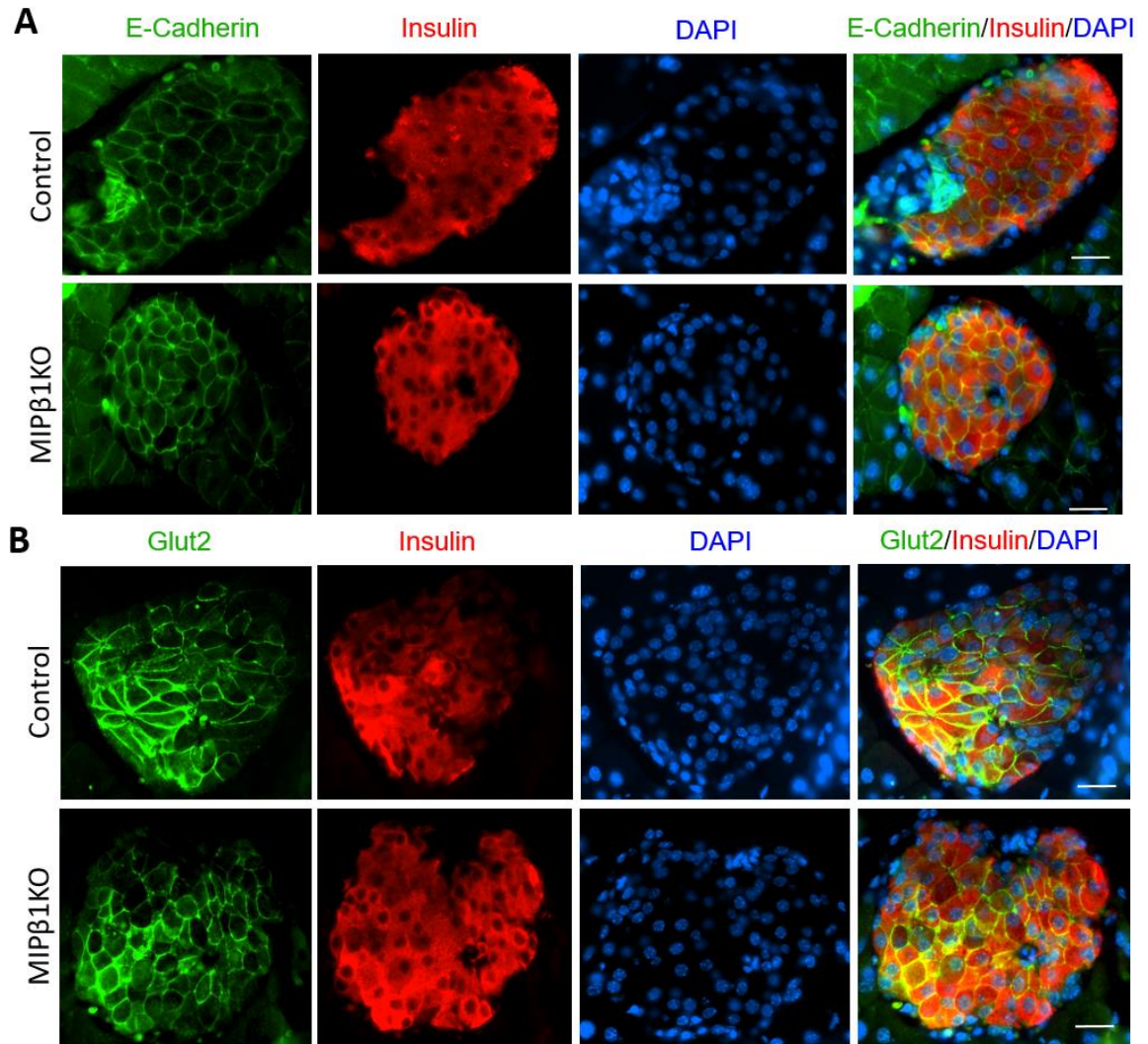


Figure 3.10 E-cadherin and Glut2 co-localization in 8 week post-tamoxifen male MIP β 1KO mice

Representative immunofluorescence staining images for islets of control and MIP β 1KO mice for **A**) cell adhesion molecule e-cadherin (green) and insulin (red) and **B**) glucose-sensing transporter Glut2 (green) and insulin (red). Nuclei were stained with DAPI (blue) ($n = 3/group$) Scale bar: 25 μ m.

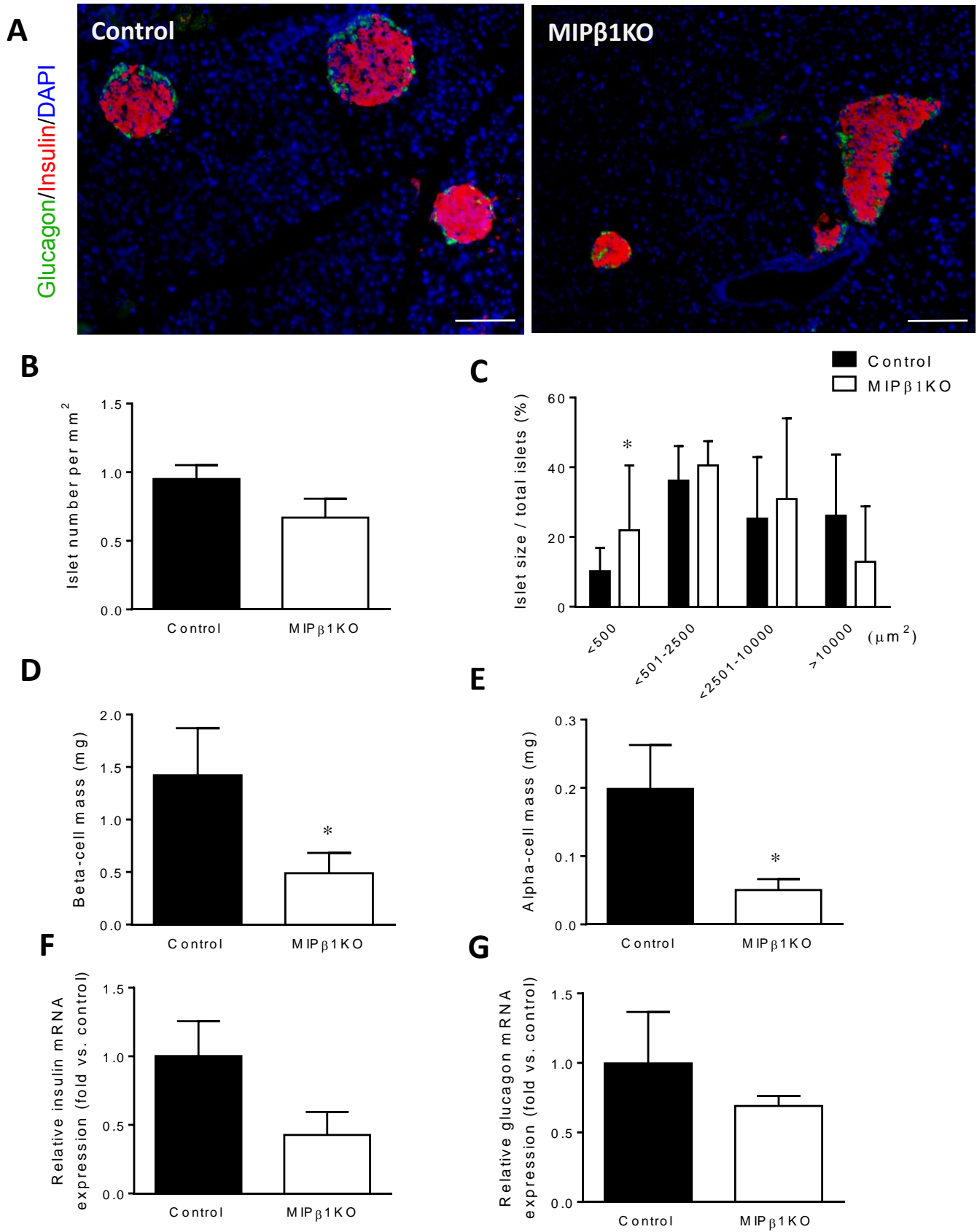


Figure 3.11 Morphometric analyses of 16 weeks post-tamoxifen female MIP β 1KO mice

A) Representative immunofluorescence images showing insulin⁺ staining (red) and DAPI (blue) in control (left) and MIP β 1KO mice (right) mice. Scale bar: 200 μ m. **B)** Islet number, **C)** islet size, **D)** beta-cell mass and **E)** alpha-cell mass of control and MIP β 1KO mice ($n = 5/group$). qRT-PCR analysis for **F)** *Insulin* and **H)** *Glucagon* mRNA of control and MIP β 1KO mice ($n = 3/group$). Black bars: control, white bars: MIP β 1KO group. Data are expressed as mean \pm SEM. * $p < 0.05$ vs. control group.

3.6 Reduction of Pdx-1 mRNA and protein levels in male MIP β 1KO mice

Because of the significant impairment in glucose tolerance and insulin secretion in male MIP β 1KO mice 8 weeks post-tamoxifen, it was important to elucidate the underlying mechanism behind the dysfunction. Pdx-1 is an important regulator of insulin transcription (Ahlgren et al. 1998) and both mRNA and protein levels were significantly reduced in the β 1KO model reported by Riopel (2011). The level of *Pdx-1* mRNA in the islets of male MIP β 1KO mice was significantly reduced by ~40% when compared to control mice ($p < 0.01$, **Figure 3.12A**), along with a significant reduction in Pdx-1 protein level as measured by western blot ($p < 0.01$, **Figure 3.12B**). Immunofluorescence staining for Pdx1 in beta-cells of male MIP β 1KO mice was consistently less intense than controls (**Figure 3.12C**). We further examined transcription factors Nkx6.1 (**Figure 3.13A**), NK2 homeobox2 (Nkx2.2) (**Figure 3.13B**), Islet-1 (Isl-1) (**Figure 3.13C**) and v-maf avian musculoaponeurotic fibrosarcoma homolog A (Mafa) (**Figure 3.13D**) using dual immunofluorescence staining or immunohistochemical staining, and found relatively similar staining intensities displayed between male MIP β 1KO mice and control mice.

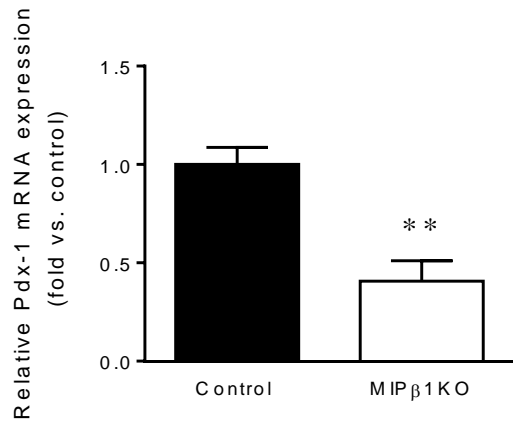
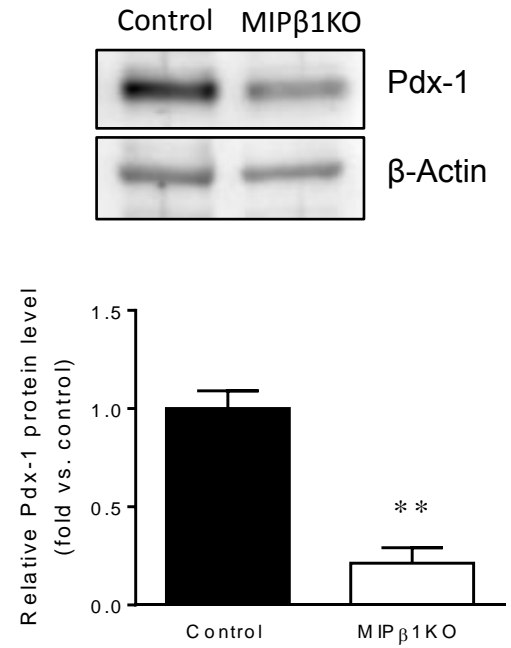
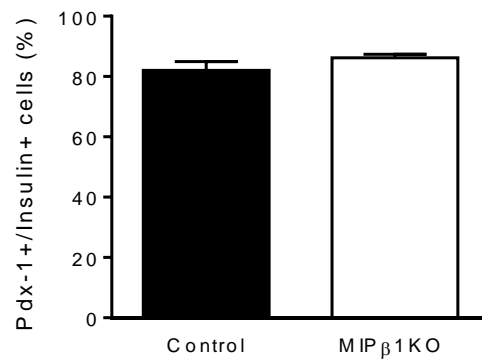
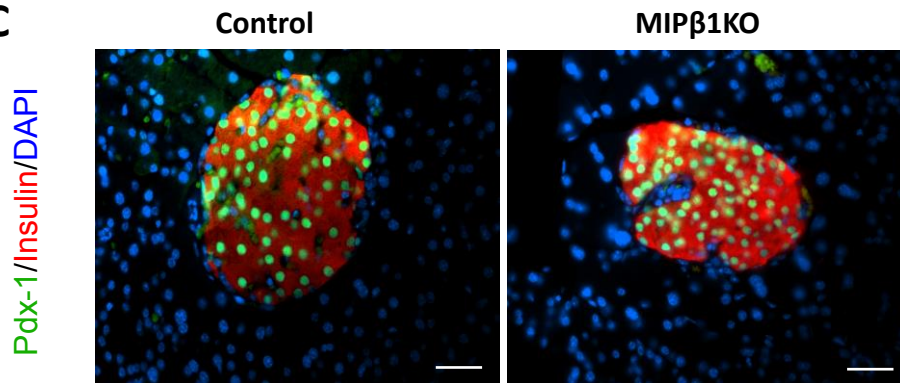
A**B****C**

Figure 3.12 Examination of Pdx-1 expression in 8 weeks post-tamoxifen male MIP β 1KO mice

A) *Pdx-1* mRNA expression and **B)** Pdx-1 protein levels in control and MIP β 1KO mice with a representative blot shown ($n = 3-6/group$). **C)** Representative immunofluorescence images for Pdx-1 (green), insulin (red) and DAPI (blue) in control and MIP β 1KO mice. Scale bar: 25 μ m. Black bars; control, white bars; MIP β 1KO group. Data are expressed as mean \pm SEM. ** $p < 0.01$ vs. control.

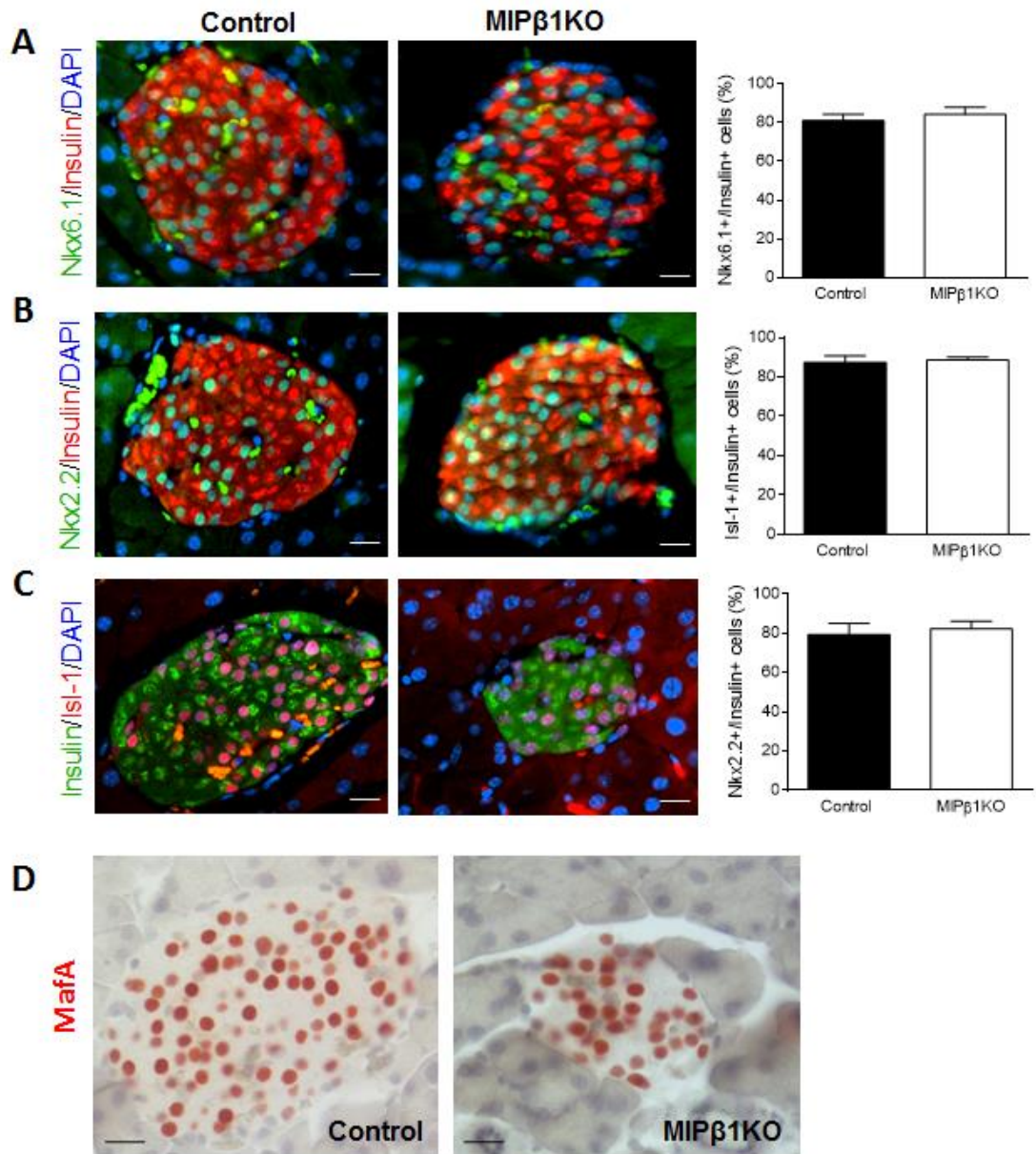


Figure 3.13 Transcription factor expression in 8 week post-tamoxifen male MIP β 1KO mice

Representative immunofluorescence images and quantification for **A)** Nkx6.1 (green) and insulin (red), **B)** Nkx2.2 (green) and insulin (red), **C)** Isl-1 (red) and insulin (green). **D)** Representative immunohistochemical staining for MafA (red) in control and MIP β 1KO mice. Black bars: control, white bars: MIP β 1KO group. Data are expressed as mean \pm SEM (n = 2-5/group). Scale bar = 25 μ m.

3.7 β 1 integrin deficiency in beta-cells does not affect islet vasculature

Immunofluorescence staining for PECAM and insulin showed no discernable differences in the vascularization of islets in 8 weeks post-tamoxifen male MIP β 1KO mice (**Figure 3.14A**). Islet capillary area and diameter showed no significant changes relative to controls (**Figure 3.14B,C**). Just as with the male MIP β 1KO mice, female MIP β 1KO mice 16 weeks post-tamoxifen had no obvious changes in islet vasculature (**Figure 3.14D**). Quantitative assessment of female MIP β 1KO islet capillary area and diameter also showed no changes compared to control mice (**Figure 3.14E,F**). These findings demonstrate that vasculature is unaltered in MIP β 1KO mice.

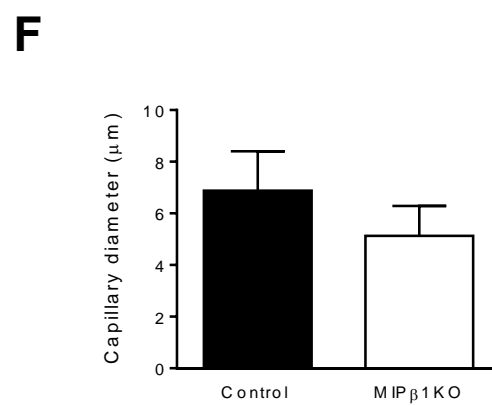
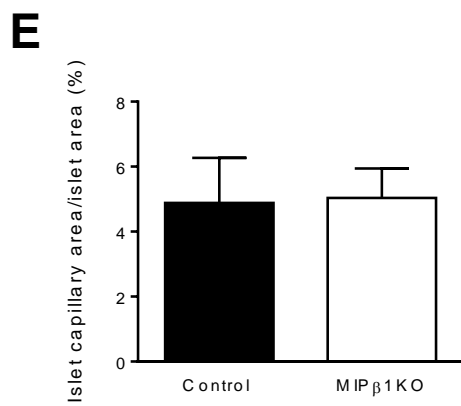
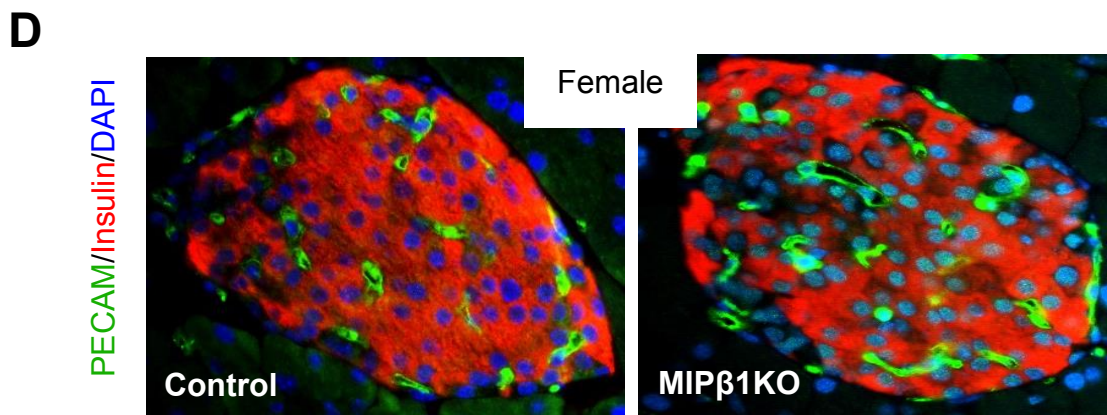
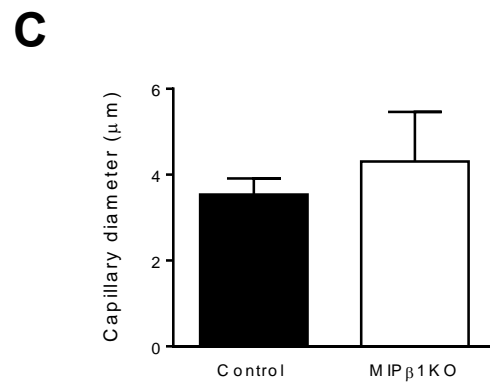
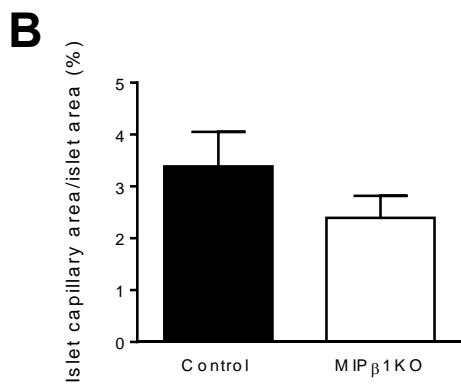
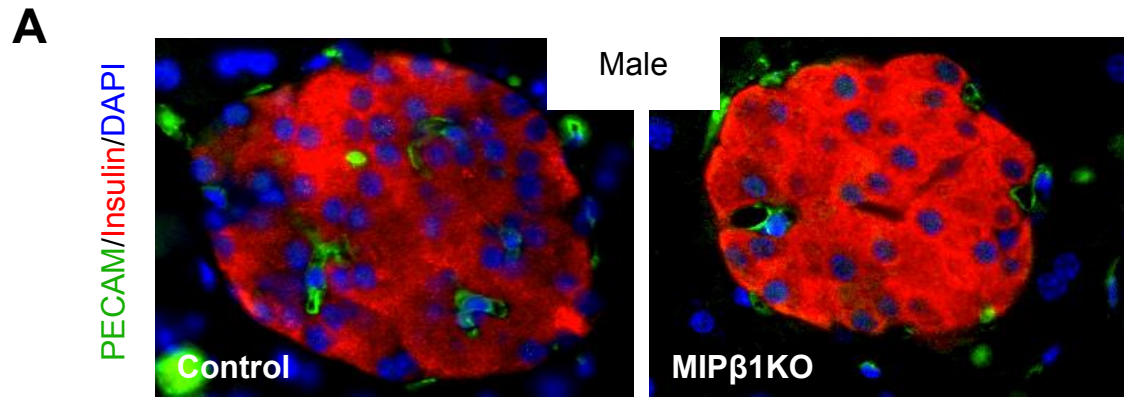


Figure 3.14 Measurement of islet vascularization in MIP β 1KO mice

A) Representative immunofluorescence staining of PECAM (green), insulin (red) and DAPI (blue) in control and male MIP β 1KO mice. Scale bar: 25 μ m. Quantification of blood vessel area (**B**) and density (**C**) in control and male MIP β 1KO mice. **D)**

Representative immunofluorescence staining of PECAM (green), insulin (red), and DAPI (blue) in female control and MIP β 1KO mice. Scale bar: 25 μ m. Blood vessel area (**E**) and density (**F**) quantification in female control and MIP β 1KO mice. Black bars: control, white bars: MIP β 1KO group. Data are expressed as mean \pm SEM ($n = 2-5/group$).

3.8 Reduction of phosphorylated-FAK, ERK1/2, and Akt protein levels with altered cell proliferation pathways in male MIP β 1KO mice

FAK and its downstream signalling molecules ERK1/2 and Akt have been shown to be important in beta-cell proliferation, survival, and function (Riopel et al. 2011, Feng et al. 2015). In line with results reported by Riopel (2011) and Diaferia (2013) using the β 1KO and RIP β 1KO models respectively, there was a significant reduction in p-FAK^{Y397} ($p < 0.001$, **Figure 3.15A**) and p-ERK1/2 ($p < 0.05$, **Figure 3.15B**) in male MIP β 1KO mice 8 weeks post-tamoxifen compared to controls. A significant decrease in p-Akt^{S473} was also observed in male MIP β 1KO mice ($p < 0.05$, **Figure 3.15**). Analysis of the proliferation marker cyclin D1 in isolated islets from male MIP β 1KO mice showed a significant reduction compared to control islets ($p < 0.05$, **Figure 3.15D**). The protein level of the apoptotic marker c-PARP was also significantly increased in male MIP β 1KO islets ($p < 0.05$, **Figure 3.15E**). Immunofluorescence staining for the proliferative marker Ki67 in male MIP β 1KO islets was similar to that of controls (**Figure 3.15G**).

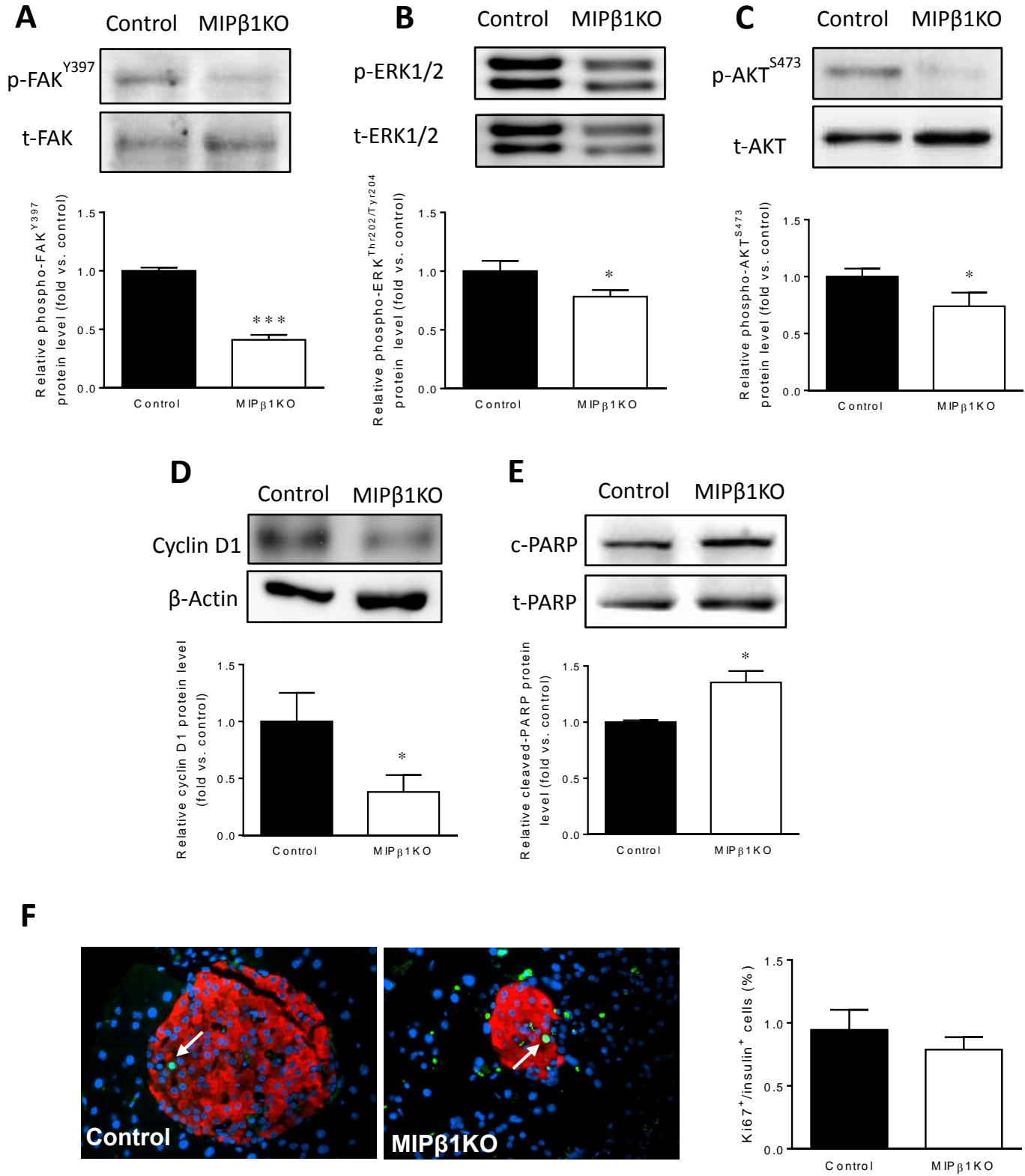


Figure 3.15 Cell signalling, proliferation, and apoptosis in 8 weeks post-tamoxifen male MIP β 1KO mice

Western blot analyses for **A)** p-FAK^{Y397}, **B)** p-ERK1/2, and **C)** p-Akt^{S473}, with representative blots shown for control and MIP β 1KO mice. **D)** Cyclin D1 and **E)** c-PARP protein levels with representative blots from control and MIP β 1KO mice. **F)** Representative immunofluorescence staining for Ki67 (green), insulin (red) and DAPI (blue), and quantification of Ki67⁺ beta-cells for control and MIP β 1KO mice. Scale bar: 25 μ m. Black bars: control, white bars: MIP β 1KO group. Data are expressed as mean \pm SEM ($n = 3-11/group$). * $p < 0.05$, *** $p < 0.001$ vs control.

3.9 Expression of other integrin subunits in male MIP β 1KO mice

The examination of other integrin subunits was conducted to see if there was any upregulation in a compensatory manner due to the knockdown of β 1 integrin in male MIP β 1KO mice 8 weeks post-tamoxifen. qRT-PCR analysis of α 3 *integrin* mRNA showed no change (**Figure 3.16A**), however qualitative assessment of immunofluorescence staining for the subunit in male MIP β 1KO mice showed an increase (**Figure 3.17A**). mRNA for α 5 *integrin* was relatively unchanged (**Figure 3.16B**) and immunofluorescence staining showed co-localization to alpha-cells with no obvious differences compared to controls (**Figure 3.17B**). mRNA levels for α 6 and α V integrins showed no change (**Figure 3.16C,D**), and there was no clear differences in immunofluorescence staining for these integrins in male MIP β 1KO islets compared to controls (**Figure 3.17C,D**).

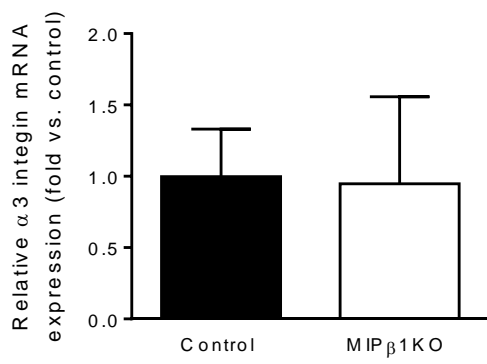
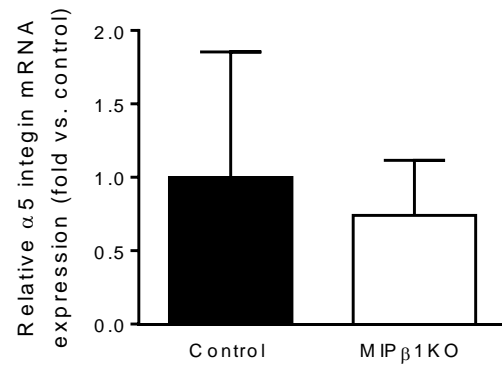
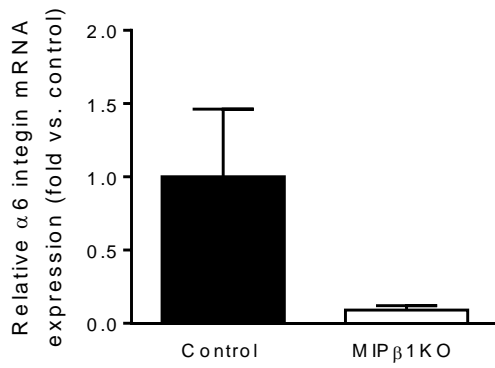
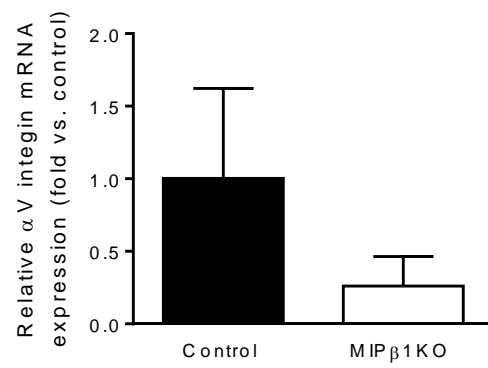
A**B****C****D**

Figure 3.16 qRT-PCR analyses for integrin alpha subunits in 8 weeks post-tamoxifen male MIP β 1KO mice

Relative mRNA expression for: **A)** $\alpha 3$ *integrin*, **B)** $\alpha 5$ *integrin*, **C)** $\alpha 6$ *integrin*, and **D)** αV *integrin* in control and male MIP β 1KO mice. Black bars: control, white bars: MIP β 1KO group. Data are expressed as mean \pm SEM ($n = 3-4/group$).

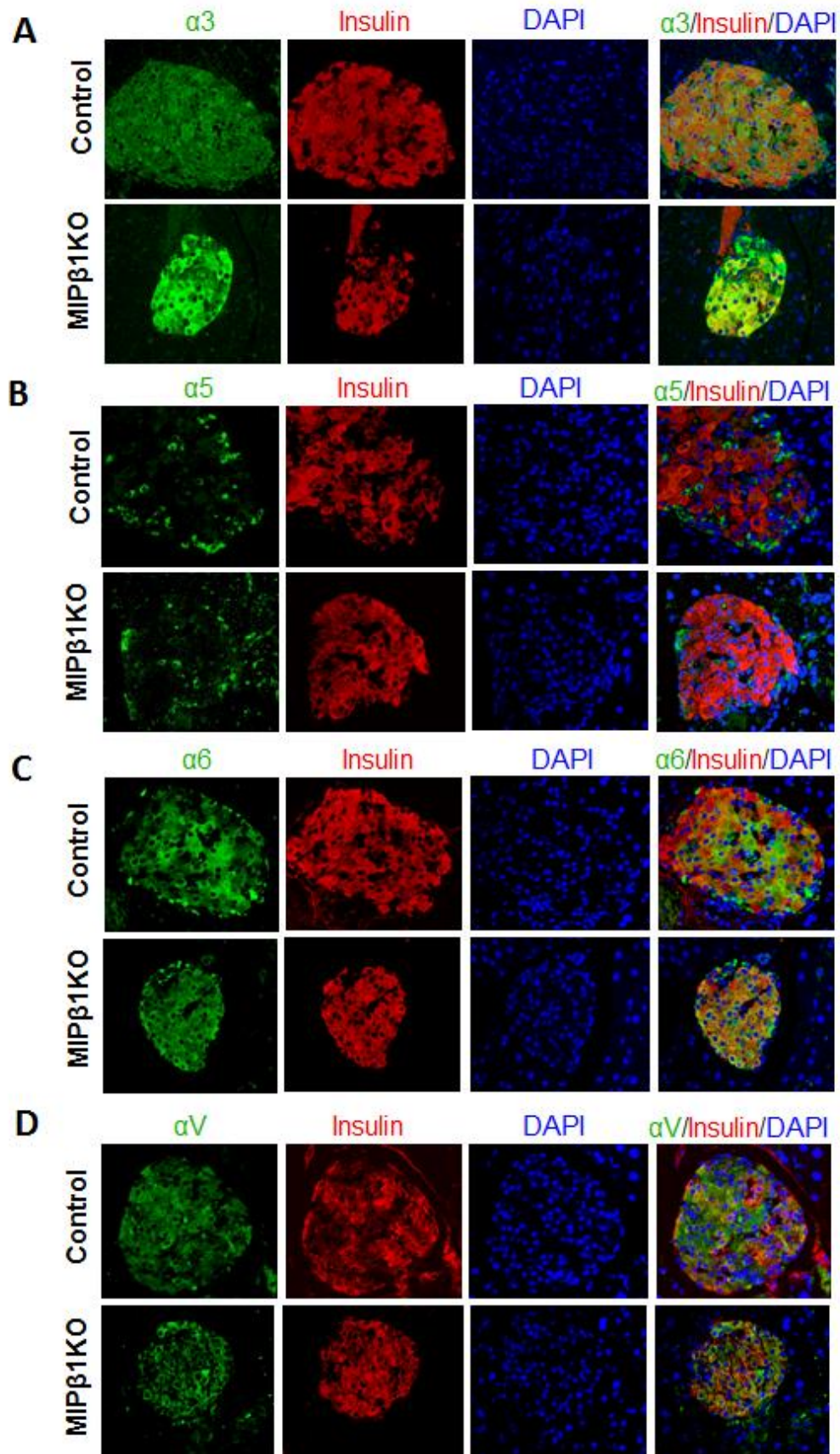


Figure 3.17 Immunofluorescence staining for integrin alpha subunits in 8 weeks post-tamoxifen male MIP β 1KO mice

Representative immunofluorescence images with separated fluorescence channels for **A)** α 3 integrin, **B)** α 5 integrin, **C)** α 6 integrin, and **D)** α V integrin (green) with insulin (red) in control and male MIP β 1KO mice. Nuclei were stained with DAPI (blue) ($n=3/group$). Scale bar: 25 μ m.

3.10 Glucose intolerance was maintained in aged MIP β 1KO mice

To investigate whether MIP β 1KO mice could recover overtime as an adaptive response through increased expression of other integrins, aged MIP β 1KO mice at 25-35 weeks post-tamoxifen were examined. Aged male MIP β 1KO mice showed significantly elevated blood glucose after an overnight fast ($p < 0.05$, **Figure 3.18A**). Aged female MIP β 1KO mice also displayed relatively high fasting blood glucose levels, but there was no statistical significance compared to control mice (**Figure 3.18B**). Similar BW was observed in all aged groups (**Figure 3.18C,D**). IPGTT in aged male MIP β 1KO mice showed significantly elevated blood glucose levels at 60, 90 and 120 minutes after glucose injection with a significantly increased overall AUC when compared to control mice ($p < 0.05-0.01$, **Figure 3.18E**). An IPGTT in the aged female MIP β 1KO mice showed significantly elevated blood glucose levels at 30, 60, 90, and 120 minutes after glucose load ($p < 0.05-0.01$) along with a significantly increased AUC ($p < 0.05 - 0.01$, **Figure 3.18F**).

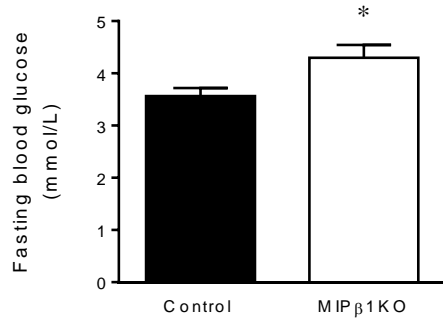
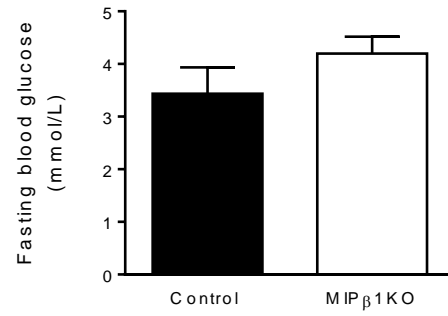
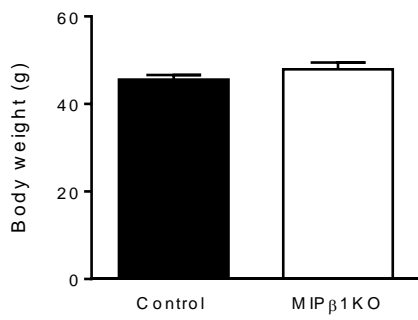
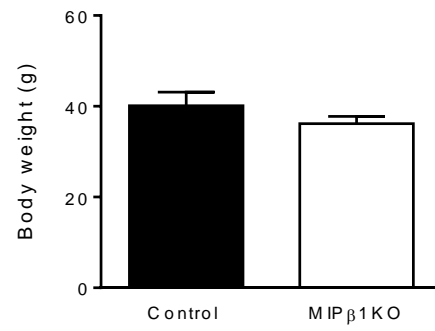
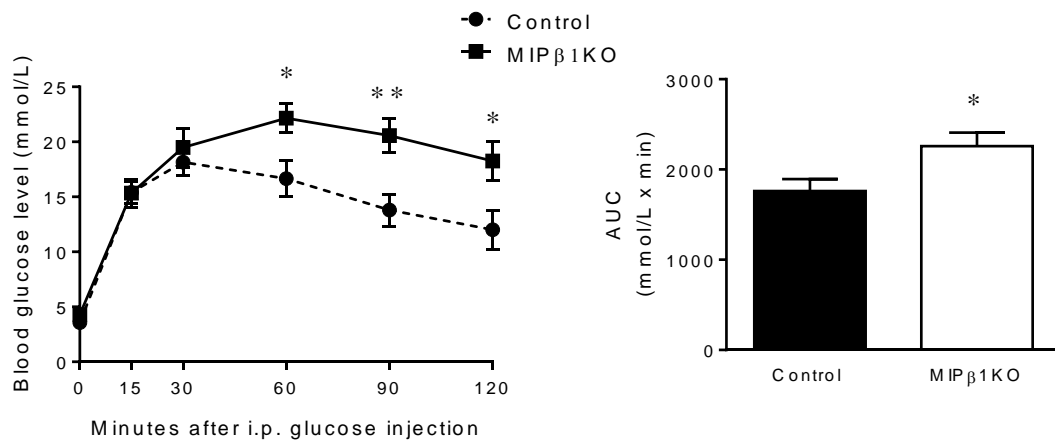
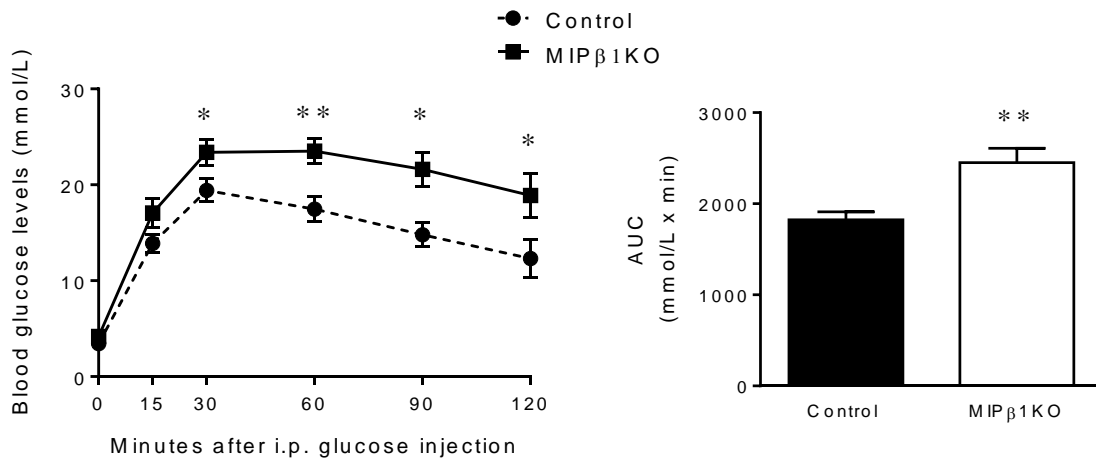
A**B****C****D****E****F**

Figure 3.18 Metabolic analyses of aged MIP β 1KO mice

Fasting blood glucose of aged **A)** male and **B)** female control and MIP β 1KO mice. Body weight for aged **C)** male and **D)** female control and MIP β 1KO mice. **E)** IPGTT analysis of control and aged male MIP β 1KO mice and the corresponding AUC. **F)** IPGTT analysis of control and aged female MIP β 1KO mice, with the corresponding AUC. Black bars: control, white bars: MIP β 1KO group. Data are expressed as mean \pm SEM ($n = 6-14/group$). * $p < 0.05$, ** $p < 0.01$ vs. control.

Chapter 4 - Discussion

This study aimed to examine the role of $\beta 1$ integrin in the beta-cells of adult mice using a beta-cell specific knockout of $\beta 1$ integrin. Based on previous literature, I hypothesized that the MIP $\beta 1$ KO mice would have impaired glucose tolerance and insulin secretion (through a reduction of SNARE proteins involved in insulin exocytosis), reduced beta-cell mass, and a reduction in FAK/MAPK/ERK and PI3K/Akt activity. My key findings confirmed my hypothesis.

4.1 Knockdown of $\beta 1$ integrin in MIP $\beta 1$ KO mice

Tamoxifen was given I.P. at 4 mg/20g BW for 3 consecutive days to produce MIP $\beta 1$ KO mice. This regimen was adapted from the dosage given in Furuyama et al. (2011), where 4 mg/ 20 g BW was given I.P. for 5 days every 48 hours. This dosage demonstrated sufficient CreER activation as indicated by x-gal staining, along with no apparent organ damage and no abnormalities within plasma samples (Furuyama et al. 2011). Consecutive dosages at such a high concentration of tamoxifen has not been used in any publications and it was observed that some male, and many female mice from both control and KO groups, became ill after the second and third round of tamoxifen administration. Various reports have been published regarding the potential toxicity of tamoxifen (Denk et al. 2015, Huh et al. 2012, Bersell et al. 2013, Phillips DH 2011). It is also possible that the surviving mice were not all receiving a consistent I.P. dose of tamoxifen, and that those receiving the higher end of the dose are the ones that did not survive. One potential factor for variability in tamoxifen dosages are human error, such as leakage of the corn oil-based tamoxifen solution from the injection site, as well as the potential for injecting into areas other than the peritoneal cavity, such as the abdomen, spleen, or even the pancreas itself.

It was apparent that a sufficient knockdown was achieved in male MIP $\beta 1$ KO mice, as verified by western blot (~40% knockdown), qRT-PCR (~60% knockdown), and an observable difference in immunofluorescence staining intensity of $\beta 1$ integrin. These values are comparable to those achieved in Riopel (2011, 2013), and despite a larger dosage of tamoxifen used in this study (4 mg/ 20 g BW for 3 consecutive days compared

to 1mg tamoxifen for 5 consecutive days), it did not lead to any clear differences in knockdown between the models. However, female mice responded differently to the specified tamoxifen dose, which requires further elaboration. Although mRNA levels showed a slight decrease in $\beta 1$ integrin along with a clear reduction of $\beta 1$ integrin in insulin positive cells as assessed by immunofluorescence staining, isolated islet protein showed no change compared to controls. Riopel (2011, 2013) also noted that female mice did not display as drastic a phenotype as male mice. Female MIP $\beta 1$ KO mice showed no significant decreases in glucose tolerance until 16 weeks of age, demonstrating there is some underlying protective factor in female mice that becomes lessened with age. Along this rationale of thinking, it is possible that the less overt phenotype observed in female mice throughout this study is primarily due to differences in the degree of $\beta 1$ knockdown due to dosage, age, or potentially through the protective effect of estrogen that has been observed in beta-cells of streptozotocin and alloxan treated female mice (Kilic et al. 2014, Le et al. 2006). It was apparent that the tamoxifen dosage used was sufficient to induce a significant knockdown of $\beta 1$ integrin in the pancreatic beta-cells of male MIP $\beta 1$ KO mice, and although there are no previous studies reporting gender differences in tamoxifen sensitivity (see Feil et al. 2009 for a review), it was clear that induction of the $\beta 1$ integrin knockdown did not increase with the dosage of tamoxifen given. The higher dosage used in this study as opposed to that used in Riopel (2011, 2013) was not sufficient to induce a significant reduction of $\beta 1$ integrin in female MIP $\beta 1$ KO mice.

4.2 Do MIP $\beta 1$ KO mice have impaired glucose tolerance and insulin secretion?

Unlike the previous study utilizing a global $\beta 1$ KO model (Riopel 2011, 2013), there was no difference in body weight, pancreatic weight and macrostructure between MIP $\beta 1$ KO and control mice. Although fasting blood glucose levels were only significantly elevated in female MIP $\beta 1$ KO mice and not males, both genders showed significantly elevated blood glucose levels during an IPGTT. Even though these findings are not in alignment with data published by Diaferia (2013), it is important to note that the knockout of $\beta 1$ integrin in our study was conducted in adult mice, without any time for compensation by

other integrins during embryonic and postnatal (p0-p21) development. The findings of glucose intolerance observed are more in agreement with published studies by Riopel (2011) and Cai (2012), where either knockdown of $\beta 1$ integrin in adults or knockout of FAK from conception leads to impaired glucose tolerance in adult life. Because there was no change in insulin tolerance in MIP $\beta 1$ KO mice, the prolonged elevation in blood glucose levels in both male and female mice are either indicative of a defect in insulin secretion, a reduction in beta-cell mass, or both. As such, an *in vivo* GSIS assay was conducted and plasma insulin levels were examined. Male MIP $\beta 1$ KO mice had significantly reduced plasma insulin levels after I.P glucose injection, indicating an overall decrease in total insulin production. However, female mice did not display a similar trend. To further assess if it was beta-cell dysfunction or some other underlying mechanism leading to reduced plasma insulin after an administered glucose load, islets were subjected to an *ex vivo* GSIS assay. Just as in Cai (2012), isolated islets had reduced insulin secretion in response to an increased concentration of glucose in the media. Basal insulin secretion levels were also reduced in male MIP $\beta 1$ KO indicating some impairment normal levels of insulin secretion. To understand what was leading to this impairment, an examination of exocytotic proteins involved in insulin secretion was conducted.

4.3 Are insulin secretory molecules altered in MIP $\beta 1$ KO mice?

It was clear in male MIP $\beta 1$ KO mice that there was reduced VAMP-2 and SNAP-25 at both the mRNA and protein level. This deficiency leads to impaired insulin vesicle docking, as the interaction between VAMP-2 on the membrane of vesicles and SNAP-25 on the plasma membrane is a requirement for proper vesicle fusion (Fasshauer 2002). Just as studies have shown that focal adhesion remodelling is required for proper glucose stimulated insulin secretion through FAK-paxillin interactions, which subsequently affect SNAP-25 levels (Rondas et al.2011, Cai et al. 2012), the $\beta 1$ integrin knockout in beta-cells of adult mice seems to have a similar effect. Although there were no changes in Stx1A and Stx3, a reduction in Munc18 protein was found. Munc18 is important in stabilizing the SNARE complex at the plasma membrane, mainly through interactions

with *Stx1A* (Thurmond 2013). No significant changes were observed in female MIP β 1KO mRNA levels of *Snap25*, *Vamp2*, *Stx1A*, and *Stx3*. The lack of a significant finding in insulin exocytotic proteins could potentially account for the indiscernible differences seen in glucose stimulated insulin secretion in female MIP β 1KO mice. These observations show that β 1 integrin is required for maintenance of normal physiological levels of insulin exocytotic machinery that are pivotal in maintaining normoglycemic levels.

4.4 Is β 1 integrin required for proper islet morphology?

Even though there was a defect in insulin secretion in MIP β 1KO mice, it was important to determine the changes of islet morphology and beta-cell mass. Both male and female MIP β 1KO mice, showed a decrease in beta-cell mass. This finding is in agreement with previous literature that sees a decrease in beta-cell proliferation when integrin is knocked out in beta-cells from conception (Diaferia et al. 2013), or knocked down globally in all *coll1a2* producing cells in adult mice (Riopel et al. 2011). In addition, when FAK, a key component in outside-in signalling of integrins is knocked down in beta-cells from conception a similar reduction in beta-cell mass is observed (Cai et al. 2012). To account for the reduction in beta-cell mass, cell cycle progression and apoptosis were examined. Akin to our previous publication (Riopel et al. 2011), a significant reduction in cyclin D1 was observed along with an increase in c-PARP in male MIP β 1KO mice, whereas females did not show significant changes in these markers, presumably from the protective effect of estrogen as mentioned previously. Despite only seeing a significant change in proliferation and apoptotic markers in male MIP β 1KO mice, this is most likely the cause for the decrease in beta-cell mass of female MIP β 1KO mice as well.

An interesting observation in the MIP β 1KO mice was a trend towards a decrease in alpha-cell mass in male mice, along with a significant reduction in female mice. In models of diet induced diabetes like the Goto-Kakizaki rat (Movassat et al. 1997) alpha-cell mass can be decreased when beta-cells are reduced. The defect in normal alpha-cell mass is attributed to abnormal islet-architecture from the distinct reduction in beta-cell population, which subsequently impacts cell-to-cell contacts within the islet, along with

reduced nutrient secretion and protein secretion important in eliciting normal ECM development in and around the islets.

With the overall decrease in beta-cell mass and changes in alpha-cell mass of MIP β 1KO mice, an overall examination of islet density was conducted. Male MIP β 1KO mice had fewer islets overall, which coincided with fewer medium (<501-2500 μm^2) and large (<2501-10000 μm^2) islets, and is similar to findings in Diaferia (2013). Female MIP β 1KO mice, however, had an increase in small islets (<500 μm^2) despite a trend towards decreased islet density. This increase in smaller islets, which was not seen in the males, clearly resulted in a greater number of islets per mm^2 compared to their male counterparts. Despite these differences, it was clear that MIP β 1KO mice have altered islet morphology compared to their control littermates.

One aspect that remained to be examined was that of transcription factors required for proper beta-cell differentiation and function. Both Pdx-1 and Nkx6.1 were reduced in the β 1KO model used in Riopel (2011) and have been shown to be important in beta-cell differentiation and proper maintenance and function in adult mice (McKinnon & Docherty 2011, Taylor et al. 2013). In the present study, male MIP β 1KO mice had a marked decrease in Pdx-1 mRNA and protein as assessed by qRT-PCR and western blot. However, there was no decrease in the number of Pdx-1⁺ cells beta-cells. This finding is in contrast to that of Diaferia (2013), where no change in Pdx-1 protein was observed. This could be due to the knockout of β 1 integrin at conception rather than in adulthood, giving beta-cells time to engage compensatory mechanisms that account for the lack of β 1 integrin and maintain normal expression levels of this transcription factor. Reduced Pdx-1 in male MIP β 1KO mice could be one factor that is responsible for the glucose intolerance, decreased insulin levels, and decreased beta-cell mass that was observed in them. Unlike the β 1KO model (Riopel et al. 2011, Riopel et al. 2013), there was no change in Nkx6.1 protein in MIP β 1KO mice. The changes in ECM composition observed in these previous studies, mainly a decrease in collagen fibers and connective tissue surrounding the islets, is a potential reason why there was a decrease in Nkx6.1 as well. The shift in ECM composition created a drastically different environment for the beta-

cells to reside, and subsequently may be the reason why Nkx6.1 was decreased in $\beta 1$ KO and not RIP $\beta 1$ KO or MIP $\beta 1$ KO mice.

4.5 Vasculature in the islets of MIP $\beta 1$ KO mice

Previous studies have shown that endothelial cells are required for proper deposition of the basement membrane, which in turn leads $\beta 1$ integrin to promote beta-cell proliferation and insulin gene expression (Nikolova, 2006). Additionally, adequate vasculature is required for beta-cells to sense changes in blood glucose as well as provide a pathway for insulin to be released and distributed throughout the body (Brissova, 2006). It has been established that PaSCs, which are myofibroblast-like cells, can promote endothelial cell proliferation via secretion of vascular endothelial growth factor (VEGF) (McCarroll et al. 2014). Based on these findings it is not surprising that vasculature was reduced in the $\beta 1$ KO model used by Riopel et al. (2011), in which both PaSCs and pericytes, cells that adhere and aid in vasculature formation in addition to ECM deposition, were both lacking $\beta 1$ integrin. Unlike this previous study where $\beta 1$ integrin was lacking in PaSCs and pericytes, our beta-cell specific knockout did not lead to a significant impairment in endothelial cell number and overall vascularization of islets. Although, these were only qualitative studies. Despite beta-cells having a role in VEGF secretion and recruitment of endothelial cells (Nikolova et al. 2006), having normal $\beta 1$ integrin levels in PaSCs and pericytes seems to overcome any deficit in VEGF-A secretion, allowing for normal islet vascularization in MIP $\beta 1$ KO mice.

4.6 Signalling in MIP $\beta 1$ KO mice

The role of $\beta 1$ integrin in regulating FAK and its downstream signalling molecules has been examined in a multitude of different cell types, including pancreatic beta-cells and beta-like cells (e.g., INS-1 cells). Our study found a significant reduction in the phosphorylation of FAK^{Y397}, and this is in alignment with several studies, all of which show that $\beta 1$ integrin is one regulator of phosphorylating FAK at tyrosine 397 (Hammer et al. 2004, Kaido et al. 2004, Wang et al. 2005, Krishnamurthy et al. 2008, Saleem et al. 2009, Riopel et al. 2011). FAK is responsible for regulating a multitude of downstream signalling molecules, one of which is ERK1/2, which has shown to be important in

maintaining function and survival in beta-cells and beta-like cells *in vitro* (Hammer et al. 2004, Krishnamurthy et al. 2008, Saleem et al. 2009) and beta-cells *in vivo* (Riopel et al. 2011, Cai et al. 2012). A significant reduction in phosphorylation of ERK1/2 was also found in the MIP β 1KO mice. Activation of ERK1/2 has been shown to play a role in beta-cell survival and Pdx-1 regulation (Hammer et al. 2004, Saleem et al. 2009, Krishnamurthy et al. 2008, Riopel et al. 2011, Dioum et al. 2010), as well as regulating glucose-stimulated insulin secretion mediated by actin remodelling (Tomas et al. 2006, Rondas et al. 2011). One-point worth noting is the fact that the RIP β 1KO model (Diaferia et al. 2013) had a reduction in ERK1/2 but showed no overt phenotype, this is most likely attributed to compensation by other integrins as mentioned throughout this discussion, which has led to the less overt phenotype in this mouse model compared to MIP β 1KO model, where the knockout was induced in adults and not from conception. An interesting finding that was not observed in the β 1KO mouse model (Riopel et al. 2011) was a decrease in pAkt^{S473}, which was also reduced in the RIP β 1KO model (Diaferia et al. 2013) and the beta-cell specific FAK knockdown model (Cai et al. 2012). Research has been published showing that FAK and Src which are downstream of integrins play a role in activation of p85 subunit of PI3K that leads to Akt^{S473} activation (Xia et al. 2004). Akt has been shown to play a significant role in cell survival by mediated apoptotic proteins such as Bcl2 while also preventing activation of caspase-9 (Song et al. 2005). As such, this pathway could also be contributing to the reduced survival of beta-cells observed in the MIP β 1KO mouse model.

4.7 Aged MIP β 1KO mice and a lack of functional compensation by other integrins

One of the more interesting aspects of integrin signalling is the ability to have compensatory outside-in signalling through increased expression of other integrin subunits when one is impaired (Diaferia et al. 2013). The low proliferative rate of beta-cells in mammals should lead to maintenance of the β 1 integrin knockdown in the majority of the beta-cell population, providing ample opportunity for compensation by other integrins within affected beta-cells (Kushner 2013). It has been shown that β 3 and β 5 integrins can maintain and enhance cellular differentiation when β 1 integrin is either

functionally blocked or deleted at the gene level (Brunetta 2012, Guan 2001, Hirsch 1998, Jeanes 2012, Retta 1998). Diaferia (2013) reported an up-regulation of vitronectin and the laminin-5 β -chain in their RIP β 1KO model, which are known ECM ligands of the α v β 3 and α 6 β 4 integrins, respectively. In the present study, the α 3 integrin subunit, known to form a heterodimer with β 1 integrin, showed no change in mRNA, whereas immunofluorescence staining showed a qualitative increase in this protein indicating a possible compensation through upregulation of α 3 integrin. Interestingly the mRNA of α v and α 6 was relatively low, but no difference at the protein level as assessed by immunofluorescence staining was observed. These two integrins are associated with other β subunits, indicating that loss of β 1 integrin did not increase other integrin expression such as α 6 β 4 and α v associated β subunits. Since there is no significant increase of other α β integrin expression in MIP β 1KO islets, mice were aged to see if they could recover from the glucose intolerant phenotypes observed at their respective time points. It was clear that the initial knockout of β 1 integrin at 3-4 weeks of age was significant enough to impact beta-cell function long-term, since the aged mice still displayed glucose intolerance, more-so than they did 8 and 16 weeks post-tamoxifen. Age, in addition to the initial knockdown of β 1 integrin, could therefore play a factor in this increase in impaired glucose metabolism observed in the aged mice due to the lack of compensation through other integrins in the beta-cells of MIP β 1KO mice.

4.8 Limitations of the study

One of the limitations in using a mouse model is that it does not directly translate to humans. There are distinct differences in ECM composition, islet organization, diet and living conditions that all directly influence the outcomes that are observed. Regarding ECM composition, it has been shown that mice and humans, for example, have overlap in terms of laminin isoforms that they interact with (such as laminin-8), yet murine islets express laminin-10 as well, which is absent in human islets (Otonkoski et al. 2008). Such small variations in ECM composition might not seem like much, but when one compares the 804G matrix (rich in laminin-5) to commercially available Matrigel (containing Laminin-1), islet cells will differentiate in Matrigel to pancreatic ductal cells, whereas the 804G matrix does not have this effect (Gao et al. 2003, Bonner-Weir et al. 2000).

Although $\beta 1$ integrin has high variability in terms of its ability to interact with a plethora of ECM ligands through the 11 different α subunits it associates with, the overlap of other integrins and differences in ECM composition and integrin expression in murine compared to human islets and beta-cells should not be dismissed.

One fundamental issue with the RIP mouse line used to drive Cre recombinase was ectopic expression found in the hypothalamus, potentially leading to differences in metabolism and energy maintenance (Wicksteed et al. 2010). Despite initial reports stating that the MIP construct was beta-cell specific (Tamarina et al. 2014), a study using more sensitive measures has detected the presence of MIP in the hypothalamus as well (Wang et al. 2014). Therefore, utilizing MIP to induce beta-cell gene knockouts face the same confounding variables as the RIP construct.

Another issue with using transgenic mouse lines is the methodology used to incorporate our transgene of interest. In the case of many transgenic mice, the human growth hormone (hGH) is included in order to increase transgene expression (Brinster et al. 1988, Palmiter et al. 1983, Palmiter et al. 1991). It was originally thought that the transgene was not transcribed and translated into growth hormone, but recent studies have shown its presence in beta-cells (Brouwers et al. 2014). The RIP-Pdx1^{late} mouse line have lower blood glucose, increased beta-cell mass and are resistant towards STZ-induced beta-cell death due to binding of hGH to prolactin receptor which stimulates serotonin production within beta-cells (Baan et al. 2015). Within the present study, we incorporated both MIP⁺/ $\beta 1$ ^{+/+} and MIP⁻/ $\beta 1$ ^{fl/fl} into the control group, but when strictly comparing MIP⁺/ $\beta 1$ ^{+/+} mice to MIP⁺/ $\beta 1$ ^{fl/fl} mice, we still found that the knockdown mice were glucose intolerant at both the adult and aged time points. Despite this finding, the presence of the hGH construct should not be ignored when assessing MIP $\beta 1$ KO mice and how the findings might accurately translate to human physiology.

One final limitation worth noting is that the decrease in $\beta 1$ integrin was roughly ~40% in beta-cells of MIP $\beta 1$ KO mice compared to controls, therefore being only a partial knockdown. Because the beta-cells still have more than 50% of remaining $\beta 1$ integrin levels, the effect of a total knockdown in adult mouse beta-cells remains unknown.

Additionally, with the corresponding amount of $\beta 1$ integrin protein present, it is possible this prevented any significant upregulation of other integrins in an attempt to compensate, unlike the compensation that was seen in the RIP $\beta 1$ KO mouse line from conception. Overall, the effects of complete $\beta 1$ integrin knockdown in adult murine beta-cells remains to be determined.

4.9 Conclusions and future directions

This study demonstrates that subnormal physiological levels of $\beta 1$ integrin in the beta-cells of murine islets leads to pathological distress, more so in males than in females as previously described. The mice are unable to overcome the deficit in $\beta 1$ integrin and results in impaired glucose tolerance and insulin secretory machinery. The reduction in $\beta 1$ integrin leads to reduced beta-cell mass and altered islet size and density, along with increased apoptosis and decreased proliferation. The signalling pathways downstream of $\beta 1$ integrin (FAK/ ERK1/2 and Akt) are also affected by reduced $\beta 1$ integrin levels, leading to the observed phenotype. A summary of the key findings of this study is presented in **Figure 4.1**.

The overall significance of this study stems from islet transplantation as a method to treat T1D. One of the fundamental issues is a lack of donor tissue, so finding optimum conditions to reproduce native environments is of utmost importance in order to maintain survivability of isolated islets, and perhaps in the future, to maintain and reproduce stem-cell derived beta-like cells. One promising avenue is the concept of encapsulating islets, or even just beta-cells themselves, to prevent an autoimmune attack (Vegas et al. 2016). However, ensuring survival of these cells requires not only protection from the immune system, but a sustainable environment as well. The importance of the ECM has been well documented throughout this dissertation, and elucidating the role of integrin receptors and their interaction with ECM ligands is paramount in constructing a long-term cure for treatment of T1D.

One future avenue of research utilizing the MIP $\beta 1$ KO model would be to assess what happens during murine embryonic development. Inducing a knockdown of $\beta 1$ integrin during both the second and third phases of development will not only provide insight into

its role during the aforementioned periods, but allowing these mice to age to adults would allow time to see if the organisms can compensate for this deficit. By determining alternative pathways or proteins that can aid in maintaining the functional state of beta-cells, or determining what is absolutely required as the animals progress from embryonic to adults, one can further the knowledge required for finding ways to treat diabetes.

Finally, finding a relationship between $\beta 1$ integrin and proteins involved in the SNARE complex that is essential for not only insulin secretion, but docking of integrins to the plasma membrane is a novel area of study. This study has shown that a reduction in $\beta 1$ integrin affects SNAP25 and Munc18 mRNA and protein, which is a novel finding. Studies examining this relationship might provide future ideas for ways to enhance beta-cell insulin secretion through ECM or integrin interactions.

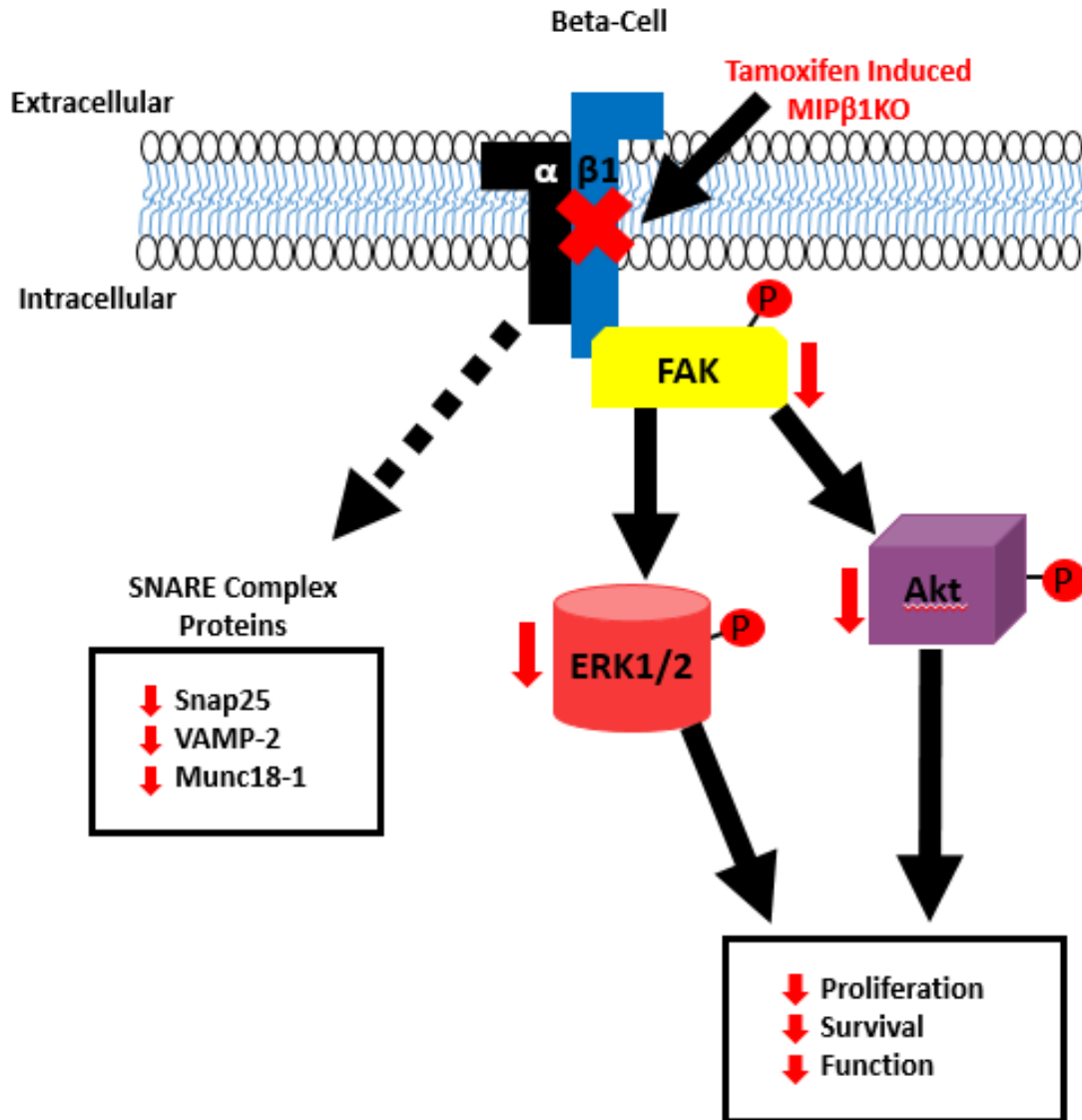


Figure 4.1 Impact of the MIP $\beta 1$ KO model in male mice

The tamoxifen induced beta-cell specific knockout of $\beta 1$ integrin lead to a multitude of impairments in male MIP $\beta 1$ KO mice. A reduction in the SNARE complex proteins Snap25, Vamp-2 and Munc18-1 was observed, however the mechanisms that lead to this reduction remain to be seen. A reduction in phosphorylated (P) FAK, ERK1/2 and Akt was also observed, and these proteins have been shown to play a role in mediating beta-cell proliferation, survival, and function.

Chapter 5 - References

Afelik S, Jensen J. Notch signaling in the pancreas: patterning and cell fate specification. *WIREs Dev Biol* 2012;2:531–544.

Afelik S, Qu X, Hasrouni E, Bukys MA, Deering T, Nieuwoudt S, et al. Notch-mediated patterning and cell fate allocation of pancreatic progenitor cells. *Development* 2012;139:1744–53.

Ahlgren U, Jonsson J, Jonsson L, Simu K, Edlund H. Beta-cell specific inactivation of the mouse *Ipfl/Pdx1* gene results in loss of beta-cell phenotype and maturity onset diabetes. *Genes Dev* 1998;12(12):1763-1768.

Allan LA, Morrice N, Brady S, Magee G, Pathak S, Clarke PR. Inhibition of caspase-9 through phosphorylation at Thr 125 by ERK MAPK. *Nat Cell Biol* 2003;5:647-654.

Apte MV, Pirola RC, Wilson JS. Pancreatic stellate cells: a starring role in normal and diseased pancreas. *Front Physiol* 2012;28(3):344.

Asfari M, Janic D, Meda P, Li G, Halban PA, Wollheim CB. Establishment of 2-mercaptoethanol-dependent differentiated insulin-secreting cell lines. *Endocrinology* 1992;130(1):167-178.

Ashcroft FM, Harrison DE, Ashcroft SJ. Glucose induces closure of single potassium channels in isolated rat pancreatic beta-cells. *Nature* 1984;312(5993):446-448.

Aszódi A, Hunziker EB, Brakebusch C, Fässler R. Beta1 integrins regulate chondrocyte rotation, G1 progression, and cytokinesis. *Genes Dev* 2003;17:2465–2479.

Aszódi A, Legate KR, Nakchbandi I, Fässler R. What mouse mutants teach us about extracellular matrix function. *Annu Rev Cell Dev Biol* 2006;22:591-621.

Baan M, Kibbe CR, Bushkofsky JR, Harris TW, Sherman DS, Davis DB. Transgenic expression of the human growth hormone minigene promotes pancreatic β -cell proliferation. *Am J Physiol Regul Integr Comp Physiol* 2015;309:R788-R794.

Bailey CJ. Metformin – an update. *Gen Pharmacol.* 1993;24:1299-1309.

Bailey CJ. Biguanides and NIDDM. *Diabetes care* 1992;15:755-772.

Bailey CJ & Puaiah JA. Effect of metformin on glucose metabolism in mouse soleus muscle. *Diabetes Metab* 1986;12:212-218.

Barczyk M, Carracedo S & Gullberg, D. Integrins. *Cell Tissue Res* 2010;339:269-280.

Belvindrah R, Graus-Porta D, Goebbels S, Nave KA, Müller U. Beta1 integrins in radial glia but not in migrating neurons are essential for the formation of cell layers in the cerebral cortex. *J Neurosci* 2007;27:13854–13865.

Bersell K, Choudhury S, Mollova M, Polizzotti BD, Ganapathy B, Walsh S, et al. Moderate and high amounts of tamoxifen in α MHC-MerCreMer mice induce a DNA damage response, leading to heart failure and death. *Dis Model Mech* 2013;6(6):1459-1469

Bonner-Weir S, Taneja M, Weir GC. In vitro cultivation of human islets from expanded ductal tissue. *Proc Natl Acad USA* 2000;97(14):7999-8004.

Boucher J, Kleinridders A, Khan CR. Insulin receptor signaling in normal and insulin-resistant states. *Cold Spring Harb Prospect Biol* 2014;6:a009191.

Bouwens L, Lu WD, Dr Krijger R. Proliferation and differentiation in the human fetal endocrine pancreas. *Diabetologia* 1997;40(4):398-404.

Brakebusch, C, Fässler, R. The Integrin-Actin Connection, an Eternal Love Affair. *EMBO J* 2003; 22(10):2324-2333.

Brakebusch C, Fässler R. Beta 1 integrin function in vivo: adhesion, migration and more. *Cancer Metastasis Rev* 2005;24:403–411.

Brakebusch C, Grose R, Quondamatteo F, Ramirez A, Jorcano JL, Pirro A, et al. Skin and hair follicle integrity is crucially dependent on beta 1 integrin expression on keratinocytes. *EMBO J.* 2000;19:3990–4003.

Brinster RL, Allen JM, Behringer RR, Gelinas RE, Palmiter RD. Introns increase transcriptional efficiency in transgenic mice. *Proc Natl Acad Sci USA* 1991;85:836-840.

Brissova M, Shostak A, Shiota M, Wiebe PO, Poffenberger G, Kantz J, et al. Pancreatic islet production of vascular endothelial growth factor-a is essential for islet vascularization, revascularization, and function. *Diabetes* 2006;55(11):2974–2985.

Brouwers B, de Faudeur G, Osipovich AB, Goyvaerts L, Lemaire K, Boesmans L. et al. Impaired islet function in commonly used transgenic mouse lines due to human growth hormone minigene expression. *Cell Metab* 2014;20:970-990.

Brown H, Meister B, Deeney J, Corkey BE, Yang SN, Larrison O, et al. Synaptotagmin III isoform is compartmentalized in pancreatic beta-cells and has a functional role in insulin exocytosis. *Diabetes* 2000;49(3):383-391.

Brunetta I, Casalotti SO, Hart IR, Forge A, Reynolds LE. β 3-integrin is required for differentiation in OC-2 cells derived from mammalian embryonic inner ear. *BMC Cell Biol* 2012;13(5).

Burkin DJ, Wallace GQ, Nicol KJ, Kaufman DJ, Kaufman SJ. Enhanced expression of the alpha 7 beta 1 integrin reduces muscular dystrophy and restores viability in dystrophic mice. *J Cell Biol* 2001;152:1207–1218.

Cai EP, Casimir M, Schroer SA, Luk CT, Shi SY, Choi D, et al. In vivo role of focal adhesion kinase in regulating pancreatic beta-cell mass and function through insulin signaling, actin dynamics, and granule trafficking. *Diabetes* 2012;61:1708-1718.

Cigolini M, Bosello O, Zancanaro C, Orlandi PG, Fezzi O, Smith U. Influence of metformin on metabolic effect of insulin in human adipose tissue in vitro. *Diabete Metab* 1984;10:311-315

Cirulli V, Beattie GM, Klier G, Ellisman M, Ricordi C, Quaranta V, et al. Expression and function of alpha(v)beta(3) and alpha(v)beta(5) integrins in the developing pancreas: roles in adhesion and migration of putative endocrine progenitor cells. *J Cell Biol* 2000;150(6):1445-1460.

Clark EA, Brugge JS. Integrins and signal transduction pathways: the road taken. *Science* 1995;268:233-239.

Collombat P, Mansouri A, Hecksher-Sorensen J, Serup P, Krull J, Gradwohl G, et al. Opposing actions of Arx and Pax4 in endocrine pancreas development. *Genes Dev* 2003;17:2591–2603.

Cordes N, Seidler J, Durzok R, Geinitz H, Brakebusch C. Beta-1-integrin-mediated signaling essentially contributes to cell survival after radiation-induced genotoxic injury. *Oncogene* 2006;25:1378-1390.

Danen EHJ & Sonnenberg A. Integrins in regulation of tissue development and function. *J Pathol* 2003;200:471-480.

Denk F, Ramer LM, Erskine EL, Nassar MA, Bogdanov Y, Signore M, et al. Tamoxifen induces cellular stress in the nervous system by inhibiting cholesterol synthesis. *Acta Neuropathol Commun* 2015;3:74-89

Diaferia GR, Jimenez-Caliani AJ, Ranjitkar P, Yang W, Hardiman G, Rhodes CJ, et al. Beta1 integrin is a crucial regulator of pancreatic beta-cell expansion. *Development* 2013;140:3360-72.

Dioum EM, Schneider JW, Cobb MH. Contribution of MAP kinases ERK1/2 in beta-cell function. *FASEBJ* 2010;24(1):Supplemental 659.5

Fasshauer D. Structural insights into the SNARE mechanism. *Biochim Biophys Acta* 2003;1641(2-3):87-97.

Feil S, Valtcheva N, Fiel R. Inducible cre mice. *Methods Mol Biol* 2009;530:343-363.

Feng ZC, Li J, Turco BA, Riopel M, Yee SP, Wang R. Critical role of c-Kit in beta cell function: increased insulin secretion and protection against diabetes in a mouse model. *Diabetologia* 2012;55:2214-2225.

Feng ZC, Popell A, Li J, Silverstein J, Oakie A, Yee SP, et al. c-Kit receptor signaling regulates islet vasculature, β -cell survival, and function in vivo. *Diabetes* 2015;64(11):3852-3866.

Fujimoto K, Polonsky KS. Pdx1 and other factors that regulate pancreatic beta-cell survival. *Diabetes Obes Metab* 2009;11(4):30-37.

Furuyama K, Kawaguchi Y, Akiyama H, Horiguchi M, Kodama S, Kuhara T, et al. Continuous cell supply from a Sox9-expressing progenitor zone in adult liver, exocrine pancreas, and intestine. *Nat Genet* 2011;43(1):34-41.

Galsuka D, Nolte LA, Zierath JR, Wallberg-Henriksson H. Effect of metformin on insulin-stimulated glucose transport in isolated skeletal muscle obtained from patients with NIDDM. *Diabetologia*. 1994;37:826-832

Gannon M, Ables ET, Crawford L, Lowe D, Offield MF, Magnuson MA, et al. Pdx-1 function is specifically required in embryonic β cells to generate appropriate numbers of endocrine cell types and maintain glucose homeostasis. *Dev Biol* 2008;314:406–417

Gao R, Ustinov J, Pulkkinen MA, Lundin K, Korsgen O, Otonkoski T. Characterization of endocrine progenitor cells and critical factors for their differentiation in human adult pancreatic cell culture. *Diabetes* 2003;52(8):2007-2015.

Giancotti FG, Guo W. Integrin signalling during tumor progression. *Nat Rev Mol Cell Biol* 2004;5:816-826.

Giancotti FG, Ruoslahti E. Integrin signaling. *Science* 1999;285:1028-1032.

Guan K, Cyzy J, Fürst DO, Wobus AM. Expression and cellular distribution of $\alpha(v)$ integrins in $\beta(1)$ integrin-deficient embryonic stem cell-derived cardiac cells. *J Mol Cell Cardiol* 2001;33(3):521-532.

Hald J, Sprinkel AE, Ray M, Serup P, Wright C, Madsen OD. Generation and characterization of Ptf1a antiserum and localization of Ptf1a in relation to Nkx6.1 and

Pdx1 during the earliest stages of mouse pancreas development. *J Histochem Cytochem* 2008;56:587–595.

Hammer E, Parnaud G, Bosco D, Perriraz N, Maedler K, Donath M, et al. Extracellular matrix protects pancreatic beta-cells against apoptosis: role for short- and long-term signaling pathways. *Diabetes* 2004;53(8):2034-2041.

Harada T, Morooka T, Ogawa S, Nishida E. ERK induces p35, a neuron-specific activator of Cdk5, through induction of Egr1. *Nat Cell Biol* 2001;3:453-459.

Harburger DS, Calderwood DA. Integrin signalling at a glance. *J Cell Sci* 2009;122:159-163.

Henseleit KD, Nelson SB, Kuhlbrodt K, Hennings JC, Ericson J, Sander M. NKX6 transcription factor activity is required for α - and β -cell development in the pancreas. *Development* 2005;132:3139–3149.

Hirsch E, Lohikangas L, Gullberg D, Johansson S, Fässler R. Mouse myoblast can fuse and form a normal sarcomere in the absence of beta1 integrin expression. *J Cell Sci* 1998;111:2397-2409.

Hoenig M & Sharp GWG. Glucose induces insulin release and a rise in cytosolic calcium concentration in a transplantable rat insulinoma. *Endocrinology* 1986;119:2502–2507.

Holland AM, Hale MA, Kagami H, Hammer RE, MacDonald RJ. Experimental control of pancreatic development and maintenance. *Proc Natl Acad Sci USA* 2002;99:12236–12241.

Hynes RO. Integrins: bidirectional, allosteric signaling machines. *Cell* 2002;110:673–687.

Huh WJ, Khurana SS, Geahlen JH, Kohli K, Waller RA, Mills JC. Tamoxifen induces rapid, reversible atrophy, and metaplasia in mouse stomach. *Gastroenterology* 2012;142(1):21-24.

Jeanes AI, Wang P, Moreno-Layseca P, Paul N, Cheung J, Tsang R, et al. Specific β -containing integrins exert differential control on proliferation and two-dimensional collective cell migration in mammary epithelial cells. *J Biol Chem* 2012;287(29):24103-24112.

Jahn R, Scheller RH. SNAREs – engines for membrane fusion. *Nat Rev Mol Cell Biol* 2006;7(9):631-643.

Kaido T, Perez B, Yebra, Hill J, Cirulli V, Hayek A, et al. α v-integrin utilization in human β -cell adhesion, spreading, and motility. *J Biol Chem* 2004b;279(17):17731-17737.

Kaido T, Yebra M, Cirulli V, Montgomery AM. Regulation of human beta-cell adhesion, motility, and insulin secretion by collagen IV and its receptor α 1 β 1. *J Biol Chem* 2004a;279(51):53762-53769.

Kalwat MA, Thurmond DC. Signaling mechanisms of glucose-induced F-actin remodeling in pancreatic islet β cells. *Exp Mol Med* 2013;45:e37

Kang Y, Huang X, Pasyk EA, Ji J, Holz CG, Wheeler MB, et al. Syntaxin-3 and syntaxin-1A inhibit L-type calcium channel activity, insulin biosynthesis and exocytosis in beta-cell lines. *Diabetologia* 2002;45:231-241.

Kantengwa S, Baetens D, Sadoul K, Buck CA, Halban PA, Rouiller DG. Identification and characterization of α 3 β 1 integrin on primary and transformed rat islet cells. *Exp Cell Res* 1997;237:394-402.

Kasai H, Takahashi N, Tokumaru H. Distinct initial SNARE configurations underlying the diversity of exocytosis. *Physiol Rev* 2012;92:1915-1964.

Kaung HL. Growth dynamics of pancreatic islet cell populations during fetal and neonatal development of the rat. *Dev Dyn* 1994;200(2):163-175.

Kawaguchi Y, Cooper B, Gannon M, Ray M, MacDonald RJ, Wright CV. The role of the transcription factor Ptf1a in converting intestinal to pancreatic progenitors. *Nat Genet* 2002;32(1):128-134.

Kilic G, Alvarez-Mercado AI, Zarrouki B, Opland D, Liew CW, Alonso LC, et al. The islet estrogen receptor- α is induced by hyperglycemia and protects against oxidative stress-induced insulin-deficient diabetes. *PLoS One* 2014;9(2):e87941-

Kim A, Miller K, Jo J, Kilimnik G, Wojcik P, Hara M. Islet architecture: a comparative study. *Islets* 2009;1(2):129-36.

Kleinman HK, Philp D & Hoffman MP. Role of the extracellular matrix in morphogenesis. *Curr Opin Biotechnol* 2003;14:526-532.

Kloker S, Major MB, Calderwood DA, Ginsberg MH, Jones DA, Beckerle MC. The kindler syndrome protein is regulated by transforming growth factor- β and involved in integrin-mediated adhesion. *J Biol Chem* 2004;279(8):6824-6833.

Krapp A, Knofler M, Frutiger S, Hughes GJ, Hagenbuchle O, Wellauer PK. The p48 DNA-binding subunit of transcription factor PTF1 is a new exocrine pancreas-specific basic helix-loop-helix protein. *EMBO Journal* 1996;15:4317-4329.

Krishnamurthy M, Li J, Al-Masri M, Wang R. Expression and function of α 1 integrins in pancreatic (INS-1) cells. *J Cell Commun Signal* 2008;2(3-4):67-79.

Kushner JA. The role of aging upon β cell turnover. *J Clin Invest* 2013;123(3):990-995.

Kushner JA, Ciemerych MA, Sicinska E, Wartschow LM, Teta M, Long S, et al. Cyclins D2 and D1 are essential for postnatal pancreatic beta-cell growth. *Mol Cell Biol* 2005;25:3752-3762.

Langerhans P (1869). "Beitrage zur mikroskopischen anatomie der bauchspeichel druse". Inaugural-dissertation. Berlin: Gustav Lange

Lambeir AM, Durinx C, Sharpé S, De Meester I. Dipeptidyl-peptidase IV from bench to bedside: an update on structural properties, functions, and clinical aspects of the enzyme DPP IV. *Crit Rev Clin Lab Sci* 2003;40(3):209-294.

Le May C, Chu K, Hu M, Ortega CS, Simpson ER, Tsai MJ, et al. Estrogens protect pancreatic beta-cells from apoptosis and prevent insulin-deficient diabetes mellitus in mice. *Proc Natl Acad Sci USA* 2006;103(24):9232-9237.

Leibiger B, Leibiger IB, Moede T, Kemper S, Kulkarni RN, Khan R et al. Selective insulin signaling through A and B insulin receptors regulates transcription of insulin and glucokinase genes in pancreatic β cells. *Mol Cell* 2001;7(3):559-70.

Liang T, Qin T, Xie L, Dolai S, Zhu D, Prentice KJ et al. New roles of syntaxin-1A in insulin granule exocytosis and replenishment. *J Biol Chem* 2013;292(6):2203-2216.

Lim ST, Mikolon D, Stupack DG, Schlaepfer DD. FERM control of FAK function: implications for cancer therapy. *Cell Cycle* 2008;7:2306–2314.

Liu S, Kapoor M, Denton C, Abraham DJ, Leask A. Loss of β 1-integrin in mouse fibroblasts results in resistance to skin scleroderma in a mouse model. *Arthritis Rheum* 2009;60(9):2817–2821.

McCarroll JA, Naim S, Sharbeen G, Russia N, Lee J, Kavallaris M, et al. Role of pancreatic stellate cells in chemoresistance in cancer cells. *Front Physiol* 2014;5:141-150.

McKinnon CM, Docherty K. Pancreatic duodenal homeobox-1, Pdx-1, a major regulator of beta cell identity and function. *Diabetologia* 2001; 44(10):1203-1214.

McLean GW, Carragher NO, Avizienyte E, Evans J, Brunton VG, Frame MC. The role of focal-adhesion kinase in cancer – a new therapeutic opportunity. *Nat Rev Cancer* 2005;5:505-515.

Mettouchi A & Meneguzzi G. Distinct roles of β 1 integrins during angiogenesis. *Eur J Cell Biol* 2006;85:243–247.

- Meulen T, Huising M. Role of transcription factors in the transdifferentiation of pancreatic islet cells. *J Mol Endocrinol* 2015;54(2):R103-R117.
- Movassat J, Saulnier C, Serradas P, Portha B. Impaired development of pancreatic beta-cell mass is a primary event during the progression to diabetes in the GK rat. *Diabetologia* 1997;40(8):916-925.
- Nikolova G, Jabs N, Konstantinova I, Domogatskaya A, Tryggvason K, Sorokin L, et al. The vascular basement membrane: a niche for insulin gene expression and beta-cell proliferation. *Dev Cell* 2006;10(3):397-405.
- Oh E, Thurmond DC. Munc18c depletion selectively impairs the sustained phase of insulin release. *Diabetes* 2009;58:1165-1174.
- Offield MF, Jetton TL, Labosky PA, Ray M, Stein RW, Magnuson MA, et al. PDX-1 is required for pancreatic outgrowth and differentiation of the rostral duodenum. *Development* 1996;122(3):983-995.
- Otonkoski T, Banerjee M, Korsgren O, Thornell LE, Virtanen I. Unique basement membrane structure of human pancreatic islets: implications for beta-cell growth and differentiation. *Diabetes Qbes Metab* 2006;10(4):119-127.
- Palmiter RD, Norstedt G, Gelinas RE, Hammer RE, Brinster RL. Methallothionein-human GH fusion genes stimulate growth of mice. *Science* 1983;222:809-814.
- Palmiter RD, Sandgren EP, Avarbock MR, Allen DD, Brinster RL. Heterologous introns can enhance expression of transgenes in mice. *Natl Acad Sci USA* 1991;88:478-482.
- Pan FC, Bankaitis ED, Boyer D, Xu X, van de Casteele M, Magnuson MA, et al. Spatiotemporal patterns of multipotentiality in *Ptf1a*-expressing cells during pancreas organogenesis and injury-induced facultative restoration. *Development* 2013;140:751-764.

Parnaud G, Hammer E, Rouiller DG, Armanet M, Halban PA, Bosco DL. Blockade of β 1 integrin-laminin-5 interaction affects spreading and insulin secretion of rat β -cells attached on extracellular matrix. *Diabetes* 2006;55(5):1413-1420.

Phillips DH. Understanding the genotoxicity of tamoxifen. *Carcinogenesis* 2011;22(6):839-849.

Retta SF, Balzac F, Ferraris P, Belkin AM, Fässler R, Humphries MJ, et al. Beta1-integrin cytoplasmic subdomains involved in dominant negative function. *Mol Biol Cell* 1998;9(4):715-731.

Riopel M, Krishnamurthy M, Li J, Liu S, Leask A, Wang R. Conditional β 1-integrin-deficient mice display impaired pancreatic β cell function. *J Pathol* 2011;224(1):45-55.

Riopel MM, Li J, Liu S, Leask A, Wang R. β 1 integrin-extracellular matrix interactions are essential for maintaining exocrine pancreas architecture and function. *Lab Invest* 2013;93(1):31-40.

Rosetti L, DeFonzo RA, Gherzi R, Stein P, Andraghetti G, Falzetti G, et al. Effect of metformin treatment on insulin action in diabetic rats: in vivo and in vitro correlations. *Metabolism* 1990;39:425-435.

Rondas D, Tomas A, Halban PA. Focal adhesion remodeling is crucial for glucose-stimulated insulin secretion and involves activation of focal adhesion kinase and paxillin. *Diabetes* 2011;60:1146-1157.

Rondas D, Tomas A, Soto-Riberio M, Wehrle-Haller B, Halban PA. Novel mechanistic link between focal adhesion remodeling and glucose-stimulated insulin secretion. *J Biol Chem* 2012;287(4):2423-2436.

Rosso F, Giordano A, Barbarisi M, Barbarisi A. From cell-ECM interactions to tissue engineering. *J Cell Physiol* 2004;199:174-180.

Ryan EA, Paty BW, Senior PA, Bigam D, Alfadhi E, Kneteman NM, et al. Five-year follow-up after clinical islet transplantation. *Diabetes* 2005;54:2060-2069.

Rother KI, Harlan DM. Challenges facing islet transplantation for the treatment of type 1 diabetes mellitus. *J Clin Invest* 2004;14:877-83.

Saleem S, Li J, Yee SP, Fellows GF, Goodyer CG, Wang R. β 1 integrin/FAK/ERK signalling pathway is essential for human fetal islet cell differentiation and survival. *J Pathol* 2009;219(2):182-192.

Scaglia L, Cahill CJ, Finegood DT, Bonner-Weir S. Apoptosis participates in the remodeling of the endocrine pancreas in the neonatal rat. *Endocrinology* 1997;138(4):1736-1741.

Schaller, M. D. (2001). Biochemical signals and biological responses elicited by the focal adhesion kinase. *Biochim Biophys Acta* 2001;1540:1-21.

Schmittgen TD, Lee EJ, Jiang J. High-throughput real-time PCR. *Methods Mol Biol* 2008;429:89-98.

Schwander M, Leu M, Stumm M, Dorchies OM, Ruegg UT, Schittny J, et al. β 1 integrins regulate myoblast fusion and sarcomere assembly. *Dev Cell* 2003;4:673-685.

Shih HP, Kopp JL, Sandhu M, Dubois CL, Seymour PA, Grapin-Bottton A, et al. A notch-dependent molecular circuitry initiates pancreatic endocrine and ductal cell differentiation. *Development* 2012;139(14):2488-2499.

Shih HP, Wang A, Sander M. Pancreas organogenesis: from lineage determination to morphogenesis. *Annu Rev Cell Dev Biol* 2013;29:81-105.

Shapiro AM, Lakey JR, Ryan EA, Korbitt GS, Toth E, Warnock GL, et al. Islet transplantation in seven patients with type 1 diabetes mellitus using a glucocorticoid-free immunosuppressive regimen. *N Engl J Med* 2000;343:230-238.

Song G, Ouyang G, Bao S. The activation of Akt/PKB signaling pathway and cell survival. *J Cell Mol Med* 2005;9(1):59-71.

Sosa-Pineda B, Chowdhury K, Torres M, Oliver G, Gruss P. The Pax4 gene is essential for differentiation of insulin-producing β cells in the mammalian pancreas. *Nature* 1997;386:399–402.

Springer TA, Dustin ML. Integrin inside-out signaling and the immunological synapse. *Curr Opin Cell Biol* 2012;24:107-15.

Straub SG, Sharp GWG. Glucose-stimulated signaling pathways in biphasic insulin secretion. *Diabetes Metab Res Rev* 2002;18:451-463.

Streuli C. Extracellular matrix remodelling and cellular differentiation. *Curr Opin Cell Biol* 1999;11:634-64

Stupack DG, Cheresch DA. Get a ligand, get a life: integrins, signaling and cell survival. *J Cell Sci* 2002;115, 3729-3738.

Takada Y, Ye X, Simon S. The integrins. *Genome Biol* 2007;8:215.1-215.9.

Tamarina NA, Roe MW, Philipson L. Characterization of mice expression ins1 gene promoter driven creERT recombinase for conditional gene deletion in pancreatic β -cells. *Islets* 2014;6(1):e27685.

Tateishi K, He J, Taranova O, Liang G, D'Alessio AC, Zhang Y. Generation of insulin secreting islet-like clusters from human skin fibroblasts. *J Biol Chem* 2008;283:31601-31607.

Taylor BL, Fen-Fen L, Sander M. Nkx6.1 is essential for maintaining the functional state of pancreatic beta cells. *Cell Rep* 2013;4(6):1262-1275.

Tellam JT, McIntosh S, James DE. Molecular identification of two novel Munc-18 isoforms expressed in non-neronal tissues. *J Biol Chem* 1995;270(11):5857-5863

Thurmond DC. Regulation of insulin action and insulin secretion by SNARE-mediated vesicle exocytosis. *Madame Curie Bioscience Database [Internet]* 2000-2013.

Trinder M, Zhou L, Oakie A, Riopel M, Wang R. β -cell insulin receptor deficiency during in utero development induces an islet compensatory overgrowth response. *Oncotarget* 2016;7:44927-44940.

Tomas A, Yerman B, Min L, Pessin JE, Halban PA. Regulation of pancreatic beta-cell insulin secretion by actin cytoskeleton remodelling: role of gelsolin and cooperation with the MAPK signalling pathway. *J Cell Sci* 2006;15(119):2156-2167.

Turner CE. Paxillin and focal adhesion signalling. *Nat Cell Biol* 2000;2(12):E231-E236.

Ungar D, Hughson FM. SNARE protein structure and function. *Annu Rev Cell Dev Biol* 2003;19:493-517.

Vegas AJ, Veisoh M, Gürtler M, Millman JR, Pagliuca FW, Bader AR, et al. Long-term glycemic control using polymer-encapsulated human stem cell-derived beta cells in immune-competent mice. *Nature Medicine* 22;2016:306-311.

Versophl EJ. Novel therapeutics for type 2 diabetes: incretin hormone mimetics (glucagon-like peptide-1 receptor agonists) and dipeptidyl peptidase-4 inhibitors. *Pharmacol Ther* 2009;124(1):113-138.

Wang CX, Song JH, Song DK, Yong VW, Shuaib A, Hao C. Cyclin-dependent kinase-5 prevents neuronal apoptosis through ERK-mediated upregulation of Bcl-2. *Cell Death Differ* 2006;13:1203-121.

Wang JH. Pull and push: talin activation for integrin signaling. *Cell Res* 2012;22(11):1512-1514.

Wang RN, Li J, Lyte K, Yashpal NK, Fellows F, Goodyear C. Role of β 1 integrin and its associated α 3, α 5, and α 6 subunits in the development of the human fetal pancreas. *Diabetes* 2005;54(7):2080-2090.

Wang RN, Paraskevas S, Rosenberg L. Characterization of integrin expression in isolated islets from hamster, canine, porcine, and human pancreas. *JHC* 1999;47(4):499-506.

Wang Z & Thurmond DC. Mechanisms of biphasic insulin-granule exocytosis- roles of the cytoskeleton, small GTPases, and SNARE proteins. *J Cell Sci* 2009;122:893-903.

Wang ZC, Wheeler MB, Belsham DD. Isolation and immortalization of MIP-GFP neurons from the hypothalamus. *Endocrinology* 2014;155(6):2314-2319.

Weimbs T, Low SH, Chapin SJ, Mostov KE, Bucher P, Hofmann K. A conserved domain is present in different families of vesicular fusion proteins: a new superfamily. *Proc Natl Acad Sci* 1997;94:3046–3051.

Wennerberg K, Armulik A, Sakai T, Karlsson M, Fassler R, Schaefer E, et al. The cytoplasmic tyrosines of integrin subunit beta1 are involved in focal adhesion kinase activation. *Mol Cell Biol* 2000;20:5758-5765.

Wheeler MB, Sheu L, Ghai M, Bouquillon A, Grondin G, Weller U, et al. Characterization of SNARE protein expression in β cell lines and pancreatic islets. *Endocrinology* 1996;137(4):1340-1348.

Wicksteed B, Brissova M, Yan W, Opland DM, Plank JL, Reinert RB, et al. Conditional gene targeting in mouse pancreatic β -cells: analysis of ectopic Cre transgene expression in the brain. *Diabetes* 2010;59(12):3090-3098.

Wollen N & Bailey CJ. Inhibition of hepatic gluconeogenesis by metformin: synergism with insulin. *Biochem Pharmacol* 1988;37:4353-4358.

Wollheim CB & Sharp GWG. Regulation of insulin release by calcium. *Physiol Rev* 1981;61(4):914-973.

Xia H, Nho RS, Kahm J, Kleidon J, Henke CA. Focal adhesion kinase is upstream of phosphatidylinositol 3-kinase/Akt in regulating fibroblast survival in response to contraction of type I collagen matrices via a beta 1 integrin viability signaling pathway. *J Biol Chem* 2004;279:33024-33034.

Yashpal NK, Li J, Wheeler MB, Wang R. Expression of β 1 integrin receptors during rat pancreas development – sites and dynamics. *Endocrinology* 2005;146(4):1798-1807.

Zaidel-Bar R, Itzkovitz, S, Ma'ayan A, Iyengar R, and Geiger B. Functional atlas of the integrin adhesome. *Nat Cell Biol* 2007;9:858-867.

Zhou Q, Law AC, Rajagopal J, Anderson WJ, Gray PA, Melton DA. A multipotent progenitor domain guides pancreatic organogenesis. *Dev Cell* 2007;13:103–114.

Zhu D, Koo E, Kwan E, Kang Y, Park S, Xie H, et al. Syntaxin-3 regulates newcomer insulin granule exocytosis and compound fusion in pancreatic beta cells. *Diabetologia* 2013;56:359-369.

Zeng Y, Ricordi C, Lendoire J, Carroll PB, Alejandro R, Bereiter DR, et al. The effect of prednisone on pancreatic islet autografts in dogs. *Surgery* 1993;113(1):98-102.

Appendices

Appendix A: Animal use protocol



2008-038-04::6:

AUP Number: 2008-038-04

AUP Title: Pancreatic Beta Cell Development: The Role of the c-Kit and Integrin Receptors

Yearly Renewal Date: 11/01/2014

The YEARLY RENEWAL to Animal Use Protocol (AUP) 2008-038-04 has been approved, and will be approved for one year following the above review date.

This AUP number must be indicated when ordering animals for this project.

Animals for other projects may not be ordered under this AUP number.

Purchases of animals other than through this system must be cleared through the ACVS office.

Health certificates will be required.

REQUIREMENTS/COMMENTS

Please ensure that individual(s) performing procedures on live animals, as described in this protocol, are familiar with the contents of this document.

The holder of this Animal Use Protocol is responsible to ensure that all associated safety components (biosafety, radiation safety, general laboratory safety) comply with institutional safety standards and have received all necessary approvals. Please consult directly with your institutional safety officers.

Submitted by: Kinchlea, Will D

on behalf of the Animal Use Subcommittee

University of Western Ontario

Permit Summary

Permit Holder Wang, Rennian
Permit # BIO-LHRI-0046 **Classification** 2
Department Physiology
Phone _____ **Ext.** _____
Email _____
Approval Date Apr 25, 2014 **Expiration Date** Apr 24, 2017
BioSafety Officer's Signature _____

Permit Conditions

- 1 INTERNAL PERMIT HOLDER RESPONSIBILITIES

Comply with UWO BioSafety Safety Policies and Standard Operating Procedures. Ensure that the Health Canada Biosafety Guidelines, relevant regulations and safe laboratory practices are followed.

 - 1.1 Receive adequate biosafety training from the institution. Permit Holders are responsible for the provision of specific training and instruction in biohazard agent handling that is necessary for the safe use of this material in their own laboratories. Supervisors must ensure that workers understand the health and safety hazards of the work or task (due diligence).
 - 1.2 Ensure that the UWO Biosafety Manual is available to all lab personnel under the permit.
 - 1.3 Report incidents of loss or theft of any biohazardous material immediately to the Biosafety Coordinator;
- 2 WORKER RESPONSIBILITIES

Be familiar with the UWO Biosafety Manual, attend all required safety training sessions and obey all safety regulations required by the UWO Biosafety Committee.

 - 2.1 Report to the Permit Holder any incident involving known or suspected exposure, personal contamination or a spill involving a biohazardous agent.

I accept the above responsibilities as a Internal Permit Holder and I am accountable for following UWO BioSafety Guidelines and Procedures Manual for Containment Level 1 and 2 Laboratories.

Permit Holder Name _____ Signed _____ Date _____

Appendix C: Biosafety approval form



<p>Researcher: Dr. Rennian Wang</p> <p>Biosafety Approval Number: BIO-LHRI-0046</p> <p>Expiry Date: April 24, 2017</p>

April 28, 2014

Dear Dr. Wang:

Please note your biosafety approval number listed above. This number is very useful to you as a researcher working with biohazards. It is a requirement for your research grants, purchasing of biohazardous materials and Level 2 inspections.

Research Grants:

- This number is required information for any research grants involving biohazards. Please provide this number to Research Services when requested.

Purchasing Materials:

- This number must be included on purchase orders for Level 1 or Level 2 biohazards. When you order biohazardous material, use the on-line purchase ordering system (www.uwo.ca/finance/people/). In the "Comments to Purchasing" tab, include your name as the Researcher and your biosafety approval number.

Annual Inspections:

- If you have a Level 2 laboratory on campus, you are inspected every year. This is your permit number to allow you to work with Level 2 biohazards.

To maintain your Biosafety Approval, you need to:

- Ensure that you update your Biohazardous Agents Registry Form at least every three years, or when there are changes to the biohazards you are working with.
- Ensure that the people working in your laboratory are trained in Biosafety.
- Ensure that your laboratory follows the University of Western Ontario Biosafety Guidelines and Procedures Manual for Containment Level 1 & 2 Laboratories.
- For more information, please see: www.uwo.ca/hr/safety/biosafety/.

Please let me know if you have questions or comments.

Regards,

Tony Hammoud
Biosafety Coordinator for Western

Curriculum Vitae

JASON PEART

EDUCATION:

Honours Double Major in Biology and Psychology, York University
Toronto, Ontario – Graduated Summer 2012.

Masters in Pathology and Laboratory Medicine, University of Western
Ontario, London, Ontario expected graduation Spring 2017

RESEARCH EXPERIENCE:

2011 Honours Thesis Research, Department of Biology, York University

Supervisor: Dr. Suraj Unniappan

Advisor: Dr. Andrew Donini

Title of the thesis: Chronic sub-cutaneous infusion of nesfatin-1 does not
affect blood glucose levels in C57BL/6 mice with type 1 diabetes

Brief description of the thesis work: C57BL/6 mice were treated with
streptozotocin and implanted with osmotic mini-pumps containing the
protein nesfatin-1. The affects of nesfatin-1 on blood glucose regulation and
pancreatic β -cell neogenesis was examined

2012 Advanced Research in Psychology, Department of Psychology, York
University

Supervisor: Dr. Janice Johnson

Title of the thesis: Does having type 1 diabetes affect desirability regarding
an intimate relationship?

Brief description of thesis work: University students were surveyed using a customized questionnaire involving online dating profiles. The purpose was to examine whether or not having type 1 diabetes impacted an individual's likelihood of being considered as a potential romantic partner

2012 Psychology 4th Year Independent Study, Department of Psychology, York University

Supervisor: Dr. Susan MacDonald,

Title of Project: A comparison of gorilla and orangutan play behavior

Brief description of final project: Gorilla and orangutan play behaviour was examined at the Toronto Zoo over multiple weeks and comparisons were made

2013- MSc Degree in Pathology and Laboratory Medicine, University of Western Ontario

Supervisor: Dr. Rennian Wang,

Brief description of project: Examining the effect of an inducible β -cell specific, β 1-integrin knockout in adult and adolescent mice

POSTER AND ORAL PRESENTATIONS:

Peart JE, Li J, Wang R. The Effect of β 1-Integrin on Pancreatic Beta-cell Survival and Function using an Inducible Beta-cell Specific β 1-Integrin Knockout Mouse Model. Poster Presentation at the 2014 Annual Pathology Research Day, Western University, April 2014.

Peart JE, Feng ZC, Riopel M, Li J, Wang R. The Effect of β 1-Integrin on Pancreatic Beta-cell Survival and Function using an Inducible Beta-cell Specific β 1-Integrin Knockout Mouse Model. Poster Presentation at the

2014 James A.F. Stevenson Distinguished Lecture and Physiology and Pharmacology Research Day, Western University, November 2014.

Peart JE, Feng ZC, Riopel M, Li J, Wang R. The Effect of β 1-Integrin on Pancreatic Beta-cell Survival and Function using an Inducible Beta-cell Specific β 1-Integrin Knockout Mouse Model. Poster Presentation at the 5th Annual Diabetes Research Day, Western University, November 2014.

Peart J, Feng Z, Riopel M, Li J, Wang R. Inducible Beta-Cell Specific β 1-Integrin Knockout Affects Islet Architecture, Beta-Cell Survival and Function. Poster Presentation at the Annual Pathology and Laboratory Medicine Research Day, Western University, March 2015

Peart J, Feng Z, Riopel M, Li J, Wang R. Inducible Beta-Cell Specific β 1-Integrin Knockout Affects Islet Architecture, Beta-Cell Survival and Function. Oral Presentation at London Health Research Day, London Ontario, April 2015

Peart J, Riopel M, Feng Z, Li J, Wang R. Inducible Beta-Cell Specific β 1-Integrin Knockout Impairs Beta-Cell Function and Survival. Poster Presentation at the 6th Annual Diabetes Research Day, Western University, November 2015

Peart J, Riopel M, Feng Z, Chen B, Li J, Wang R. Inducible Beta-Cell Specific β 1-Integrin Knockout Impairs Beta-Cell Function and Survival. Poster Presentation at the 9th Annual Diabetes Research Day, Western University, November 2015

CONFERENCE PUBLICATIONS:

Jason E Peart, Jinming Li, Rennian Wang. (2014). Inducible Beta-Cell Specific β 1-Integrin Knockout Affects Islet Architecture, Beta-Cell Survival and Function. Canadian Journal of Diabetes. Canadian Diabetes Association and the Canadian Society of Endocrinology and Metabolism 17th Annual Professional Conference and Annual Meeting, Winnipeg, Canada, 2014-10-25 (S17). Elsevier Inc.,

PUBLICATIONS:

Jason Peart, Jinming Li, Hojun Lee, Matthew Riopel, Zhi-Chao Feng, Rennian Wang. Critical role of β 1 integrin in postnatal beta-cell function and expansion. Oncotarget (pending revisions).